

**SOIL STRUCTURE ANALYSIS OF TURBOGENERATOR FOUNDATION USING
PLAXIS 2D**



A Final Report on

Submitted in partial fulfillment of the requirements for the award of the degree of

MASTER OF ENGINEERING

In

CIVIL ENGINEERING

(With Specialization in Geotechnical Engineering)

Of

ASSAM SCIENCE & TECHNOLOGY UNIVERSITY SESSION 2020-22



Submitted By

MISS MOITREYEE MAHANTA

Roll No: PG-C-008

ASTU Roll No: 210620062008

ASTU Registration No: 006306221 of 2021-2023.

Under the Guidance of

DR. JAYANTA PATHAK
Professor and Head of Department
Department of Civil Engineering

DR. SASANKA BORAH
Assistant Professor
Department of Civil Engineering

Assam Engineering College Jalukbari, Guwahati-781013, Assam

DECLARATION

I hereby declare this work entitled “Soil Structure Analysis of “Turbogenerator foundation using PLAXIS 2D” is accorded for the award for the degree of “MASTER OF ENGINEERING” in CIVIL ENGINEERING, with specialization in Geotechnical engineering, submitted to the department of civil engineering ,Assam Engineering College ,Guwahati is an authentic record of my own work carried out under the supervision and guidance of Dr. Jayanta Pathak, Professor and Head of Department of Civil Engineering, Assam Engineering College, Guwahati, and Dr. Sasanka Borah, Assistant Professor, Department of Civil Engineering, Assam Engineering College.

Dated:
Place: Guwahati

.....
(Moitreyee Mahanta)
M.Tech 4th Semester
Department of Civil Engineering
Assam Engineering College
Jalukbari, Guwahati-781013

CERTIFICATE

This is to certify that the work presented in the project report entitled “Soil Structure Analysis of Turbogenerator foundation using PLAXIS 2D” is submitted by Moitreyee Mahanta, Roll No: PG-C-008, ASTU Roll No. 210620062008 a student of M.Tech 4th semester, Department of Civil Engineering, Assam Engineering College, to the Assam Science and Technology University in partial fulfillment of the requirement for the award of the degree of Master of Technology, in Civil Engineering with specialization in Geotechnical Engineering under our guidance and supervision.

Dr. Jayanta Pathak

Professor and Head of Department
Department of Civil Engineering
Assam Engineering College
Jalukbari, Guwahati-781013

Date:

Dr Sasanka Borah

Assistant Professor
Department of Civil Engineering
Assam Engineering College
Jalukbari, Guwahati-781013

Date:

Certificate From The Head Of The Department

This is to certify that the dissertation entitled “Soil Structure Analysis of Turbogenerator foundation using PLAXIS 2D” has been submitted by Moitreyee Mahanta, bearing Roll No: PG-C-008, ASTU Roll No. 210620062008 a student of M.Tech 4th semester, Department of Civil Engineering, Assam Engineering College, to the Assam Science and Technology University in partial fulfilment of the requirement for the award of the degree of Master of Technology in Civil Engineering with specialization in Geotechnical Engineering.

Dated:

Place: Guwahati

.....

Dr. Jayanta Pathak

(Professor & Head of the Department)

Department of Civil Engineering

Assam Engineering College

Jalukbari, Guwahati-781013

ACKNOWLEDGEMENT

At the very onset I would like to express my profound gratitude and sincere thanks to my respected guide Dr. Jayanta Pathak, Professor and Head of Dept. of Civil Engineering, Assam Engineering College, Guwahati and Dr. Sasanka Borah, Assistant Professor, Department of Civil Engineering, Assam Engineering College for their invaluable supervision, guidance and constructive suggestions throughout the course of this work and particularly for their diligent scrutiny and correction of the manuscript.

I offer my heartiest thanks to my friends and family members for their constant inspiration and encouragement.

I also thank all the faculty members and staff of the Department of Civil Engineering.

Dated:
Place: Guwahati

.....
(Moitreyee Mahanta)
M.Tech 4th Semester
Department of Civil Engineering
Assam Engineering College
Jalukbari, Guwahati-781013

ABSTRACT

This study focuses on investigating the impact of a turbogenerator foundation on a concrete block foundation situated in close proximity to a two-story steel frame structure. The analysis is conducted using the PLAXIS 2D computer software. The primary objective is to understand the dynamic response of the foundations under varying loading conditions and to demonstrate the effectiveness of PLAXIS 2D in facilitating this study.

The study encompasses several key steps. Initially, parameters are determined for the soil surrounding the foundations, including relevant properties such as density, shear modulus, and damping. Additionally, material characteristics for the concrete footing and the structural steel of the frame are considered.

Specifications for the turbogenerator, including its weight, rotation frequency, and vibration amplitude, are adopted from the company manual. To streamline calculations and modelling, an axisymmetric model is chosen, assuming symmetry around a central axis.

The analysis proceeds through three distinct phases. The first phase involves evaluating the foundation response without any loading, establishing a baseline for subsequent comparisons. In the second phase, the effects of turbogenerator vibrations on the foundations are analysed, considering the dynamic loading induced by the rotating turbogenerator. The third phase examines the post-vibration behaviour of the foundations after the turbogenerator comes to a stop.

Results obtained from the PLAXIS 2D analysis are interpreted using the software's in-built curve generator, facilitating graphical representation and comprehensive analysis of the data. By employing this approach, the study not only sheds light on the dynamic response of foundations to varying loads but also underscores the user-friendly and graphical capabilities of PLAXIS 2D.

In conclusion, this research contributes to the understanding of foundations subjected to dynamic loading from turbogenerators, utilizing advanced modelling techniques and specialized software tools. The insights gained have implications for foundation design in similar scenarios, while the study highlights the efficacy of PLAXIS 2D for investigating dynamic foundation behaviour in a visually informative manner.

Table of Content

CHAPTER 1.....	1
1.1 Definition:	1
1.2 History of Turbogenerator:	3
1.3 Operating Principle:	3
1.4 Cooling System:.....	4
1.5 Applications of Turbogenerators	4
1.6 Overview of Study:	4
CHAPTER 2.....	5
2.1 Introduction	5
2.2 Review of Literature.....	5
CHAPTER 3.....	11
3.1 Introduction	11
3.2 Criteria for Design	11
3.3 Information Needed for Design	11
3.4 Sizing of Foundation	12
3.5 Primary Load And Load Combination for Static Analysis.....	12
3.6 Representation of the model.....	14
4.1 Introduction	15
4.2 Mode of Analysis	15
4.3 Property of Soil	15
4.3.1 Property of Clay Layer	16
4.3.2 Properties of Sand Layer:	17
4.4 Properties of Structural Steel:	18
4.5 Properties of foundation concrete:	18
4.6 Properties of Turbogenerator:.....	19
CHAPTER 5.....	20
5.1 Introduction:	20
5.2 Test Program:	20
5.3 Procedure.....	21
CHAPTER 6.....	25
6.1 Introduction:	25
6.2 Calculation Phase:.....	25
6.3 Output Mesh and Point/Node Selection:	25

6.4	The Curve Generator:	26
6.5	Results.....	27
6.6	Results after starting of the Turbogenerator:	28
6.6.1	: Point on the surface of soil:	28
6.6.2	At the bottom of the steel frame foundation	29
6.6.3	At the middle of the clay layer	29
CHAPTER 7.....		30
7.1	Introduction	30
7.2	Generalized discussion of the effects on bearing capacity of soil.....	30
7.3	Generalized discussion of the effects on settlement of soil.....	30
7.4	Different soil parameters used in Plaxis 2D	31
7.5	Effects of soil parameters on model.....	32
CHAPTER 8.....		304
8.1	Introduction	34
8.2	Young's Modulus of Soil:.....	34
8.2.1	Typical values of Young's modulus for granular material (MPa) (based on Obrzud & Truty 2012 compiled from Kezdi 1974 and Prat et al. 1995):	34
8.2.2	Typical values of Young's modulus for cohesive material (MPa) (based on Obrzud & Truty 2012 compiled from Kezdi 1974 and Prat et al. 1995):	35
8.3	Angle of friction:	35
8.3.1	Typical values of soil friction angle [°]:.....	35
8.3.2	Correlation between SPT-N value, friction angle, and relative density:	38
8.4	Cohesion:	38
8.4.1	Typical values of soil cohesion for different soils [kPa]:.....	38
8.5	Dry unit weight:	41
8.5.1	Typical values of soil cohesion for different soils (kN/m ³):	41
8.6	Soil bearing capacity:	42
8.6.1	Typical values of soil bearing capacity (kPa):	42
8.7	Soil permeability coefficient:	43
8.7.1	Typical values of soil permeability:	43
8.8	Soil porosity:	45
8.8.1	Typical values of soil void ratio for different soils:	45
8.9	Void ratio:.....	47
8.9.1	Typical values of soil void ratio for different soils:	47
8.10	Young's Modulus of Steel:.....	49

8.10.1	The typical values of Young's modulus for different types of steel (GPa):.....	49
8.11	Turbo generator proportions	50
CHAPTER 9.....		51
9.1	Introduction	51
9.2	Description of different types of models	51
9.2.1	CONCRETE MODEL	51
9.2.2	Importance of Concrete Modeling	51
9.2.3	Features of the Concrete Model	51
9.3	Applications of Concrete Model	53
9.4	MOHR-COLUMB MODEL.....	54
9.4.1	Importance of Mohr-Columb Model.....	54
9.4.2	Features of the Mohr-Columb Model	54
9.5	Applications of the Mohr-Coulmb Model	55
9.6	HARDENING SOIL MODEL	55
9.6.1	Importance of Soil Hardening Model.....	56
9.6.2	Features of Soil Hardening Model.....	56
CHAPTER 10.....		58
10.1	Introduction	58
10.2	Methodology	58
10.3	Different models prepared for performing the analysis	58
10.3.1	Cohesionless Soil i.e., clay.	58
10.4	Findings.....	63
10.4.1	Cohesive soil i.e. clay.....	63
10.5	RESULTS.....	65
10.5.1	FOR A TWO LAYERED SOIL SYSTEM.....	68
CHAPTER 11.....		72
11.1	Introduction	72
11.2	Water Table effects through Plaxis 2D.....	72
11.3	Water Table effect on Cohesionless soil.	72
11.4	The effects of water table in Cohesionless soil.....	73
11.5	Comparing the load vs settlement, we get.....	74
11.6	Effects of water table in cohesive soil.....	75
11.7	Comparing the load vs settlement we get.....	76
11.8	Mitigation of rising water levels.	76

CHAPTER 12.....	78
12.1 Introduction	78
12.2 Rayleigh damping.....	78
12.3 Damping analysis in cohesionless soil	78
12.4 Results of analysis performed.....	80
12.4.1 Without damping.	80
12.4.2 With damping.....	80
12.5 Damping analysis in cohesive soil.....	81
12.6 Results of analysis performed.....	82
12.6.1 Without damping.	82
12.6.2 With damping.....	82
12.7 Damping analysis in Two Layered soil.....	82
12.8 Results of analysis performed.....	84
12.8.1 Without damping.	84
12.8.2 With Damping	85
CHAPTER 13.....	87
13.1 Introduction	87
13.2 Methodology	87
13.3 Analytical calculation of safe distance in cohesive soil.....	87
13.3.1 Generation of geometry and mesh.....	87
13.4 Analytical calculation of safe distance in cohesionless soil.	90
13.4.1 Generation of geometry and mesh.....	90
13.5 Analytical calculation of safe distance in two layered soil.....	93
13.5.1 Generation of geometry and mesh.....	93
CHAPTER 14.....	96
14.1 GENERAL	96
14.2 Soil-Structure Interaction:	96
14.3 Vibration and Settlement Analysis:.....	96
14.4 Damping Analysis:.....	96
14.5 Water Table Analysis:.....	97
14.6 Calculation of safe distance:	97
14.7 Validation and Optimization:	98
14.8 Future Scope:.....	98

List of Figure

Figure 1.1 A typical turbogenerator in an industrial complex.....	1
Figure 1.2 Table Top Turbogenerator Foundation.....	2
Figure 1.3 Table Top Turbogenerator Foundation with Vibration Isolator.....	2
Figure 3.1 Torque due to normal operation.....	13
Figure 3.2 Layout of the system.....	14
Figure 3.3 Representation of the turbo generator model in Plaxis2D.....	14
Figure 4.1 Layout of the model made in Plaxis 2D.....	15
Figure 5.1 Model Properties taken from Plaxis 2D.....	21
Figure 5.2: Soil and Footing Properties denoted in Plaxis 2D.....	22
Figure 5.3: Layout of the model made in PLAXIS 2D.....	22
Figure 5.4: Adding the Turbogenerator Frequency in Plaxis 2D.....	23
Figure 5.5: The four phases of calculation done in Plaxis 2D.....	23
Figure 5.6: Mesh Generation done in PLAXIS 2D.....	24
Figure 6.1: Calculation Phase taken in PLAXIS 2D.....	25
Figure 6.2: Selection of nodes/points in the output section of PLAXIS 2D.....	26
Figure 6.3: The Curve Generator inbuilt in PLAXIS 2D.....	27
Figure 6.4: Result obtained by considering the dead loading phase in the turbogenerator in PLAXIS 2D.....	27
Figure 6.5: Phase 2: On surface of soil.....	28
Figure 6.6: Phase 2: At the bottom of the steel foundation.....	29
Figure 6.7: Phase 2: At the middle of the clay layer.....	29
Figure 8.1: Model of the generator as taken from the company journal.....	50
Figure 9.1: Analysed concrete model in PLAXIS 2D.....	53
Figure 9.2: Mohr-Columb Model in PLAXIS 2D.....	55
Figure 9.3: Hardening Soil Model in Plaxis 2D.....	57
Figure 10.1: Layout of the model.....	58
Figure 10.2: Generation of the Mesh in PLAXIS 2D.....	60
Figure 10.3: Node Selection.....	60
Figure 10.4: Result generated in the in-situ generator with no loading in PLAXIS 2D.....	61
Figure 10.5: Result generated in the in-situ generator after starting of turbogenerator in PLAXIS 2D.....	61
Figure 10.6: Result generated in the in-situ generator after starting of turbogenerator in PLAXIS 2D.....	62
Figure 10.7: Result generated in the in-situ generator after starting of turbogenerator in PLAXIS 2D.....	62
Figure 10.8: Layout of the model.....	63
Figure 10.9: Generation of Mesh.....	65
Figure 10.10: Selection of Nodes.....	65
Figure 10.11: Result generated in the in-situ generator with no loading in PLAXIS 2D.....	66
Figure 10.12: Result generated in the in-situ generator after starting of turbogenerator in PLAXIS 2D.....	66
Figure 10.13: Result generated in the in-situ generator after starting of turbogenerator in PLAXIS 2D.....	67

Figure 10.14: Result generated in the in-situ generator after starting of turbogenerator in PLAXIS 2D	67
Figure 10.15: Layout of the Model.....	68
Figure 10.16: Generation of Mesh	69
Figure 10.17: Selection of Nodes	69
Figure 10.18: Result generated in the in-situ generator with no loading in PLAXIS 2D.....	70
Figure 10.19: Result generated in the in-situ generator after starting of turbogenerator in PLAXIS 2D	70
Figure 10.20: Result generated in the in-situ generator after starting of turbogenerator in PLAXIS 2D	71
Figure 10.21: Result generated in the in-situ generator after starting of turbogenerator in PLAXIS 2D	71
Figure 11.1: System with Global water level.....	73
Figure 11.2: Manually raised water level to study the effects.....	73
Figure 11.3: Graphical representation of comparing the load vs settlement.....	74
Figure 11.4: System with Global water level.....	75
Figure 11.5: Manually raised water level to study the effects.....	75
Figure 11.6: Graphical representation of comparing the load vs settlement.....	76
Figure 12.1: Damping is introduced.....	79
Figure 12.2: Generation of mesh	79
Figure 12.3: Result generated in in-situ generator analysis performed without damping.....	80
Figure 12.4: Result generated in in-situ generator analysis performed with damping	80
Figure 12.5: Damping is introduced into the soil layer	81
Figure 12.6: Mesh is generated.....	81
Figure 12.7: Result generated in in-situ generator analysis performed without damping.....	82
Figure 12.8: Result generated in in-situ generator analysis performed with damping	82
Figure 12.9: Damping is introduced for Sand layer.....	83
Figure 12.10: Damping is introduced for clay layer	83
Figure 12.11: Generation of mesh	84
Figure 12.12: Result generated in in-situ generator analysis performed without damping.....	84
Figure 12.13: Result generated in in-situ generator analysis performed with damping	85
Figure 13.1: The foundation and machine are modelled as separate entities	87
Figure 13.2: Generation of mesh	88
Figure 13.3: The dynamic time vs. displacement graph is shown below.....	88
Figure 13.4: Tabulated data showing minimal to no deformation for the safe distance in PLAXIS 2D	89
Figure 13.5: Tabulated data showing minimal to no deformation for the safe distance in PLAXIS 2D	89
Figure 13.6: Tabulated data showing minimal to no deformation for the safe distance in PLAXIS 2D	90
Figure 13.7: The foundation and machine are modelled as separate entities	91
Figure 13.8: Generation of mesh	91
Figure 13.9: Selection of nodes.....	92
Figure 13.10: The dynamic time vs. displacement graph is shown below.....	92
Figure 13.11: The foundation and machine are modelled as separate entities	93
Figure 13.12: Generation of mesh	93

Figure 13.13: Selection of nodes.....	94
Figure 13.14: The dynamic time vs. displacement graph is shown below.....	94

List of Tables

Table 4.1: Properties of Clay Layer	16
Table 4.2: Properties of Sand Layer.....	17
Table 4.3: Properties of Steel	18
Table 4.4: Properties of Foundation Concrete	19
Table 4.5: Properties of Turbogenerator	19
Table 8.1: Standard Dimension Table of Prime Rating (3300V, 6600V)	50
Table 10.1: Properties of Sand Layer.....	59
Table 10.2: Properties of clay layer	64
Table 14.1: Vibration and Settlement Analysis of types of Soil.....	96
Table 14.2: Damping Analysis in various steps of soil.	97
Table 14.3: Water Table Analysis of soil.	97
Table 14.4: Calculated safe distance of various types of soil.	97

CHAPTER 1

INTRODUCTION

1.1 Definition:

A turbo generator is a generator connected to a shaft of a gas or steam turbo to generate electrical energy. Huge steam powered turbo generators supply electricity mainly to the world. These generators are also used in steam powered turbo-electric vessels. Small turbo generators powered by gas turbos are often used as APUs (auxiliary power units), especially for aircraft.

The turbo-generator forms the heart of a power plant. It is the most vital and expensive equipment of a power plant complex and is generally housed inside a turbo-generator building. A turbo-generator consists of a turbine-generator and other auxiliaries like condenser, pipelines carrying superheated steam etc. Turbo-generator falls under high-speed rotary type machines and its capacity varies from 2 MW to 2000 MW (referred from https://en.wikipedia.org/wiki/Turbo_generator). The turbo-generator foundation consists of turbo-generator and its auxiliaries mounted on a table top foundation. The foundation can be either made of steel or RCC. A RCC table top type foundations are commonly adopted. The top deck, column and bottom raft together constitute the turbo-generator foundation. Sometimes the turbogenerator foundation is mounted on vibration isolator. A typical turbogenerator in an industrial complex is shown in Figure 1.1.



Figure 1.1 A typical turbogenerator in an industrial complex

(https://en.wikipedia.org/wiki/Turbo_generator#/media/File:Turbogenerator01.jpg)

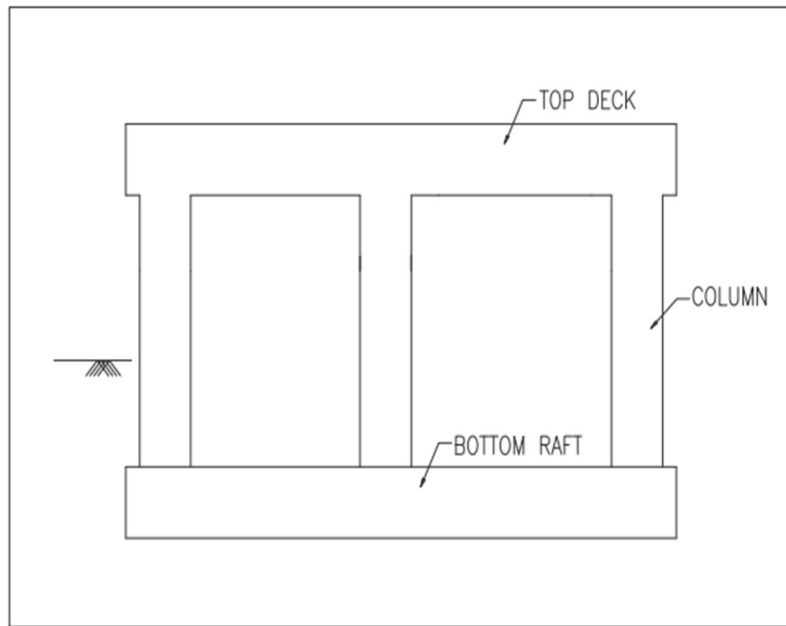


Figure 1.2 Table Top Turbogenerator Foundation

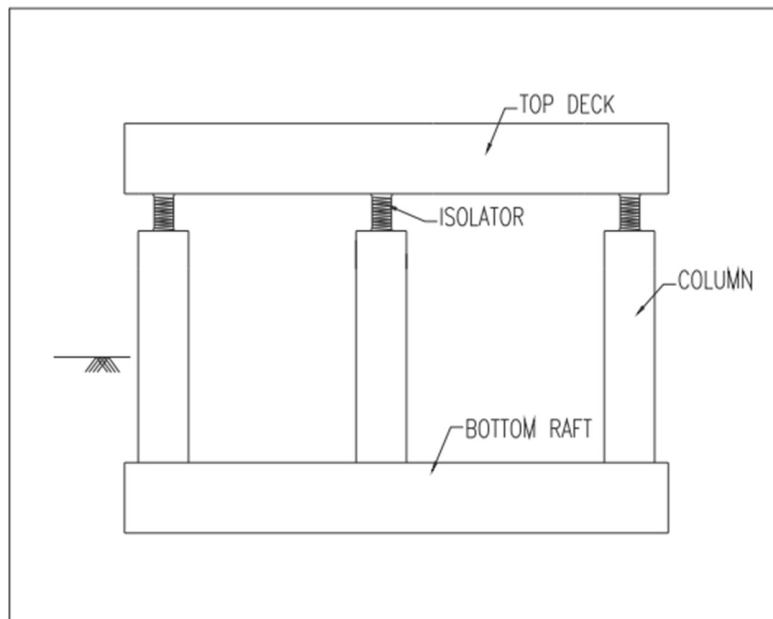


Figure 1.3 Table Top Turbogenerator Foundation with Vibration Isolator

1.2 History of Turbogenerator:

The first turbo generator known as an electric generator was powered through a water turbine. A turbo generator with DC steam powered using a dynamo was demonstrated by an Engineer namely "Charles Algernon Parsons" in the year 1887. After that, the first large industrial AC turbo generator was supplied with megawatt power to a nuclear power plant in the year 1901, Elberfeld, Germany. (C. Ginet, 2010)

1.3 Operating Principle:

Turbo generators operate on the principle of electromagnetic induction. When the turbo is connected to a generator, the kinetic energy (CU) of the steam cancels the turbo's fan blades and the generator's rotor spins to generate electricity. Construction of turbo generators includes stators, stator frames, stator cores, stator windings, bushings, excitation systems, cooling systems, rotors, rotor shafts, rotor windings, retaining rings, rotor wedges, etc.

It can be done using various components of the rotor fan. The parts of the turbo generator are described below. The stator is the stationary part of the generator and the stator frame is the heaviest part of the generator. The body of the stator is completely gas-encapsulated and its construction is made of high quality austenitic and mild steel. This frame is used to reduce vibration and withstand the pressure of the gas boiler.

The stator core contains thin laminations, each of which is manufactured in several separate segments. The main feature of the stator core is that it provides mechanical support and efficiently transports magnetic flux. Thin fins are used here to reduce eddy currents.

The stator windings have three-phase and pitched two-layer windings that allow the fifth and seventh harmonics to match. The openings and ends of the three-phase winding are insulated from the stator frame using bushings to provide high voltage insulation. These bushings are connected to the stator frame at the end of the exciter.

The rotor shaft is a sturdy single piece made of vacuum cast steel in which the slots are located. The rotor body edge is provided with 60% of longitudinal slots with field winding.

The rotor is a rotating part of the turbo generator thus it protects the winding from the centrifugal force effects and they are protected by rotor slot wedges. The cooling air in the turbo generator is dispersed by an axial fan disposed on the shaft of the rotor.

For example, in a 250 MW rotor type, two axial flow fans are used in both the excitation end and the turbo, and a 500 MW axial fan is mainly used on the edge of the turbo. As soon as both the rotor and the stator are created, all of these parts are connected through the implementation. The suggestion is a method of generating a magnetic field by current.

Turbo generators are particularly exciting machines. The excitation system continuously provides the flow of C fields corresponding to the interfacial winding. Brushless

pathogens have two abstracts such as three domestic areas and permanent magnetic pilots.

1.4 Cooling System:

The cooling system in the turbo generator is mainly used to dissolve the heat generated by different losses and extend the life of the insulating material. This system is separated into three parts, such as air cooling, hydrogen, water cooling. The rotation speed of a turbo generator is typically 1500 rpm or 3000 rpm with two or four poles at a frequency of 50 Hz and 1800 rpm or 3600 rpm with two or four poles at a frequency of 60 Hz. Speed, parts of this generator can cause high mechanical load. In turbo generators, the rotor is typically forged using alloys and solid steel to mechanically strengthen the rotor.

1.5 Applications of Turbogenerators

1. Turbo generators are used to connect to the shafts of steam or gas turbos to generate electricity.
2. Large steam-based turbo generators provide electricity
3. These turbos are used by turbid vessels operated by current.
4. Small targets are often operated by gas turbos, so they often use APUs (auxiliary power supply units).
5. Turbo generators can be used as auxiliary power supply units.
6. A motor generator using diesel fuel for controlling motor on sites
7. These generators are used when emergency and standby power is required when supply capacity of power supply current occurs.
8. Turbo generators are used in hospitals during power outages.
9. Used in various power plants such as solar power plants, thermal power plants, and hydropower plants.

1.6 Overview of Study:

This was an overview of turbo generators and their possible uses. This generator is used to convert energy from machinery to electricity by exchanging fuels such as wind, steam, solar and fossil fuels.

In the following chapters, the design of the foundation for such turbo-generators is studies in depth and furthermore the soil-structure interaction of such foundations.

CHAPTER 2

REVIEW OF LITERATURE

2.1 Introduction

In this chapter previous contributions in the form of studies into soil-structure interaction and turbo generator foundations is discussed

2.2 Review of Literature

1. **Jagtap, H. P., Bewoor, A. K., Kumar, R., Ahmadi, M. H., & Chen, L. (2020)** analyzed the performance and availability optimization to improve maintenance schedule for the turbo- generator subsystem of a thermal power plant using particle swarm optimization.

They concluded that the applicability of the Markov approach and particle swarm optimization are employed and reported in this study. The optimum availability parameters of the turbo-generator subsystem are obtained. The Markov approach-based availability equations are derived for availability simulation modeling, and the results are obtained.

The study recommended the maintenance priority of subsystems of the TGS as per the criticality level obtained by the Markov approach. Furthermore, the system performance is evaluated, and the optimum availability level is obtained by using the PSO method. The PSO based study results advocate in rescheduling CBM based vibration monitoring frequency of turbine governing, which in turn reduces the required monitoring time. In addition, it is recommended to use PM predominantly for turbine lubrication and generator excitation system. In fact, maintenance planning depends on the criticality of the equipment. The frequency of system failure facilitates the allocation of maintenance resources. Besides, the required time to repair data of the system for maintenance activities can be used in actual maintenance planning and allocating the availability of the plant. For example, maintenance planning of the turbine-generator system to improve is recommended, as the criticality analysis results prioritize the system after criticality analysis, which in turn gives inputs/supports the maintenance planning department (MTP). In addition, the optimized availability parameters viz. failure rate (λ) and the repair rate (μ) are obtained using the particle swarm optimization method. These optimized parameters are used to recommend the optimized condition-based maintenance, preventive maintenance, and breakdown maintenance activities and used effectively for allocating resources for maintenance. This study could be further extended for validating PSO based availability analysis results with other optimization techniques such as ant colony algorithm, genetic algorithm, etc.

2. **Rajkumar, K., Ayothiraman, R., & Matsagar, V. A. (2021)** studied the influence of soil- structure interaction (SSI) on a torsionally coupled turbo-generator (TG) machine foundation is studied under earthquake ground motions and beneficial effects of base isolators in the TG foundation under earthquake ground motions were also studied duly, considering the effects of SSI. A typical TG foundation is analyzed using a three-dimensional finite element (FE) model. Two superstructure

eccentricity ratios are considered to represent the torsional coupling. Soft soil properties are considered to study the effects of SSI. This research concludes that the effects of torsional coupling alter the natural frequencies, if ignored, could lead to unsafe design. Deck accelerations and displacements are increased with an increase in superstructure eccentricity. On the other hand, the deck accelerations and displacements are greatly reduced with the help of base isolators, thus confirming the beneficial use of base isolators in machine foundations to protect the sensitive equipment from the strong earthquake ground motions. However, the effects of SSI reduce the natural frequencies of the TG foundation resting on soft soil conditions and activate the higher mode participation, resulting in amplifying the response.

FE analysis is carried out to evaluate the dynamic response of a typical base-isolated TG foundation subjected to different earthquake ground motions. The effects of torsional coupling in machine foundation are also studied and the results are compared with the torsional uncoupled case. Soft soil conditions are considered to analyze the effects of SSI and the results are compared with the fixed-base condition. From the results of the present study, the following conclusions are drawn:

- i) The SSI effects decrease the natural frequency of the entire structure-foundation-soil system, which is significant in higher modes, especially for TG foundation resting on soft soil strata. Also, the dynamic response of such machine foundations is greatly affected by the presence of superstructure eccentricities. The natural frequencies in lower modes are further reduced by the superstructure eccentricities
 - ii) The SSI effects increase the deck acceleration and lateral displacement in TG foundation resting on soft soil strata. In addition, the deck acceleration and lateral displacement are also increased in such machine foundations when the superstructure eccentricities are considered. Due to the excitation in torsional modes, the horizontal displacement in the other direction is also increased significantly with an increase in eccentricity ratio.
 - iii) Since the TG foundations are rigid as compared to the conventional low-rise buildings, the forces exerted on the superstructure are severe under earthquake ground motions. Hence, the base isolators are beneficial in TG foundations, by which the superstructure accelerations are greatly reduced. In addition, the relative deck displacements are also greatly reduced with the help of base isolators. Hence, base isolators are beneficial to protect sensitive equipment from damaging earthquake events.
3. **Smart, M. G., Friswell, M. I., & Lees, A. W. (2000)** made a study to estimate the turbogenerator foundation parameters: model selection and regularization. They concluded that using measured foundation responses, analytical rotor and bearing models and a known state of unbalance, it is possible to estimate a foundation dynamic stiffness model for a rotor-bearing-foundation system. The linear method, based on forces acting on the foundation, is quickly solved but suffers from the fact that the response contains global, rather than local, modes. The nonlinear method on the other hand provides more accurate models at the expense of longer computation times. The models showed some predictive capacity with

respect to different excitations, but the magnitudes of the peaks in the predicted response were often significantly in error. It is believed that this is due to three things: an inaccurate bearing model, changes in the bearing characteristics from run to run and the fact that the system is not entirely stationary. Model order selection and regularization was necessary for the models to have this predictive capacity. The tools used for this were equation error plots, with the model order with a low error chosen, and the singular value decomposition, with a cut-off level being specified below which the data were assumed to only represent noise. However, these methods are subjective and require some user judgement. Therefore, the estimation method was broadly successful, with further work required to improve the predictive capacity of the estimated models.

4. **Tripathy, S., & Desai, A. K. (2015)** analysed a turbo generator frame foundation using SAP: 2000 v 17.1 software.

In their work, the winkler spring soil model, solid Finite element modelling and dynamic analysis of Turbo generator foundation were considered. The frequency dependent soil impedance (stiffness & damping) for various mode shapes are addressed in this study. The soil foundation system was simulated in SAP: 200017.1. software and dynamic response of foundation was analyzed. The results are compared and validated with the mode shapes and frequencies published in the book "Foundations for Industrial Machines" published by Dr. KG Bhatia.

They conclude that the design of large dynamic equipment foundations located in high seismic regions is based on a multitude of factors. Both the dynamic requirements and seismic requirements based on site conditions play a very important role. For finite element analysis, SAP 2000 issued to create a model for static and dynamic analysis. The Eigen values increase with each mode and one of the values shall be near to the operating frequency of the machine. The Resonance condition observed at 47 Hz. It means resonance condition cannot be avoided but for safety of Turbo generator Frame Foundation to reduce transient resonance condition, the Machine can be speed up during the frequency overlapping.

5. **Jayarajan, P., & Kouzer, K. M. (2014)** performed the dynamic analysis of turbo-generator machine foundations.

Their paper focuses on the first two steps of the analysis and accordingly details the various aspects involved in the development of a realistic finite element model required for dynamic analysis. The response of the foundation was then obtained through free vibration analysis (Eigen analysis) and harmonic forced vibration analysis

The dynamic analysis of turbine foundations needs attention to detail both in modelling and interpretation of the results. The paper highlighted various issues related to the mathematical modelling of structure, machine and soil for dynamic analysis of the foundation system. Finite element method provides an efficient tool for the modelling and dynamic analysis of turbo- generator foundations. SAP2000 provided a real computational environment for the modelling of structure, machine and soil in a single model and to perform the free and forced vibration analysis.

6. **Fleischer, P. S., & Trombik, P. G. (2008, October)** analysed a Turbo generator machine foundations subjected to earthquake loadings. Their paper focused on the investigations and studies on foundation stability, proposes simplified design

principles for large machine foundations and will show specific requirements for turbo generators, which are sometimes in contradiction to seismic design demands. For practicable design of pedestals, foundation supports and machine anchorages, it was preferred to transfer seismic loads to static equivalent forces. Here, apart from local parameters such as ground acceleration and soil amplifications, the main concern is the load distribution over the height. Especially for compact raft foundations, the soil-structure-interaction is an eminent attribute, as first eigenfrequencies are in strong dependence to the bedding situation, and are often situated within the critical earthquake frequency range with regard to the soil amplification.

7. **Madhu Priya, M., Chandru, P., Vijaya Sarathy, R., & Jose Ravindra Raj, B. (2016)** performed a study on the dynamic Analysis and structural design Of Turbo Generator frame foundations.

An extensive study about the dynamic loads and static loads, frequency, amplitude, eccentricity and code/standards of machine foundation is carried out and observed the procedure for the design of machine foundation. A very less Research work has been done on turbo generator foundation. As a result, it has been concluded that the dynamic analysis of turbine generator foundations needs attention to detail both in modelling and interpretation of the results and also to consider the issues on mathematical modelling of structure, soil and machine for dynamic analysis.

8. **Sun, Y. H., & Zhang, Q. (2013)** studied on optimization of dynamic characteristics of turbo generator foundation. The study first used the vibration mode superposition method to solve the structural vibration response and sensitivity through establishing the dynamic equations and optimization model of the foundation, and then determined the optimization variables, constraints and objectives according to the process conditions, and at last undertook multivariate optimization research on a 1000MW turbo-generator foundation. Finally, an optimization scheme which reduces both the linear displacement of foundation vibration and the amount of concrete used was obtained. The analysis results showed that the optimization method adopted in this study had higher efficiency and could achieve better technical and economic benefits.

Their study makes an analysis on the optimization of 1000MW-level turbo generator foundation based on the rich experiences of turbo generator foundation design in China, according to the requirements of "Code for Design of Dynamic Machine Foundation". Finally, the results of design with a structural weight reduction by 1700 tons (670 m³) relative to the initial design, a reduction of the maximum vibration linear displacement of the disturbing force point, and a reduction of the amplitude differences between disturbing force points, is obtained.

The design presented was favorable for the turbo generator unit's power running environment. The following conclusions are achieved by summarizing the optimization and analysis process:

- i. In the design of a turbo generator foundation under dynamic load, attentions should be paid to dynamic optimization besides static optimization, in order to more effectively ensure that the unit runs smoothly.

- ii. By selecting different weight coefficients, dynamic optimization schemes that satisfy different object requirements can be obtained. Furthermore, the scheme that reduces the amount of concrete used while reducing the control point's maximum amplitude can be obtained, so that the dynamic performance of the foundation is improved in addition to saving investments.
- iii. The post section sizes have great impact on the stiffness of the foundation, and appropriately reducing the cross-section areas is good for improvement of the whole foundation dynamic performance.
- iv. The cross beams and longitudinal beams of roof are much restricted by technology conditions, but better effects are still feasible if adjustments are made appropriately.
- v. The stiffness of a two-floor platform also has certain effects on the dynamic characteristics of the foundation.

9. **Hokmabadi, A. S., & Fatahi, B. (2016)** studied the influence of foundation type on seismic performance of buildings considering soil–structure interaction.

Their paper describes how a 3D numerical simulation was used to conduct a series of parametric studies on a 15-storey full-scale (prototype) structure with different types of foundations including a fixed base, a shallow foundation, a floating pile foundation, and a pile-raft foundation. Material (and geometric nonlinearities have been considered in the 3D numerical simulation. Influence of Foundation Type on Seismic Performance. The results of this 3D numerical simulation showed that the properties of the in-situ soil influenced the characteristics of the excitation where the peak accelerations at the surface of the soft soil were more than those on the bedrock for low to moderate levels of acceleration. However, at higher levels of acceleration, the low stiffness and nonlinearity of the soft soil prevented peak accelerations as large as those recorded at the bedrock to develop. Moreover, the earthquakes consisted of greater proportions of long-period (low frequency) motions after passing through the deposits of soft soil. The nonlinear behavior of the soft soil influenced the dynamic characteristics of the ground motion by shifting the peaks in the amplification curve to the right (longer periods),and reducing the amplitudes of the peak ground accelerations. In general, the ratio of the structural base shear for cases that included the interaction between the soil–structure to that of the fixed-base was less than one, demonstrating the effect of the SSI in reducing the base shear of the structure. The reduction ratio for the base shear is a function of the foundation type. The results of this study indicated that the structure supported by the pile-raft foundation and the floating pile foundation experienced more base shear than the structure supported by the shallow foundation. Moreover, the amount and trend of this reduction in the structural shear forces differed for different levels in the superstructure. On this basis, practicing engineers must recognize that the reduction factor for the maximum base shear due to SSI cannot be generalized to every level of the superstructure. The predicted maximum rocking angles of the superstructure indicated that the structure supported by the shallow foundation experienced the most severe rocking compared to the floating pile and pile-raft foundations because the pile elements in both foundations reduced the maximum

uplift and the rocking experienced by the structure. Moreover, the structure supported by the pile-raft foundation experienced on average 20% less rocking than the structure supported by the floating pile foundation because the compressive stresses generated in one side of the floating pile foundation meant that the piles experienced more settlement here than in the pile-raft foundation where the compressive stresses were distributed over a larger area, which in turn, reduced the settlement. Eventually, considering the rocking-dissipation, the results of this study may help the practicing engineers when selecting the proper type of foundation type for their structures. Accordingly, the types of foundations that experienced a considerable amount of rocking during an earthquake, dissipated much more earthquake energy than other types of foundations and demonstrated that rocking-dissipation directed less shear forces to the superstructure and reduced the structural demand of the superstructure

10. **Star, L. M., Givens, M. J., Nigbor, R. L., & Stewart, J. P. (2015)** in their study, performed the Field-testing of structure on shallow foundation to evaluate soil-structure interaction effects.

In this paper, they described a sequence of experiments in which the same structure is subjected to forced vibrations at multiple sites representing varying degrees of base flexibility.

They concluded that the field testing to measure soil-structure interaction (SSI) effects is useful to evaluate the applicability of analytical models for realistic field conditions and to guide the selection of model parameters. A test program was designed to provide high quality data for validation of SSI models under realistic boundary conditions, a wide range of load amplitudes, and a wide frequency range. Forced vibration tests were performed on a portable steel column structure. The test structure was reconfigurable to provide alternate structural stiffnesses and tests were performed with shaking applied in both the short and long directions of the oblong structure. The tests were performed at three test sites with different soil conditions including: the UCLA Structures Laboratory (nearly fixed-base conditions), the Wildlife Liquefaction Array (very soft clays and silts), and the Garner Valley Downhole Array (medium dense sands). The Garner Valley Downhole Array has an additional permanently installed structure that was also instrumented. Forced vibration loading was provided by two different shakers installed on the structure and by a shaker truck. In addition, earthquake loading events were recorded.

CHAPTER 3

DESIGN OF TURBO GENERATOR FOUNDATION

3.1 Introduction

In this section, the specific design parameters followed for turbo generator foundations are discussed as per IS 2974-3 (1992): Code of practice for design and construction of machine foundations, Part 3: Foundations for rotary type machines (Medium and high frequency).

3.2 Criteria for Design

The basic principle of TG foundation remains same compared to other machine foundation

1. No resonance should occur and hence the natural frequency of foundation system should not coincide with the operating frequency of the machine. The foundation is high tuned when its fundamental frequency is greater than the operating speed or low tuned when its fundamental frequency is lower than the operating speed.
2. The amplitudes of motion at operating frequencies should not exceed the limiting amplitudes, which are generally specified by machine manufacturers.
3. An eccentricity of 3% of base dimension along which the center of gravity gets displaced may be allowed. The reason to limit eccentricities is to minimize secondary moments that could significantly influence the natural frequencies of the foundation.

3.3 Information Needed for Design

The following data needs to be provided by machine manufacturer to the designer for the design of Turbo Generator foundations.

1. Loading diagram showing magnitude and location of static and dynamic loads exerted by machine on its foundation.
2. Speed of turbine and generator
3. Critical speeds of the machine Critical speed is the angular speed at which the rotating shaft undergoes dynamic instability with increase in lateral amplitude. This develops when the angular speed is in resonance with natural frequency of lateral vibration of shaft. The critical speed concept helps to identify the operational region of rotor bearing system, probable mode shapes and approximate location of peak amplitude.
4. Mass moment of inertia of machine components
5. Drawings showing the embedded parts, openings, grooves for foundation bolts, etc.
6. Piping layout, ducting etc.

Apart from above the following points shall be taken care while designing a turbogenerator foundation:

- The total mass of the frame plus the raft shall not be less than three times the mass of the machine

- The mass of the top deck plus mass of half the length of the column shall not be less than the mass of the supported turbine and its auxiliaries on the top deck. A minimum gap of 25 mm shall be maintained between top deck of turbo generator foundation and floor of turbine building to avoid transfer of vibration to the floor.
- The clear distance in any direction between adjacent foundations and turbo generator foundation shall be large enough to avoid transmission of detrimental vibration amplitudes through the surrounding. Foundation spacing is intended to ensure that the soil response of adjacent foundations is independent as far as possible. A spacing of 2.5 times the width of the smallest foundation is recommended, because the volumes of soil under stress from adjacent foundations will not overlap in that case. In such cases vibration isolation pads are to be installed on the adjacent sides of the foundations to avoid transfer of vibration.
- The stress in the soil due to turbogenerator foundation depends not only on the maximum displacement characterizing the vibration, on the amplitude and frequency, but also on the static pressure to which the soil is subjected. The settlement caused by vibration increases with pressure. Therefore, the pressure permitted must be smaller than that permitted for static load. Hence, the stress induced in soil shall not exceed 50% of the allowable bearing capacity of the soil.

3.4 Sizing of Foundation

1. **Top Deck:** The proportioning of the deck is basically governed by the machine manufacturer's drawing giving the sole plate locations and opening details for the various parts of the machine.
2. **Columns:** The following guidelines may be followed for column sizing:

As far as possible pairs of columns should be provided under each transverse girder

- a) Compressive stresses and elastic shortening should be kept uniform in all the columns as far as possible
- b) **Base Raft:** The bottom of the raft shall not be placed above the level as suggested by the geotechnical consultant where the thickness (t) of the slab shall not be less than, $t = 0.07L^{4/3}$, where L is the average distance between columns.

3.5 Primary Load And Load Combination for Static Analysis

1) Dead load (DL):

Dead load includes self-weight of the foundation and dead weight of machine and its auxiliaries. The weight of machine component are supplied by machine manufacturer.

2) Operation load (OL):

The operation loads supplied by machine manufacturer includes friction forces, torque loads, thermal elongation, vacuum in condenser, piping forces etc

- a) Torque loads Forces due to steam in turbine section impose a torque on the stationary turbine casing in the direction opposite to the direction of rotation of rotor. The turbine manufacturer provides this data.

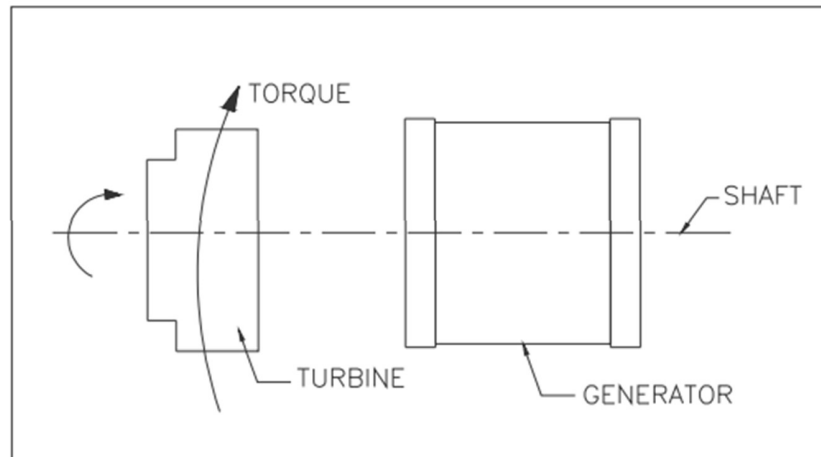


Figure 3.1 Torque due to normal operation

- b) Vacuum in condenser:

In a thermal power plant, the mode of cooling the steam in the turbine is done either by air cooled condenser or water-cooled condenser. Water cooled condenser are mounted on the base raft. Whereas the air-cooled condenser also called ACC is a separate unit outside the T.G building to which the steam is taken through a separate pipe. In case of turbine mounted on TG raft, load due to vacuum in condenser needs to be considered. The pressure on the turbine casing is atmospheric and the pressure in the condenser is below atmospheric pressure. The differential pressure between the turbine casing and the condenser results in a suction or a vacuum load transferred to the deck slab through turbine base plates. The magnitude of the vacuum load is significantly large and may be several times the weight of condenser.

- c) Frictional load

The heat emitted by pipes carrying superheated steam, circulation of steam through turbine casing itself give rise to temperature gradients between foundation components causing additional stress on them. Heat buildup in turbine casing and bed plates induces thermal loading on the foundation. The expansion of casing and base plate of the machine relative to the concrete deck results in frictional loads on the slab.

- 3) **Normal machine unbalance force (NUL):** Imbalance in rotating machinery is the common source of harmonic excitation. The cause of this defect may be due to material

imperfection, tolerances etc. of the rotor leading to centrifugal force in the system and the vibration force is imparted to the bearings as a result of centrifugal forces. Due to unsatisfactory balancing of rotating parts in practice the mass centroid of rotating part does not coincide with center of rotation (refer figure 4). In the course of operation the initial defective balancing may be increased at an alarming rate in consequence of the loosening, corrosion or breakage of the turbine blades. With generators the warming up of the rotor, a displacement of the coils or variation in the material of the rotor may upset the balance. Also, the defects of the lubrication system, deficiency of the packing and uneven warming up rotating parts may cause expansion resulting in vibrations which do not follow simple harmonic motion. But undergo complicated changes just like the centrifugal forces produced by them. This fact is however neglected and all mechanical forces are considered as centrifugal ones. For the computation of dynamic effect, the data of weight of rotating parts & their point of application is necessary.

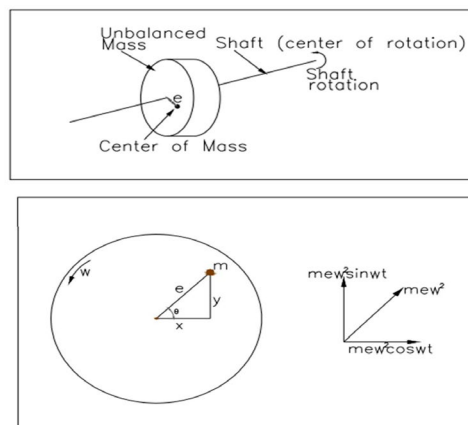


Figure 3.2 Layout of the system

3.6 Representation of the model

The turbogenerator used in our project is represented by this model in Figure 3.3.

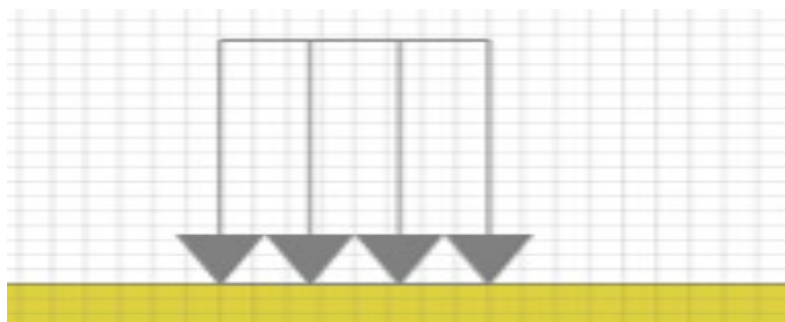


Figure 3.3 Representation of the turbo generator model in Plaxis2D

CHAPTER 4

METHODOLOGY

4.1 Introduction

In this section, the methodology of a model and analysis is discussed in brief.

4.2 Mode of Analysis

In this Chapter, we will model a typical turbogenerator running at a specific frequency on a double storey steel frame structure. The structure is made of structural steel of Fe-415 and is on a M25 concrete block foundation length of 14 m with a height of 10 m.

The underlying soil is a cohesive soil up to 15 m and below layer consists of sand. We take 25 m of sand layer for our analysis. The turbogenerator lies at a distance of 5 m from the steel frame with a height of 2.5 m and width of 5 m respectively running at 50 Hz frequency.

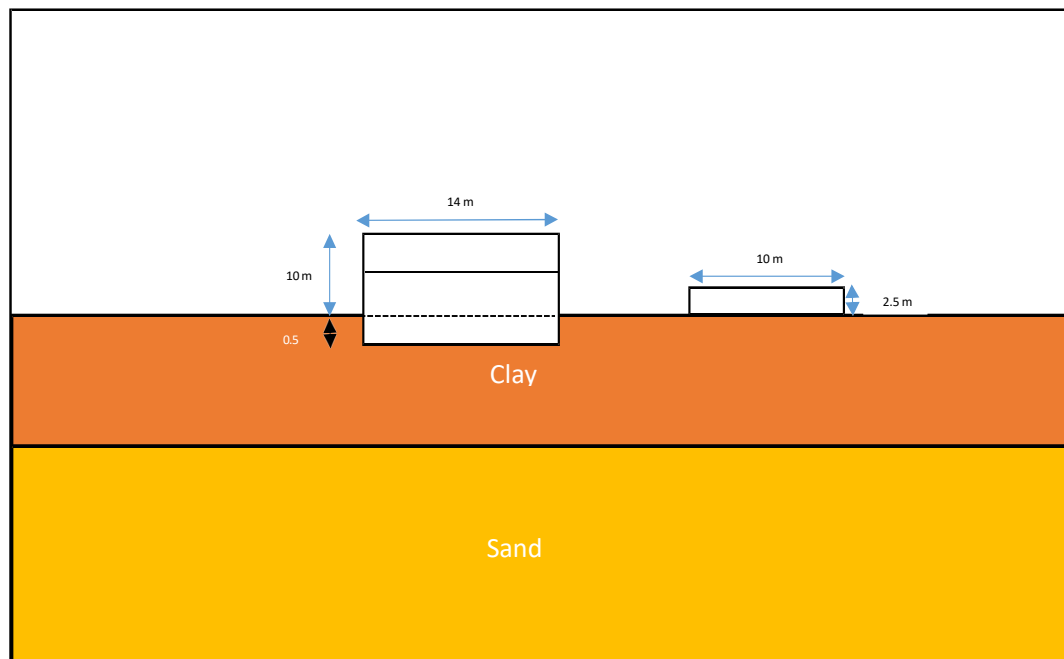


Figure 4.1 Layout of the model made in Plaxis 2D

4.3 Property of Soil

The properties of soil needed to be input into the software, are taken from Appendix C¹ of the APPC manual for Geotechnical Engineers. Namely, the Young's Modulus of soil is taken from Table C.2¹ and the Poisson's Ratio is taken from Table C.4¹ of the Appendix C cited above.¹

4.3.1 Property of Clay Layer

The properties of the clay layer are shown in the table 4.1 below.

Table 4.1: Properties of Clay Layer

Parameter	Name	Value	Unit
General			
Material Model	Model	HS Small	-
Type of Material nature	Type	Drained	-
Soil unit weight (Unsaturated)	γ_{unsat}	16	kN/m ³
Soil Unit Weight (Saturated)	γ_{sat}	20	kN/m ³
Parameters			
Young's Modulus (Constant)	E	2×10^4	kN/m ²
Poisson's Ratio	σ	0.2	-
Initial Conditions			
Cohesion	c	10	-
Friction angle	φ	18	Degrees
Dilatancy angle	ϕ	0	Degrees

4.3.2 Properties of Sand Layer:

The properties of underlying sand layer are shown in the table 4.2 below.

Table 4.2: Properties of Sand Layer

Parameter	Name	Value	Unit
General			
Material Model	Model	HS Small	-
Type of Material nature	Type	Drained	-
Soil unit weight (Unsaturated)	γ_{unsat}	20	kN/m ³
Soil Unit Weight (Saturated)	γ_{sat}	20	kN/m ³
Parameters			
Young's Modulus (Constant)	E	3 x 10 ⁴	kN/m ²
Poisson's Ratio	σ	0.2	-
Initial Conditions			
Cohesion	c	2	-
Friction angle	φ	28	Degrees
Dilatancy angle	ϕ	0	Degrees

4.4 Properties of Structural Steel:

The properties of structural steel is taken from IS 800: 2007 - General Construction In Steel - Code Of Practice (Third Revision).

They are summarized in the table 4.3 below

Table 4.3: Properties of Steel

Parameter	Name	Value	Unit
Material Type	-	Elastic, Isotropic	-
Normal Stiffness	EA	9 x 10 ⁶	kN/m
Flexural Rigidity	EI	6.75 x 10 ⁴	kNm ² /m
Weight	w	10	kN/m/m
Poisson's ratio	V	0.0	

4.5 Properties of foundation concrete:

The footing is assumed to be constructed of M25 Concrete and hence the Modulus of Elasticity (Young's Modulus) is calculated as per Article 6.2.3.1 of IS 456:2000 and can be calculated as :

$$E = 5000\sqrt{25} = 2.5 \times 10^4 \text{ kN/m}^2$$

$$\text{Moment of Inertia of the circular footing} = I = \pi * \frac{R^4}{4} = \pi * \frac{0.5^4}{4} = 0.049$$

$$\text{Area of the Footing will be given by} = A = \pi \times R^2 = \pi \times 0.5^2 = 0.785 \text{ m}^2$$

Putting the above values in the respective formulas of Flexural Rigidity and Stiffness, it was found and tabulated, the said properties of the concrete material as given below.

The concrete is assumed to be Isotropic and elastic in nature for ease.

Table 4.4: Properties of Foundation Concrete

Parameter	Name	Value	Unit
Material Type	Type	Elastic; Isotropic	-
Stiffness	EA	7.6 x 10 ⁶	kN/m
Flexural Rigidity	EI	2.4 x 10 ⁴	kNm ² /m
Weight	W	5.0	kN/m/m
Poisson's Ratio	σ	0.0	-

4.6 Properties of Turbogenerator:

The properties of turbogenerator are taken from standard manual of turbogenerators provided by 'MEIDEN-Alternator JG2000 series' of their standard units and are referred in table 4.5.

Table 4.5: Properties of Turbogenerator

Parameter	Value	Unit
Weight	58	kN
Width	10	M
Height	2.5	M
Frequency	50	Hz

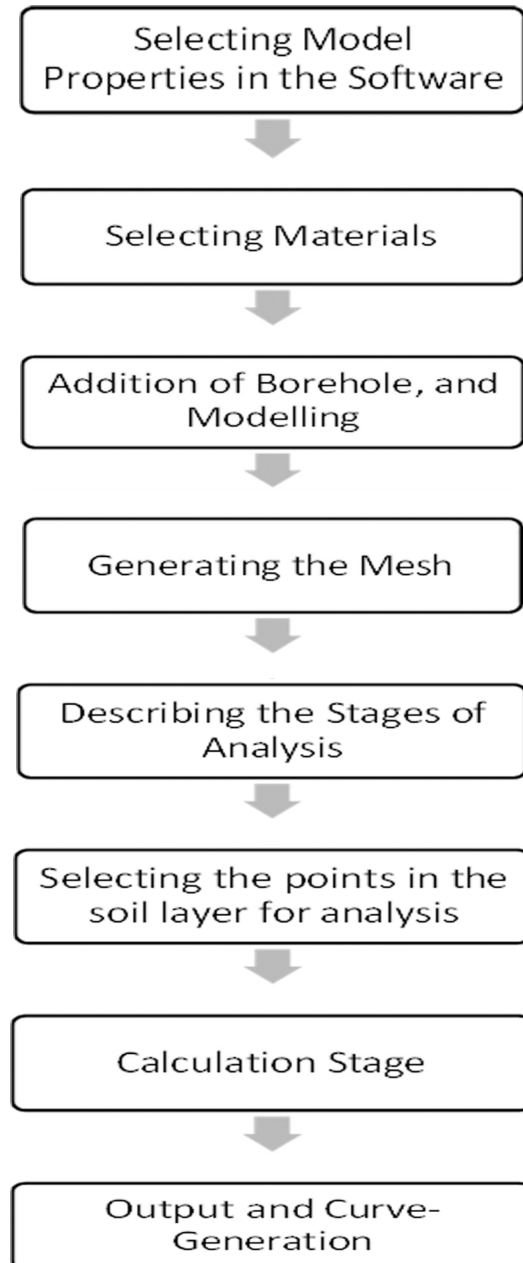
The above data after entering into the software is used there afterwards to construct the model and further our analysis.

CHAPTER 5

PROCEDURE OF ANALYSIS

5.1 Introduction:

This chapter describes about the different tests performed in the software. The following flowchart shows the procedure of software analysis in brief:



5.2 Test Program:

There are basically two main objectives of the test program:

1. To simulate the effect of a turbogenerator running at 50 Hz on a concrete foundation on a nearby steel frame structure and see the variations of displacements of the soil at 3 points.

2. To display the said results via the in-situ curve manager of the software and conclude with stating the stability of the soil concerned at 3 points, namely:
 - a. A point on the surface of the soil.
 - b. A point at the bottom of the steel frame foundation.
 - c. A point at the middle of the clay layer below the steel frame.

Thus, after careful planning the entire test program is divided into four phases as follows:

1. PHASE 1: Without any Load conditions applied.
2. PHASE 2: Taking the self-weight of the frame and generator only, i.e, Live Load + Dead Load.
3. PHASE 3: Starting the Turbo-generator and the vibrations, i.e Live Load + Dead Load + Dynamic Load.
4. PHASE 4: Stopping of the Turbogenerator.

5.3 Procedure

1. The model space of the project with boundary is defined constrains as shown below in Figure 5.1.
 - Axis symmetrical Model is chosen for ease of dynamic load calculations.
 - Model space limits are chosen at a range of 20 m each.
 - S.I. Units are chosen.

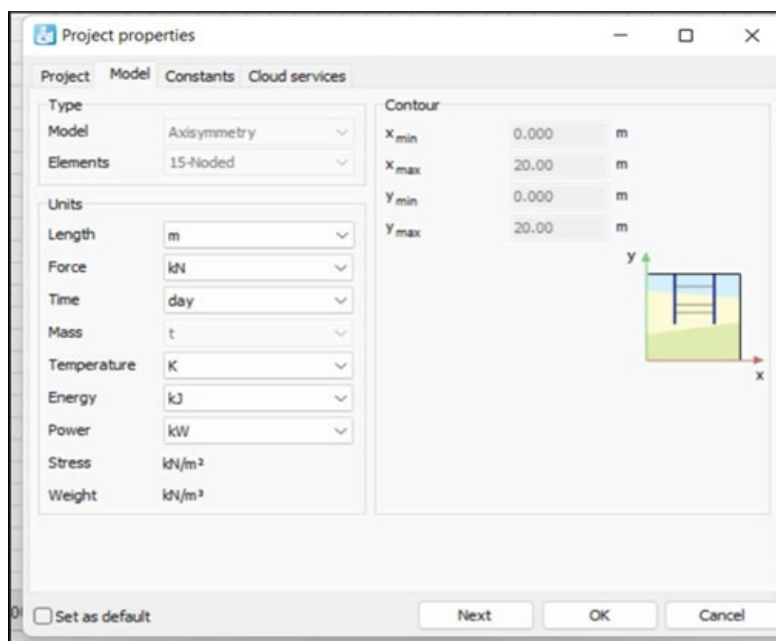


Figure 5.1 Model Properties taken from Plaxis 2D

- The soil material, steel as well as the footing material is defined as per Table 5.1 and Table 5.2, and Table 5.3 respectively.

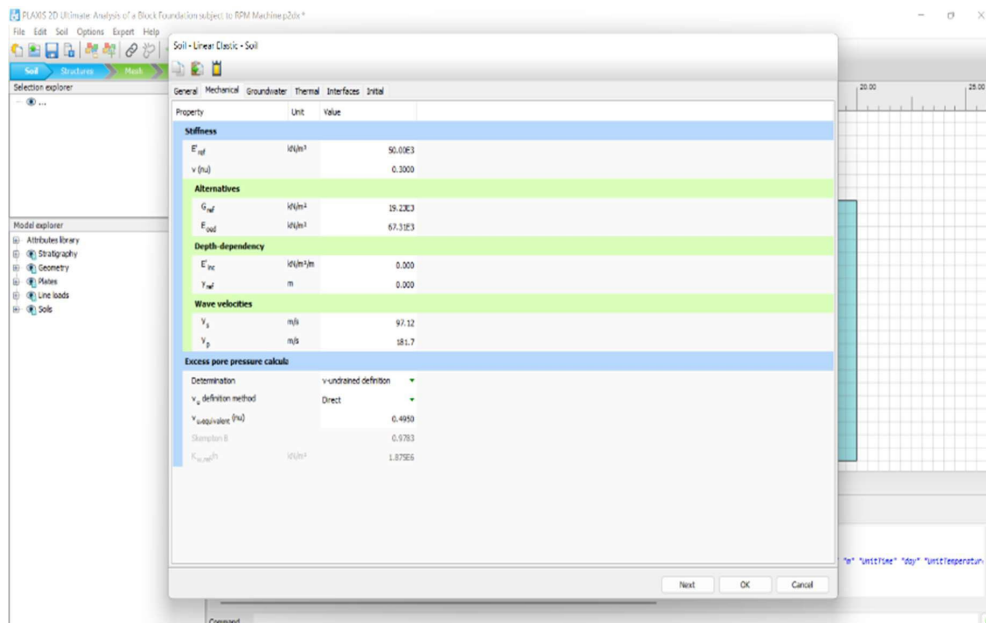


Figure 5.2: Soil and Footing Properties denoted in PLAXIS 2D

- Two boreholes of depth 15 m and 25 m respectively at coordinates (0,0) and (-15,0) are made and the material is set as Clay and Sand respectively which is earlier defined.
- Similarly, a Plate of length 14 m and 10 m is added below which will represent the foundations of the steel frame and the turbo generators which is at 5 m from the frame.
- A Line Load is added to the turbogenerator foundation which will represent the machine and then the model is ready to define the loading conditions for analysis as shown.

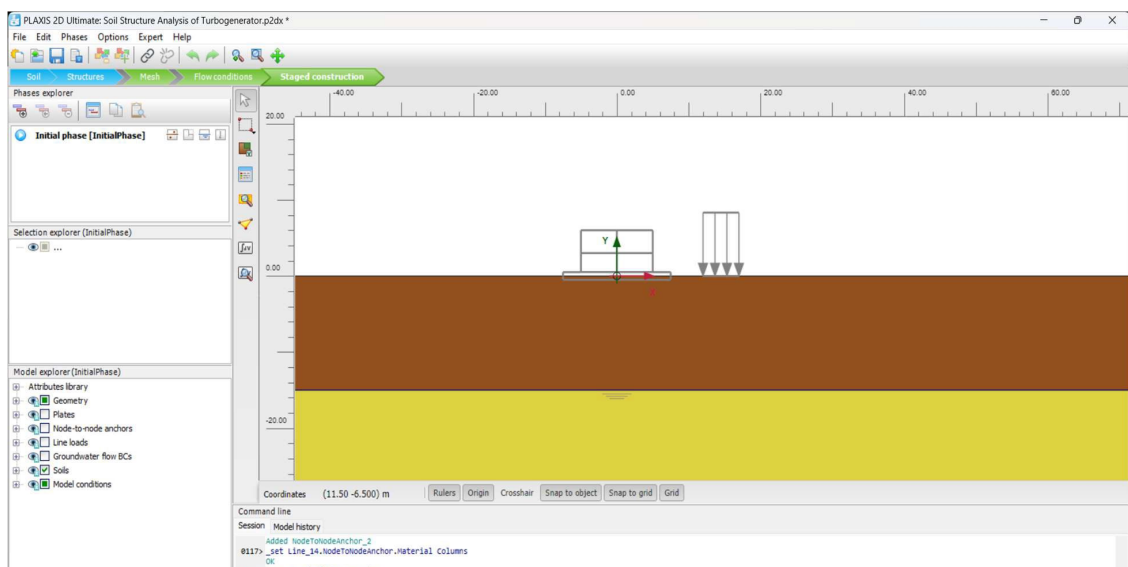


Figure 5.3: Layout of the model made in PLAXIS 2D

6. The mesh is generated and the loading conditions are defined as follows:

- Stage 1: Initial Condition with no loading
- Stage 2: Only Dead Load of Footing is Considered.
- Stage 3: Starting the Turbo Generator.
- Stage 4: Stopping the Turbo generator.

Note: The properties of the Live Load is set as a harmonic motion of weight 5 units with an amplitude of 50 and a frequency of 50 Hz.

7. The Calculations are performed by the software and the results are obtained.

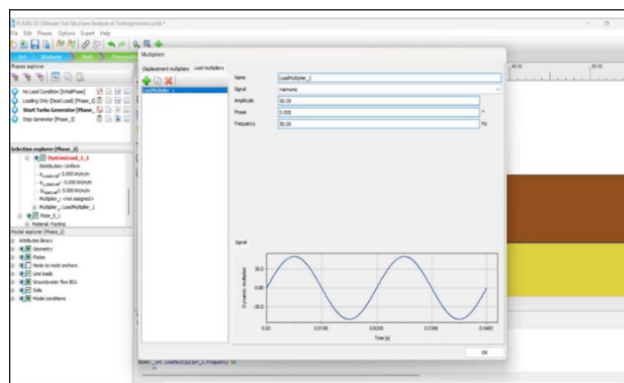


Figure 5.4: Adding the Turbogenerator Frequency in Plaxis 2D

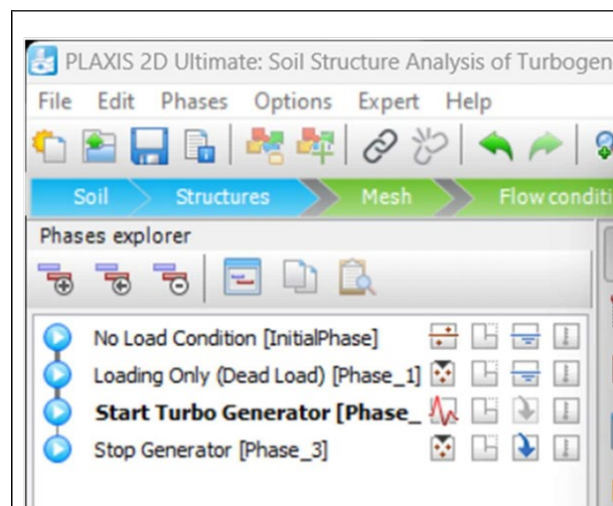


Figure 5.5: The four phases of calculation done in PLAXIS 2D

8. Mesh Generation: After the modelling is done, the mesh is generated as shown below.

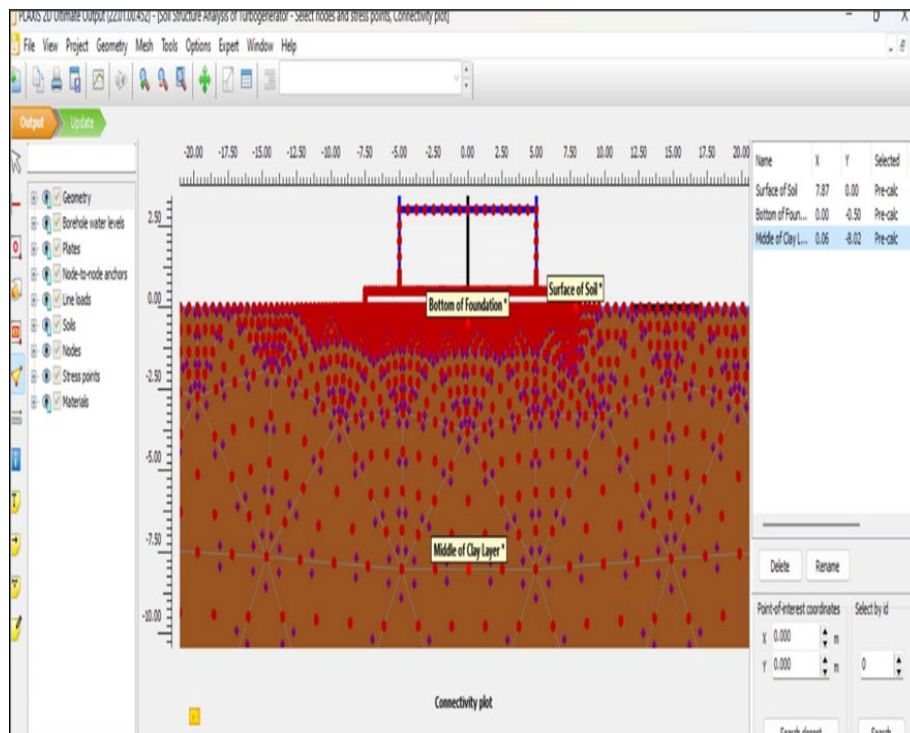


Figure 5.6: Mesh Generation done in PLAXIS 2D

CHAPTER 6

OUTPUT MECHANISM

6.1 Introduction:

In this chapter, it is attempted to understand the mechanism via which the software vis-à-vis PLAXIS 2D displays the results after calculations.

6.2 Calculation Phase:

After the layout is done the software performs the necessary calculations as shown in Figure 6.1.

The time frame is kept as low as 5 seconds to speed up the calculations which may take hours for each node of the mesh.

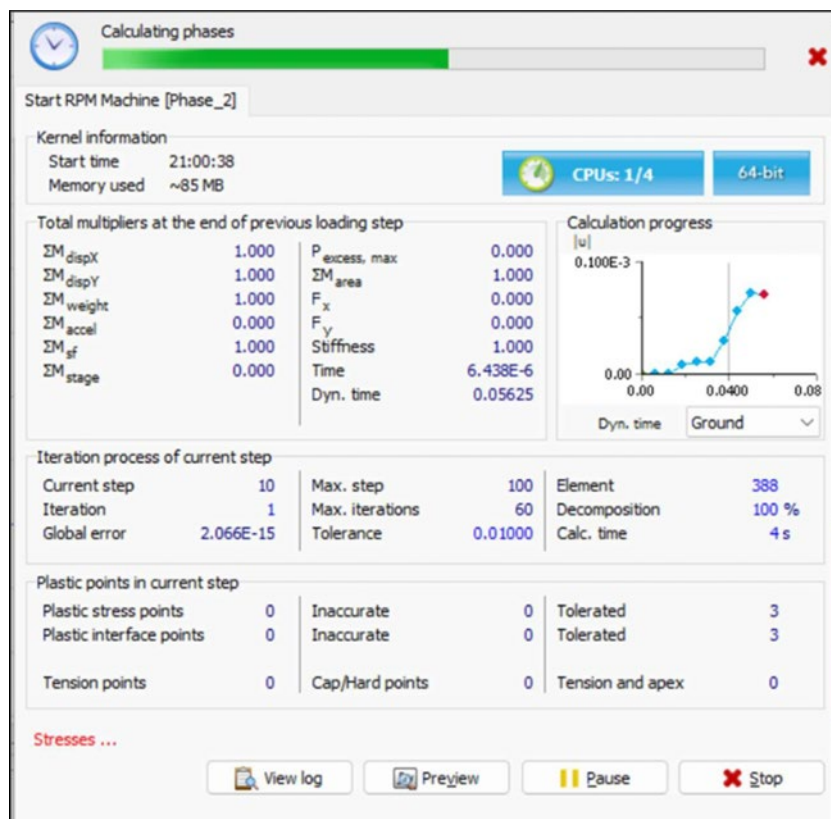


Figure 6.1: Calculation Phase taken in PLAXIS 2D

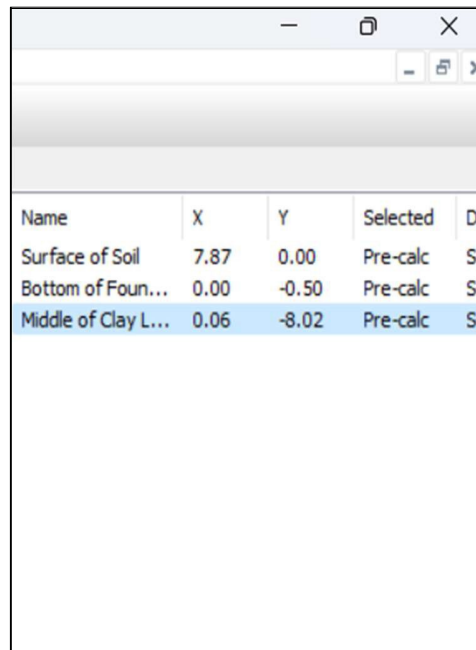
6.3 Output Mesh and Point/Node Selection:

In the mesh formed, the specific points needed for the analysis are chosen.

These points are:

- Point 1: On the surface just below the soil.
- Point 2: Bottom of the steel frame foundation.
- Point 3: Middle of the clay layer.

After selecting the points, the mesh is updated for the final time for results.



Name	X	Y	Selected	Data
Surface of Soil	7.87	0.00	Pre-calc	Sc
Bottom of Foun...	0.00	-0.50	Pre-calc	Sc
Middle of Clay L...	0.06	-8.02	Pre-calc	Sc

Figure 6.2: Selection of nodes/points in the output section of PLAXIS 2D

6.4 The Curve Generator:

While PLAXIS 2D provides an array of tools for analysis, it was aimed to provide the results in a graphical and user-friendly manner. For this purpose, the help of the inbuilt Curve Generator provided to us by the software was taken.

The curve manager is a tool that allows us to display various factors of analysis in the form of graphs.

The factors include but are not limited to:

1. Total Displacements.
2. Total Acceleration
3. Dynamic Time
4. Total Strain
5. Total Velocity
6. Pore Pressure
7. Groundwater Flow
8. Force

After selecting the parameters, the Curve Generator displays the required Graph along with relevant scale and legend as required.

For our analysis, it was aimed to display the results in the form of Time v/s Total Vertical Displacement graphs.

The two points are selected separately for the results.

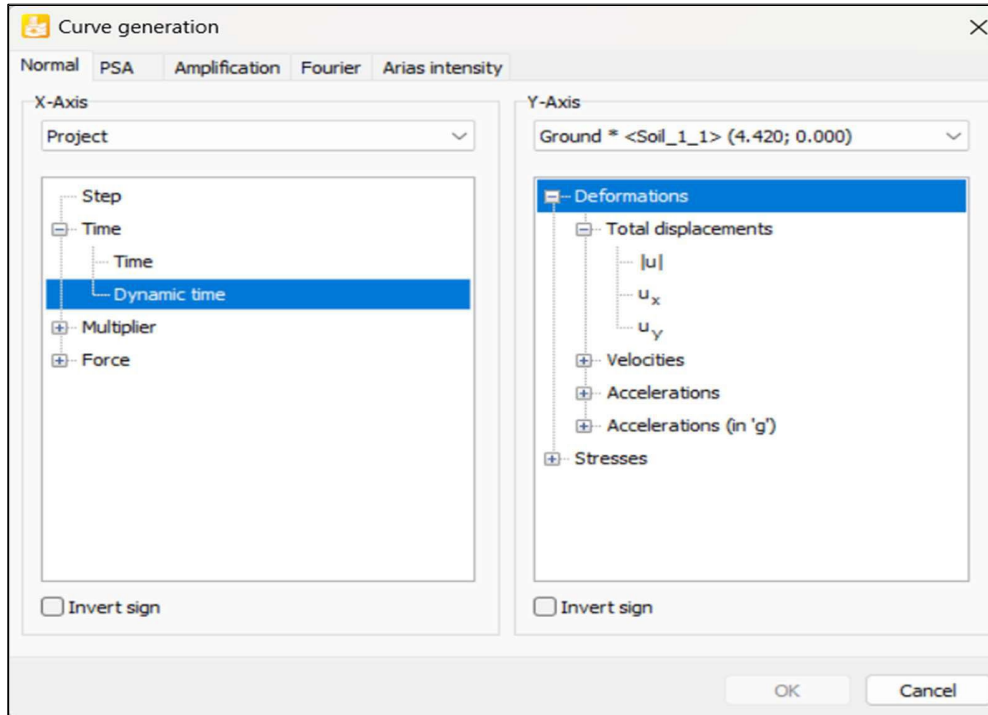


Figure 6.3: The Curve Generator inbuilt in PLAXIS 2D

6.5 Results

Plotting the graph between Dynamic Time and Total Displacement in the vertical direction, the following curves for each phase are obtained.

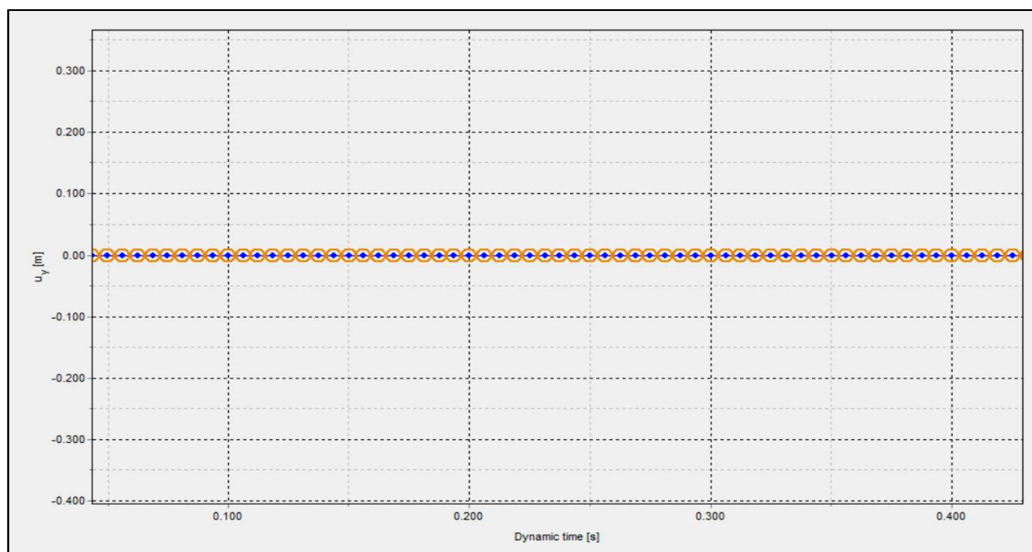


Figure 6.4: Result obtained by considering the dead loading phase in the turbogenerator in PLAXIS 2D

Inference: As expected there is no significant displacement in the soil.

The result is same for all points under consideration as is expected with minimal to no displacements in the vertical direction.

6.6 Results after starting of the Turbogenerator:

6.6.1 Point on the surface of soil:

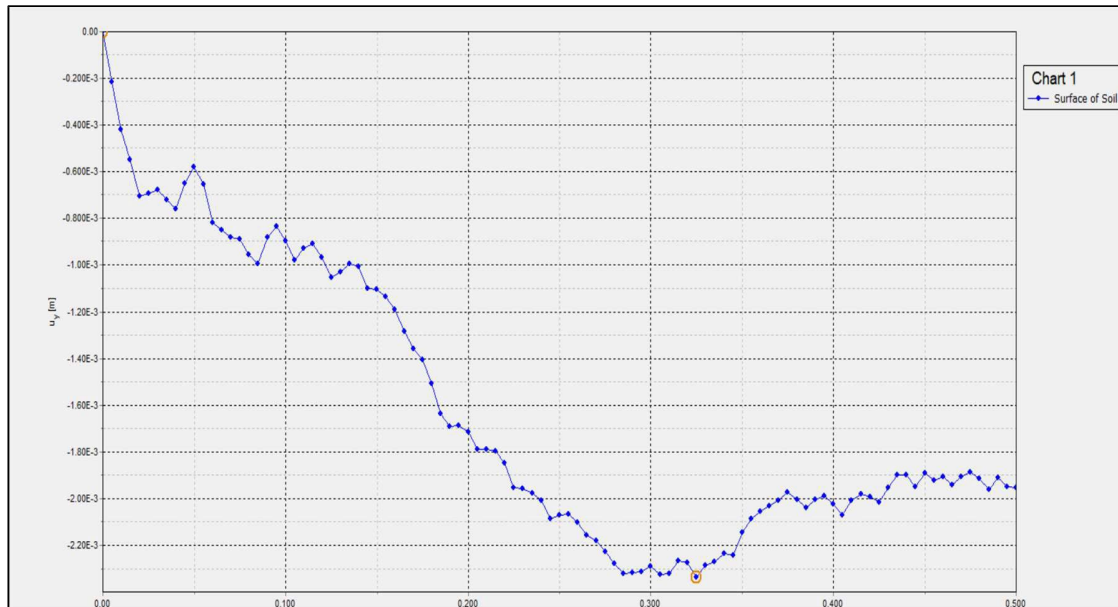


Figure 6.5: Phase 2: On surface of soil

Inference: There is a sharp deformation in the soil in the vertical direction with a maximum value of 2.25×10^{-3} m in the soil and the mesh is deformed.

The surface of the soil therefore is expected to be deformed severely at the start of the operation.

6.6.2 At the bottom of the steel frame foundation

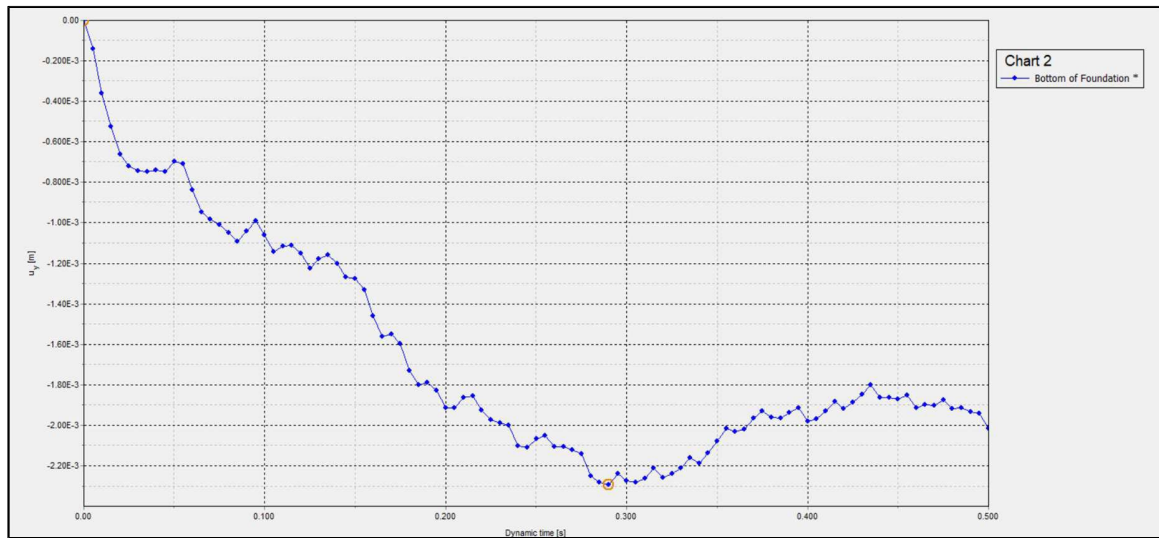


Figure 6.6: Phase 2: At the bottom of the steel foundation.

Inference: There are significant deformations with a peak value of around 2.2×10^{-3} m. Though the deformations are similar in pattern with that of the surface of the soil layer.

6.6.3 At the middle of the clay layer

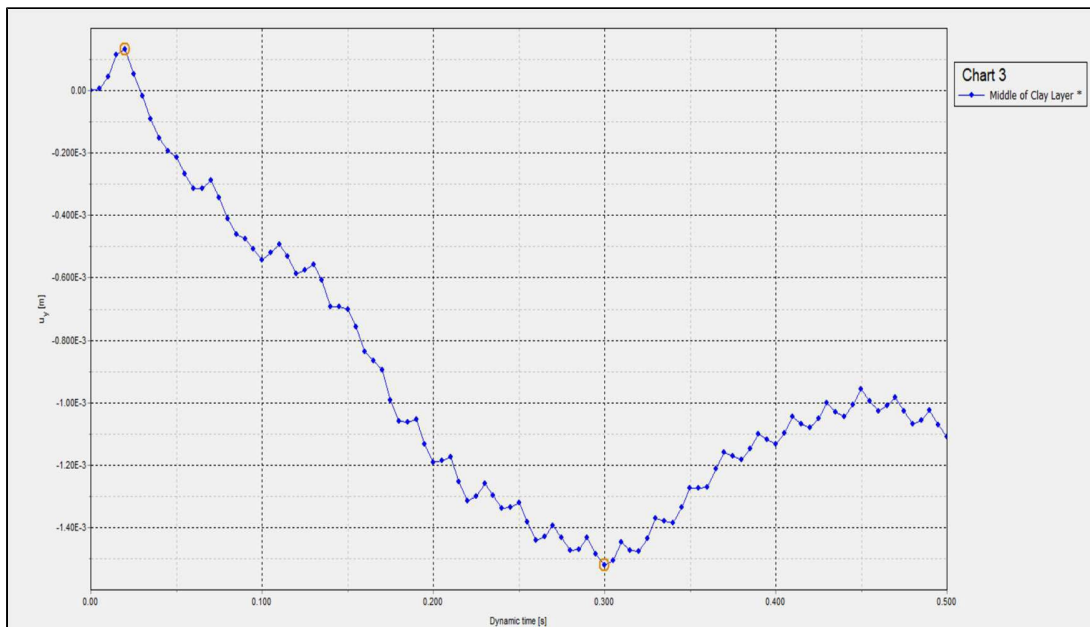


Figure 6.7: Phase 2: At the middle of the clay layer.

Inference: While the pattern remains, same there is a comparatively less value of deformation at the end of the operation with a value of about 1.45×10^{-3} m in the vertical direction.

CHAPTER 7

EFFECT OF SOIL PARAMETERS

7.1 Introduction

Bearing capacity of both topsoil and subsoil layers would to a great extent controls the foundation selection. For low bearing capacity soil, stronger and suitable foundation is selected compared to where the soil has more bearing capacity. Bearing capacity and the settlement are the two important parameters in the field of geotechnical engineering. Finite element analysis has been used by different investigators in conjunction with plasticity theory, to predict bearing capacity of footings. Many investigators attributed the beneficial changes in properties of soil and increase in the load carrying capacity of the soil by various methods like compaction, preloading, grouting, densification using vibratory equipment, using in situ reinforcement, using geotextiles, chemical stabilization etc.

7.2 Generalized discussion of the effects on bearing capacity of soil.

- The important parameters which govern the bearing capacity of soil are cohesion, unit weight of soil, depth of proposed foundation, width of foundation and angle of internal friction.
- In case of local shear failure, the values of ultimate bearing capacity determined for circular and square shaped footings are found to be higher than strip and rectangular footings. This trend is different for non-cohesive soil.
- The effect of water table correction on safe bearing capacity is predominant for non-cohesive soil. Safe bearing capacity of non-cohesive soil is reduced to about 50% when water table may reach up to ground level.

7.3 Generalized discussion of the effects on settlement of soil.

- Soil Type: Different soil types exhibit varying settlement behaviours. For instance:
 - Cohesive soil: These soils tend to experience more consolidation settlement over time due to their low permeability. The process of consolidation can lead to gradual settlement as water is squeezed out from the soil.
 - Cohesionless soil: These soils may experience immediate settlement upon the load application but generally have higher bearing capacities compared to cohesive soils.
- Soil Compaction: The degree of compaction of the soil beneath the foundation is vital. Proper compaction is essential to reduce settlement caused by soil compression. Insufficient compaction can lead to uneven settlement and potential foundation failure.
- Soil Moisture Content: Moisture content affects soil volume and its ability to support loads. Changes in moisture content can lead to soil expansion or contraction, causing differential settlement, which is undesirable for the foundation.

- **Shear Strength:** The shear strength of soil determines its resistance to deformation under lateral loads. A higher shear strength can help reduce lateral settlement and potential tilting of the foundation.
- **Groundwater Level:** The depth of the groundwater table can impact the soil's strength and stability. High groundwater levels can reduce the effective stress in the soil, potentially causing additional settlement.

7.4 Different soil parameters used in Plaxis 2D

PLAXIS 2D is a widely used finite element analysis (FEA) software for geotechnical engineering applications. In PLAXIS 2D, various soil parameters are used to define the mechanical behaviour of the soil and analyse the response of geotechnical structures. Some of the essential soil parameters used in this software include:

1. **Soil Type and Material Models:** PLAXIS 2D supports various soil material models to represent different soil types, including linear elastic, Mohr-Coulomb, Hardening Soil, Soft Soil, and Hardening Soil Small-Strain models, among others. These material models define how the soil responds to stress and strain.
2. **Elastic Modulus (E):** The elastic modulus represents the stiffness of the soil. It is used in linear elastic material models to describe the stress-strain behaviour of the soil within the elastic range.
3. **Poisson's Ratio (ν):** Poisson's ratio is a dimensionless parameter that defines the lateral strain response of the soil concerning axial strain. It is used in linear elastic material models.
4. **Strength Parameters:** For Mohr-Coulomb and Hardening Soil models, the key strength parameters are:
 - Cohesion (c): The cohesion intercept of the Mohr-Coulomb failure envelope.
 - Friction Angle (ϕ): The angle of internal friction of the soil, defining the slope of the Mohr-Coulomb failure envelope.
5. **Young's Modulus at Small Strains (E50):** For Hardening Soil Small-Strain model, the small-strain stiffness of the soil is represented by E50.
6. **Small Strain Stiffness (G0):** In the Hardening Soil Small-Strain model, G0 is used to define the initial stiffness at small strains.
7. **Plasticity Parameters:** For Soft Soil and Hardening Soil models, additional parameters are used to define the plastic behaviour of the soil, such as the yield stress and the plastic modulus.
8. **Creep Parameters:** In Soft Soil and Hardening Soil models, parameters such as the time characteristic, the viscous coefficient, and the ageing parameter are used to define the creep behaviour of the soil.

9. **Groundwater Parameters:** PLAXIS 2D allows users to define hydrostatic or non-hydrostatic pore pressure distributions within the soil to simulate the effect of groundwater.
10. **Initial Stress State:** The initial stress state, including initial vertical effective stress and horizontal stresses, is essential for the analysis of geotechnical problems.

These soil parameters are crucial in accurately modelling the behaviour of the soil and predicting the response of geotechnical structures under various loading conditions in PLAXIS 2D. It is essential to calibrate these parameters based on laboratory tests, field measurements, or empirical correlations to obtain reliable and realistic simulation results.

7.5 Effects of soil parameters on model.

PLAXIS 2D, soil parameters play a significant role in determining the behavior of geotechnical structures and the response of the soil under various loading conditions. The effects of different soil parameters in PLAXIS 2D can be observed in several ways:

1. **Deformation and Settlement:** The choice of soil parameters, such as elastic modulus and Poisson's ratio, affects the deformation and settlement of the soil and the structure. Stiffer soils will experience less settlement and deformation under the same load compared to softer soils.
2. **Shear Strength and Stability:** Soil parameters like cohesion and friction angle directly influence the shear strength of the soil. The Mohr-Coulomb and Hardening Soil models use these parameters to define the failure envelope. A lower cohesion or higher friction angle can lead to reduced stability and increased potential for slope failure or bearing capacity issues.
3. **Plastic Behavior and Creep:** For Soft Soil and Hardening Soil models, plasticity parameters control the plastic behavior and creep of the soil. These parameters determine how the soil will undergo permanent deformation under sustained loads or cyclic loading conditions.
4. **Foundation Bearing Capacity:** The bearing capacity of a foundation is significantly influenced by the soil parameters used in the analysis. Properly calibrated cohesion, friction angle, and other strength parameters are essential for accurate bearing capacity predictions.
5. **Earth Pressure and Retaining Wall Design:** In PLAXIS 2D, the soil parameters affect the lateral earth pressure exerted on retaining walls and other structures. Accurate representation of soil properties is crucial for reliable retaining wall design.
6. **Slope Stability Analysis:** Soil parameters have a direct impact on slope stability analysis. By correctly defining the shear strength parameters, engineers can assess the safety factor of slopes and evaluate potential failure mechanisms.
7. **Settlement and Consolidation:** Soil parameters like initial vertical effective stress, consolidation coefficient, and compressibility influence the consolidation settlement

behavior of cohesive soils. Proper modeling of these parameters is essential for predicting long-term settlement.

8. Groundwater Flow and Pore Pressure: The effects of groundwater on the stability and deformation of structures can be analyzed by specifying appropriate groundwater parameters in PLAXIS 2D. These parameters include hydraulic conductivity, initial pore pressure, and drainage conditions.

9. Dynamic Analysis: Soil parameters also impact the response of the soil and structures under dynamic loading conditions, such as earthquakes or machine vibrations. Accurate representation of soil properties is crucial for reliable dynamic analysis.

The accuracy and reliability of PLAXIS 2D simulations depend on the proper calibration of soil parameters. These parameters are obtained through laboratory testing, in-situ testing, or based on well-established correlations.

CHAPTER 8

DEFINED SOIL STEEL AND TURBOGENERATOR PROPERTIES

8.1 Introduction

Defined soil and steel properties are taken down from various renowned research journals as stated below. The standard dimensions and multiple vibration ranges of the turbo generator is taken from the 'MEIDEN-Alternator JG2000 series.'

8.2 Young's Modulus of Soil:

Soil Young's modulus (E), commonly referred to as soil elastic modulus, is an elastic soil parameter and a measure of soil stiffness. It is defined as the ratio of the stress along an axis over the strain along that axis in the range of elastic soil behaviour. The elastic modulus is often used for estimation of soil settlement and elastic deformation analysis.

Soil elastic modulus can be estimated from laboratory or in-situ tests or based on correlation with other soil properties. In laboratory, it can be determined from triaxial test or indirectly from oedometer test. On field, it can be estimated from *Standard penetration test*, *Cone penetration test*, *pressure meter* or *indirectly from dilatometer test*.

8.2.1 Typical values of Young's modulus for granular material (MPa) (based on Obrzud & Truty 2012 complied from Kezdi 1974 and Prat et al. 1995):

USCS	Description	Loose	Medium	Dense
GW,SW	Gravels/Sand well graded	30-80	80-160	160-320
SP	Sand, Uniform	10-30	30-50	50-80
GM, SM	Sand, Gravel Silty	7-12	12-20	20-30

8.2.2 Typical values of Young's modulus for cohesive material (MPa) (based on Obrzud & Truty 2012 compiled from Kezdi 1974 and Prat et al. 1995):

USCS	Description	Very soft to soft	Medium	Stiff to very Stiff	Hard
ML	Silts with Slight plasticity	2.5-8	10-15	15-40	40-80
ML,CL	Silts with low plasticity	1.5-6	6-10	10-30	30-60
CL	Clays with low-medium plasticity	0.5-5	5-8	8-30	30-70
CH	Clays with high plasticity	0.35-4	4-7	7-20	20-32
OL	Organic Silts	-	0.5-5	-	-
OH	Organic Clays	-	0.5-4	-	-

8.3 Angle of friction:

Soil friction angle is a shear strength parameter of soils. Its definition is derived from the Mohr-Coulomb failure criterion and it is used to describe the friction shear resistance of soils together with the normal effective stress. Soil friction angle is a shear strength parameter of soils. Its definition is derived from the Mohr-Coulomb failure criterion and it is used to describe the friction shear resistance of soils together with the normal effective stress.

In the stress plane of Shear stress-effective normal stress, the soil friction angle is the angle of inclination with respect to the horizontal axis of the Mohr-Coulomb shear resistance line.

8.3.1 Typical values of soil friction angle [°]:

USCS	Description	Min	Max	Specific Value
GW	Well graded gravel, sandy gravel, with little or no fines	33	40	
GP	Poorly graded gravel, sandy gravel, with little or no fines	32	44	

GW, GP	Sandy gravels – Loose			35
GW,GP	Sandy gravels – Loose			50
GM	Silty gravels, silty sandy gravels	30	40	
GC	Clayey gravels, clayey sandy gravels	28	35	
SW	Well graded sands, gravelly sands, with little or no fines	33	43	
SW	Well-graded clean sand, gravelly sands – Compacted			38
SW	Well-graded sand, angular grains – Loose			33
SW	Well-graded sand, angular grains – Dense			45
SP	Poorly graded sands, gravelly sands, with little or no fines	30	39	
SP	Poorly-graded clean sand – Compacted			37
SP	Uniform sand, round grains – Loose			27
SP	Uniform sand, round grains – Dense			34
SW, SP	Sand	37	38	
SW, SP	Loose sand	29	30	
SW, SP	Medium sand	30	36	
SW, SP	Dense sand	36	41	
SM	Silty sands	32	35	
SM	Silty clays, sand-silt mix - Compacted			34
SM	Silty sand - Loose	27	33	

SM	Silty sand - Dense	30	34	
SC	Clayey sands	30	40	
SC	Clayey sands, sandy-clay mix - compacted			31
SM,SC	Loamy sand, sandy clay Loam	31	34	
ML	Inorganic silts, silty or clayey fine sands, with slight plasticity	27	41	
ML	Inorganic silt - Loose	27	30	
ML	Inorganic silt - Dense	30	35	
CL	Inorganic clays, silty clays, sandy clays of low plasticity	27	35	
CL	Clays of low plasticity - compacted			28
OL	Organic silts and organic silty clays of low plasticity	22	32	
MH	Inorganic silts of high plasticity	23	33	
MH	Clayey silts - compacted			25
ML	Silts and clayey silts - compacted			32
CH	Inorganic clays of high plasticity	17	31	
CH	Clays of high plasticity - compacted			19
OH	Organic clays of high plasticity	17	35	
ML, OL, MH, OH	Loam	28	32	
ML, OL, MH, OH	Silt Loam	25	32	
ML, OL, CL, MH, OH, CH	Clay Loam, Silty Clay Loam	18	32	

OL, CL, OH, CH	Silty clay	18	32	
CL, CH, OH, OL	Clay	18	28	
Pt	Peat and other highly organic soils	0	10	

8.3.2 Correlation between SPT-N value, friction angle, and relative density:

SPT N ₃ [Blows/0.3 m - 1 ft]	Soil packing	Relative Density [%]	Friction angle [°]
<4	Very loose	< 20	<30
4-10	Loose	20-40	30-35
10-30	Compact	40-60	35-40
30-50	Dense	60-80	40-45
>50	Very Dense	> 80	>45

8.4 Cohesion:

The cohesion is a term used in describing the shear strength soils. Its definition is mainly derived from the Mohr-Coulomb failure criterion and it is used to describe the non-frictional part of the shear resistance which is independent of the normal stress. In the stress plane of Shear stress-effective normal stress, the soil cohesion is the intercept on the shear axis of the Mohr-Coulomb shear resistance line

8.4.1 Typical values of soil cohesion for different soils [kPa]:

Description	USCS	min	max	Specific value
Well graded gravel, sandy gravel, with little or no fines	GW	-	-	0
Poorly graded gravel, sandy gravel, with little or no fines	GP	-	-	0
Silty gravels, silty sandy gravels	GM	-	-	0
Clayey gravels, clayey sandy gravels	GC	-	-	20

Well graded sands, gravelly sands, with little or no fines	SW	-	-	0
Poorly graded sands, gravelly sands, with little or no fines	SP	-	-	0
Silty sands	SM	-	-	22
Silty sands - Saturated compacted	SM	-	-	50
Silty sands - Compacted	SM	-	-	20
Clayey sands	SC	-	-	5
Clayey sands - Compacted	SC	-	-	74
Clayey sands -Saturated compacted	SC	-	-	11
Loamy sand, sandy clay Loam – compacted	SM, SC	50	75	
Loamy sand, sandy clay Loam – saturated	SM, SC	10	20	
Sand silt clay with slightly plastic fines - compacted	SM, SC	-	-	50
Sand silt clay with slightly plastic fines - saturated compacted	SM, SC	-	-	14
Inorganic silts, silty or clayey fine sands, with slight plasticity	ML	-	-	7
Inorganic silts and clayey silts – compacted	ML	-	-	67
Inorganic silts and clayey silts - saturated compacted	ML	-	-	9
Inorganic clays, silty clays, sandy clays of low plasticity	CL	-	-	4
Inorganic clays, silty clays, sandy clays of low plasticity – compacted	CL	-	-	86
Inorganic clays, silty clays, sandy clays of low plasticity - saturated compacted	CL	-	-	13

Mixture if inorganic silt and clay – compacted	ML-CL	-	-	65
Mixture if inorganic silt and clay - saturated compacted	ML-CL	-	-	22
Organic silts and organic silty clays of low plasticity	OL	-	-	5
Inorganic silts of high plasticity - compactd	MH	-	-	10
Inorganic silts of high plasticity - saturated compacted	MH	-	-	72
Inorganic silts of high plasticity	MH	-	-	20
Inorganic clays of high plasticity	CH	-	-	25
Inorganic clays of high plasticity – compacted	CH	-	-	103
Inorganic clays of high plasticity - saturated compacted	CH	-	-	11
Organic clays of high plasticity	OH	-	-	10
Loam – Compacted	ML, OL, MH, OH	60	90	
Loam – Saturated	ML, OL, MH, OH	10	20	
Silt Loam – Compacted	ML, OL, MH, OH	60	90	
Silt Loam – Saturated	ML, OL, MH, OH	10	20	
Clay Loam, Silty Clay Loam – Compacted	ML, OL, CL, MH, OH, CH	60	105	
Clay Loam, Silty Clay Loam – Saturated	ML, OL, CL, MH, OH, CH	10	20	
Silty clay, clay - compacted	OL, CL, OH, CH	90	105	
Silty clay, clay - saturated	OL, CL, OH, CH	10	20	
Peat and other highly organic soils	Pt	-	-	

8.5 Dry unit weight:

Soil unit weight, as referred to as specific weight, is the weight per unit volume of soil. It may refer to

- Wet unit weight: Unit weight of the soil when the pore are fully or partially filled with water.
- Dry unit weight: Unit weight of the soil the pores are filled only with air without any water.

$$\gamma_d = \frac{\gamma}{(1+w)}$$

Where:

γ_d : dry unit weight

γ : unit weight

w : soil water content.

8.5.1 Typical values of soil cohesion for different soils (kN/m³):

USCS	Description	Average value (kN/m ³)
GW	Well graded gravel, sandy gravel, with little or no fines	21 ± 1
GP	Poorly graded gravel, sandy gravel, with little or no fines	20.5 ± 1
GM	Silty gravels, silty sandy gravels	21.5 ± 1
GC	Clayey gravels, clayey sandy gravels	19.5 ± 1.5
SW	Well graded sands, gravelly sands, with little or no fines	20.5 ± 2
SP	Poorly graded sands, gravelly sands, with little or no fines	19.5 ± 2
SM	Silty sands	20.5 ± 2.5
SC	Clayey sands	18.5 ± 1.5
ML	Inorganic silts, silty or clayey fine sands, with slight plasticity	
CL	Inorganic clays, silty clays, sandy clays of low plasticity	

OL	Organic silts and organic silty clays of low plasticity	
MH	Inorganic silts of high plasticity	
CH	Inorganic clays of high plasticity	
OH	Organic clays of high plasticity	
Pt	Peat and other highly organic soils	

8.6 Soil bearing capacity:

Allowable bearing capacity: The maximum pressure that can be applied to the soil from the foundation so that the two requirements are satisfied:

Acceptable safety factor against shear failure below the foundation

Acceptable total and differential settlement

Ultimate bearing capacity: The minimum pressure that would cause the shear failure of the supporting soil immediately below and adjacent to the foundation.

8.6.1 Typical values of soil bearing capacity (kPa):

Soil type	Bearing value (kPa)	Remarks
Dense gravel or dense sand and gravel	> 600	Width of foundation not less than 1 m. Water table at least at the depth equal to the width of foundation, below base of foundation.
Dense dense gravel or medium dense sand and gravel	200-600	-
Loose gravel or loose sand and gravel	< 200	-
Compact sand	> 300	-
Medium dense sand	100 - 300	-
Very stiff boulder clays and hard clays	300 - 600	Susceptible to long term consolidation settlement
Stiff clays	150 - 300	-
Firm clays	75 -150	-

Soft clays and silts	< 75	-
Very soft clays and silts	-	-

8.7 Soil permeability coefficient:

The soil permeability is a measure indicating the capacity of the soil or rock to allow fluids to pass through it. It is often represented by the permeability coefficient (k) through the Darcy's equation:

$$V=ki$$

Where v is the apparent fluid velocity through the medium i is the hydraulic gradient, and K is the coefficient of permeability (hydraulic conductivity) often expressed in m/s

K depends on the relative permeability of the medium for fluid constituent (often water) and the dynamic viscosity of the fluid as follows.

$$k = \frac{\gamma_w * K}{\eta}$$

Where γ_w is the unit weight of water η is the dynamic viscosity of water K is an absolute coefficient depending on the characteristics of the medium (m²)

The permeability coefficient can be determined in the laboratory using falling head permeability test, and constant head permeability test. On the field, the permeability can be estimated using Lugeon test.

8.7.1 Typical values of soil permeability:

Description	USCS	min (m/s)	max (m/s)	Specific value (m/s)
Well graded gravel, sandy gravel, with little or no fines	GW	5.00E-04	5.00E-02	
Poorly graded gravel, sandy gravel, with little or no fines	GP	5.00E-04	5.00E-02	
Silty gravels, silty sandy gravels	GM	5.00E-08	5.00E-06	
Alluvial sand and gravel	(GM)	4.00E-04	4.00E-03	

Clayey gravels, clayey sandy gravels	GC	5.00E-09	5.00E-06	
Well graded sands, gravelly sands, with little or no fines	SW	1.00E-08	1.00E-06	
Very fine sand, very well sorted	(SW)			8.40E-05
Medium sand, very well sorted	(SW)			2.23E-03
Coarse sand, very well sorted	(SW)			3.69E-01
Poorly graded sands, gravelly sands, with little or no fines	SP	2.55E-05	5.35E-04	
Clean sands (good aquifers)	(SP-SW)	1.00E-05	1.00E-02	
Uniform sand and gravel	(SP-GP)	4.00E-03	4.00E-01	
Well graded sand and gravel without fines	(GW-SW)	4.00E-05	4.00E-03	
Silty sands	SM	1.00E-08	5.00E-06	
Clayey sands	SC	5.50E-09	5.50E-06	
Inorganic silts, silty or clayey fine sands, with slight plasticity	ML	5.00E-09	1.00E-06	
Inorganic clays, silty clays, sandy clays of low plasticity	CL	5.00E-10	5.00E-08	
Organic silts and organic silty clays of low plasticity	OL	5.00E-09	1.00E-07	
Inorganic silts of high plasticity	MH	1.00E-10	5.00E-08	
Inorganic clays of high plasticity	CH	1.00E-10	1.00E-07	
Compacted silt	(ML-MH)	7.00E-10	7.00E-08	
Compacted clay	(CL-CH)	-	1.00E-09	

Organic clays of high plasticity	OH	5.00E-10	1.00E-07	
Peat and other highly organic soils	Pt	-	-	

8.8 Soil porosity:

Soil void ratio (e) is the ratio of the volume of voids to the volume of solids:

$$e = \frac{V_v}{V_s}$$

Where V_v is the volume of the voids (empty or filled with fluid), and V_s is the volume of solids.

Void ratio is usually used in parallel with soil porosity (n), which is defined as the ratio of the volume of voids to the total volume of the soil. The porosity and the void ratio are inter-related as follows:

$$e = \frac{n}{1-n} \text{ and } n = \frac{e}{1+e}$$

The value of void ratio depends on the consistence and packing of the soil. It is directly affected by compaction. Some typical values of void ratio for different soils are given below only as general guidelines.

8.8.1 Typical values of soil void ratio for different soils:

Description	USCS	min	max	Specific value
Well graded gravel, sandy gravel, with little or no fines	GW	0.26	0.46	
Poorly graded gravel, sandy gravel, with little or no fines	GP	0.26	0.46	
Silty gravels, silty sandy gravels	GM	0.18	0.28	
Gravel	(GW-GP)	0.30	0.60	
Clayey gravels, clayey sandy gravels	GC	0.21	0.37	
Glatial till, very mixed grained	(GC)	-	-	0.25

Well graded sands, gravelly sands, with little or no fines	SW	0.29	0.74	
Coarse sand	(SW)	0.35	0.75	
Fine sand	(SW)	0.40	0.85	
Poorly graded sands, gravelly sands, with little or no fines	SP	0.30	0.75	
Silty sands	SM	0.33	0.98	
Clayey sands	SC	0.17	0.59	
Inorganic silts, silty or clayey fine sands, with slight plasticity	ML	0.26	1.28	
Uniform inorganic silt	(ML)	0.40	1.10	
Inorganic clays, silty clays, sandy clays of low plasticity	CL	0.41	0.69	
Organic silts and organic silty clays of low plasticity	OL	0.74	2.26	
Silty or sandy clay	(CL-OL)	0.25	1.80	
Inorganic silts of high plasticity	MH	1.14	2.10	
Inorganic clays of high plasticity	CH	0.63	1.45	
Soft glacial clay	-	-	-	1.20
Stiff glacial clay	-	-	-	0.60
Organic clays of high plasticity	OH	1.06	3.34	
Soft slightly organic clay	(OH-OL)	-	-	1.90
Peat and other highly organic soils	Pt	-	-	
soft very organic clay	(Pt)	-	-	3.00

8.9 Void ratio:

Soil void ratio (e) is the ratio of the volume of voids to the volume of solids:

$$e = \frac{V_v}{V_s}$$

Where V_v is the volume of the voids (empty or filled with fluid), and V_s is the volume of solids.

Void ratio is usually used in parallel with soil porosity (n), which is defined as the ratio of the volume of voids to the total volume of the soil. The porosity and the void ratio are inter-related as follows:

$$e = \frac{n}{1-n} \text{ and } n = \frac{e}{1+e}$$

The value of void ratio depends on the consistence and packing of the soil. It is directly affected by compaction. Some typical values of void ratio for different soils are given below only as general guidelines.

8.9.1 Typical values of soil void ratio for different soils:

Description	USCS	min	max	Specific value
Well graded gravel, sandy gravel, with little or no fines	GW	0.26	0.46	
Poorly graded gravel, sandy gravel, with little or no fines	GP	0.26	0.46	
Silty gravels, silty sandy gravels	GM	0.18	0.28	
Gravel	(GW-GP)	0.30	0.60	
Clayey gravels, clayey sandy gravels	GC	0.21	0.37	
Glacial till, very mixed grained	(GC)	-	-	0.25
Well graded sands, gravelly sands, with little or no fines	SW	0.29	0.74	
Coarse sand	(SW)	0.35	0.75	
Fine sand	(SW)	0.40	0.85	
Poorly graded sands, gravelly sands, with little or no fines	SP	0.30	0.75	
Silty sands	SM	0.33	0.98	
Clayey sands	SC	0.17	0.59	

Inorganic silts, silty or clayey fine sands, with slight plasticity	ML	0.26	1.28	
Uniform inorganic silt	(ML)	0.40	1.10	
Inorganic clays, silty clays, sandy clays of low plasticity	CL	0.41	0.69	
Organic silts and organic silty clays of low plasticity	OL	0.74	2.26	
Silty or sandy clay	(CL-OL)	0.25	1.80	
Inorganic silts of high plasticity	MH	1.14	2.10	
Inorganic clays of high plasticity	CH	0.63	1.45	
Soft glacial clay	-	-	-	1.20
Stiff glacial clay	-	-	-	0.60
Organic clays of high plasticity	OH	1.06	3.34	
Soft slightly organic clay	(OH-OL)	-	-	1.90
Peat and other highly organic soils	Pt	-	-	
soft very organic clay	(Pt)	-	-	3.00

Definition of steel properties used

8.10 Young's Modulus of Steel:

Young's modulus (E) is a fundamental mechanical property of steel that measures its stiffness and elasticity. It represents the ratio of stress to strain within the elastic range of steel behaviour. Young's modulus is crucial for estimating the deformation and structural response of steel components.

8.10.1 The typical values of Young's modulus for different types of steel (GPa):

Steel Type	Young's Modulus (GPa)
Carbon Steel	200-220
Stainless Steel	190-210
Tool Steel	200-230
High-Speed Steel	200-240
Alloy Steel	190-210
Low-Alloy Steel	200-220
Spring Steel	210-240
Structural Steel	190-210
Cast Steel	160-180

8.11 Turbo generator proportions

Standard Dimension Table of Gas Turbine Driven Alternators

Table 8.1: Standard Dimension Table of Prime Rating (3300V, 6600V)

Output (kVA)		Dimensions (mm)								Mass (kg)	
50 (Hz)	60 (Hz)	L	A	B	D	M	I	C	IE		
-	250	1505	625	705	625	670	745	224	90	280M	950
250	300									280L	950
300	400									280LL	1030
400	500	1625	685	765	725	720	800	250	115	315S	1240
500	625									315M	1340
625	750	1665	660	780	805	805	900	300	105	355S	1650
750	875	1835	745	865						355M	1810
875	1000									355X	2000
1000	1250	1975	780	910	910	845	940	350	105	400M	2330
1250	1500									400L	2540
1500	2000	2205	870	1030	975	950	1085	400	90	450S	3400
2000	2500	2225								450M	3770
2500	3000	2285	870	1030	1115	1100	1185	450	110	500S	4610
3000	3500									500M	4920
3500	4000	2410	950	1080	1260	1260	1355	500	135	560SS	6600
4000	4500									560S	7150
4500	5000	2650	1055	1210	1260	1260	1355	500	135	560M	7900
5000	-									560L	8500

These properties are taken from the company’s journal “MEIDEN-Alternator JG2000 series”

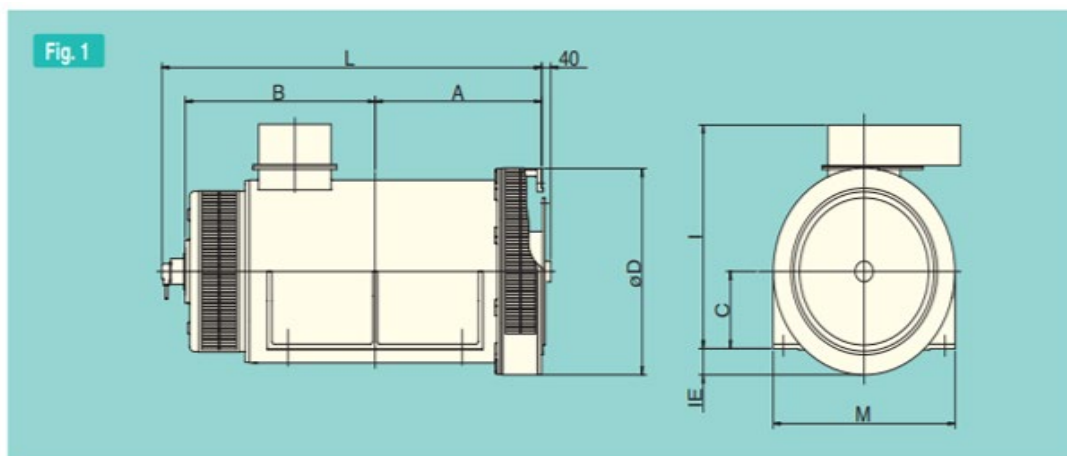


Figure 8.1: Model of the generator as taken from the company journal

CHAPTER 9

SOIL MODELS OF PLAXIS 2D

9.1 Introduction

In PLAXIS 2D, various soil models are available to represent the mechanical behaviour of different types of soil under different loading conditions. These soil models allow to attain the response of soils and analyse the behaviour of geotechnical structures. Each soil model in PLAXIS 2D has its strengths and limitations, for this project emphasis on Hardening soil model is given. In this chapter various soil models are also described along with their applications and limitations.

9.2 Description of different types of models

9.2.1 CONCRETE MODEL

The concrete material model represents the mechanical behaviour of concrete elements in geotechnical structures. The concrete material model allows to simulate the response of concrete elements such as piles, diaphragm walls, or other structural components interacting with the surrounding soil. The concrete material model is essential for the analysis and design of geotechnical structures where the behaviour of concrete is a critical factor.

9.2.2 Importance of Concrete Modeling

Concrete is a crucial material in many geotechnical projects such as foundations, retaining walls, and tunnels. Accurate modeling of concrete behavior is essential for assessing structural performance and ensuring safety.

9.2.3 Features of the Concrete Model

1. **Linear Elastic Behaviour:** The concrete model assumes linear elastic behaviour under small strains, allowing for accurate representation of elastic deformation in concrete elements.
2. **Tension Cut-off:** Concrete is generally not considered to carry tensile stresses in geotechnical applications. The concrete model in PLAXIS 2D incorporates a tension cut-off to prevent the generation of tensile stresses in the concrete elements. This ensures realistic modelling of concrete behaviour, especially in situations where cracking may occur.
3. **Cracking and Stiffness Reduction:** When subjected to high tensile stresses, concrete can undergo cracking. The concrete model in PLAXIS 2D incorporates stiffness reduction after cracking to reflect the nonlinear behaviour of cracked concrete. This feature enables to assess the effects of cracking on the structural integrity of concrete elements.
4. **Concrete Strength Properties:** Engineers can define the concrete's compressive strength, tensile strength, and other relevant properties to accurately represent

its resistance to axial and bending stresses. This allows for precise simulation of concrete behaviour in different loading scenarios.

5. **Hardening:** The concrete model includes the option for strain hardening, which allows to capture the material's increased strength after cracking. This feature is particularly significant in reinforced concrete structures, where strain hardening can influence the overall structural response.
6. **Element Types:** PLAXIS 2D offers various element types suitable for modelling concrete elements, such as beams, piles, and diaphragm walls. These element types are specifically designed to represent the behaviour of concrete structures accurately.
7. **Material Anisotropy:** The concrete model supports material anisotropy, allowing engineers to account for different mechanical properties in different directions, which is relevant for concrete elements with complex geometries or reinforcement layouts.
8. **Time-Dependent Behaviour:** The concrete model in PLAXIS 2D can incorporate time-dependent behaviour, enabling engineers to analyse long-term effects, such as creep and shrinkage, in concrete elements.
9. **Nonlinear Analysis:** The concrete model is compatible with nonlinear analysis in PLAXIS 2D, allowing engineers to explore the response of concrete structures under large deformations and complex loading conditions.

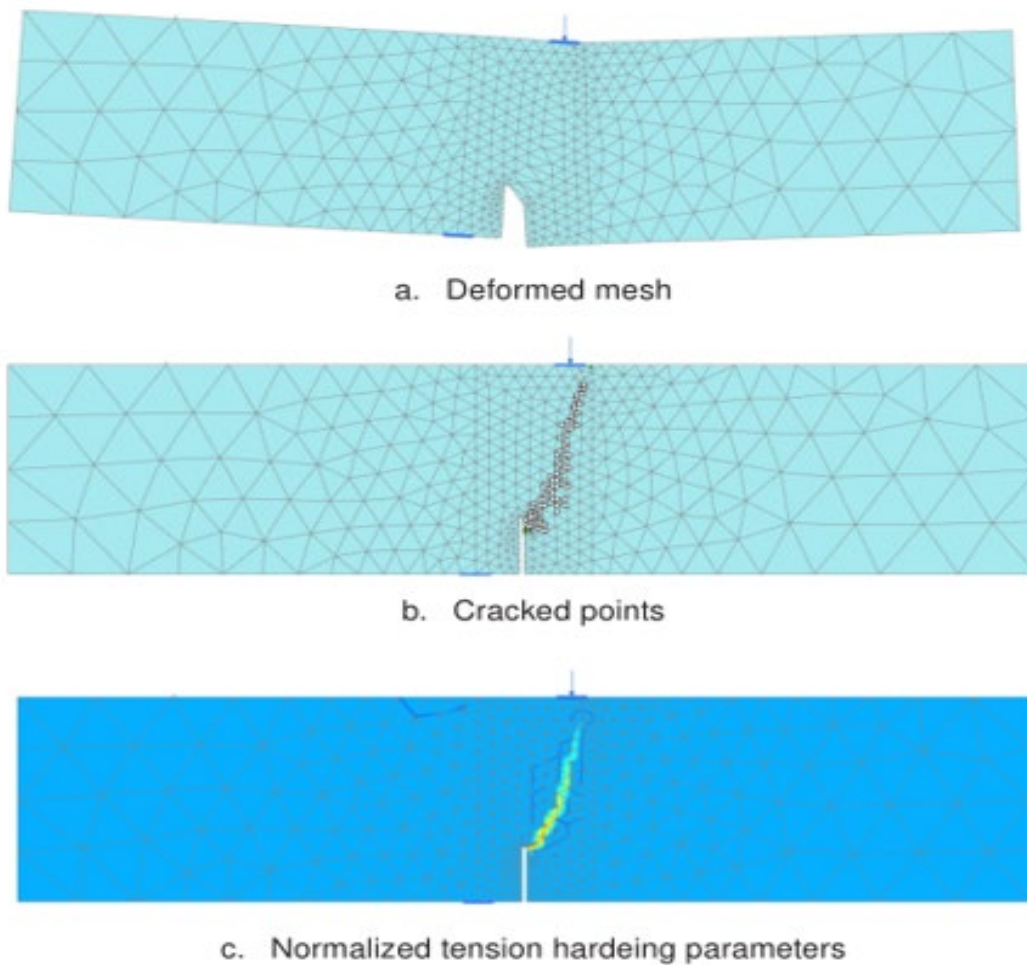


Figure 9.1: Analysed concrete model in PLAXIS 2D

(https://communities.bentley.com/cfs-file/__key/communityserver-wikis-components-files/00-00-00-01-05/Use_5F00_of_5F00_ShotCrete_5F00_UDSM_5F00_notchedbeammixedfracturemode_5F00_abc.png)

9.3 Applications of Concrete Model

- Foundation design
- Retaining wall design
- Tunnel analysis

The concrete modeling capabilities of Plaxis 2D provide engineers with a powerful tool for analyzing and designing geotechnical structures involving concrete. Accurate representation of concrete behavior allows for improved decision-making, enhanced safety, and optimized designs in various geotechnical projects.

9.4 MOHR-COLUMB MODEL

The Mohr-Coulomb model is a widely used soil model to simulate the mechanical behaviour of both cohesive and granular soils. The Mohr-Coulomb model is a linearly elastic-perfectly plastic model that represents the shear strength and stress-strain relationship of the soil.

9.4.1 Importance of Mohr-Columb Model

The Mohr-Coulomb model is extensively used to represent the behavior of soils and rocks in geotechnical engineering. It allows to analyze and predict the response of these materials under different loading and boundary conditions.

9.4.2 Features of the Mohr-Columb Model

1. **Stress-Strain Relationship:** The Mohr-Coulomb model follows a linear stress-strain relationship under small-strain conditions, allowing for accurate representation of the soil elastic behaviour.
2. **Yield Surface:** The Mohr-Coulomb model is defined by a yield surface, represented by a linear equation in the deviatoric stress space. The yield surface defines the limit beyond which the soil starts to undergo plastic deformation.
3. **Cohesion (c):** The cohesion parameter represents the intercept of the yield surface on the deviatoric stress axis. It reflects the soil's shear strength in the absence of normal stress.
4. **Friction Angle (ϕ):** The friction angle parameter defines the slope of the yield surface and represents the shear strength increase with increasing normal stress. It characterizes the internal friction of the soil.
5. **Plasticity Condition:** When the stress state exceeds the yield surface, the soil undergoes plastic deformation. PLAXIS 2D automatically switches from the elastic to the plastic behaviour when the plasticity condition is satisfied.
6. **Plastic Flow Rule:** Once the soil is in the plastic state, it follows a plastic flow rule, ensuring that the stress state remains on the yield surface. This rule governs the redistribution of stresses during plastic deformation.
7. **Hardening and Softening:** The Mohr-Coulomb model in PLAXIS 2D allows for both hardening i.e., increasing shear strength with plastic deformation and softening i.e. decreasing shear strength with plastic deformation behaviours, enabling simulation of soil behaviour under different loading conditions.
8. **Dilation:** The Mohr-Coulomb model allows for dilation, which means the volume expansion of soil during shearing. This characteristic is essential for capturing the behaviour of granular soils.
9. **Time-Dependent Behaviour:** Although the Mohr-Coulomb model is primarily a static model, it can be combined with time-dependent components to simulate time-dependent soil behaviour, such as creep and consolidation.

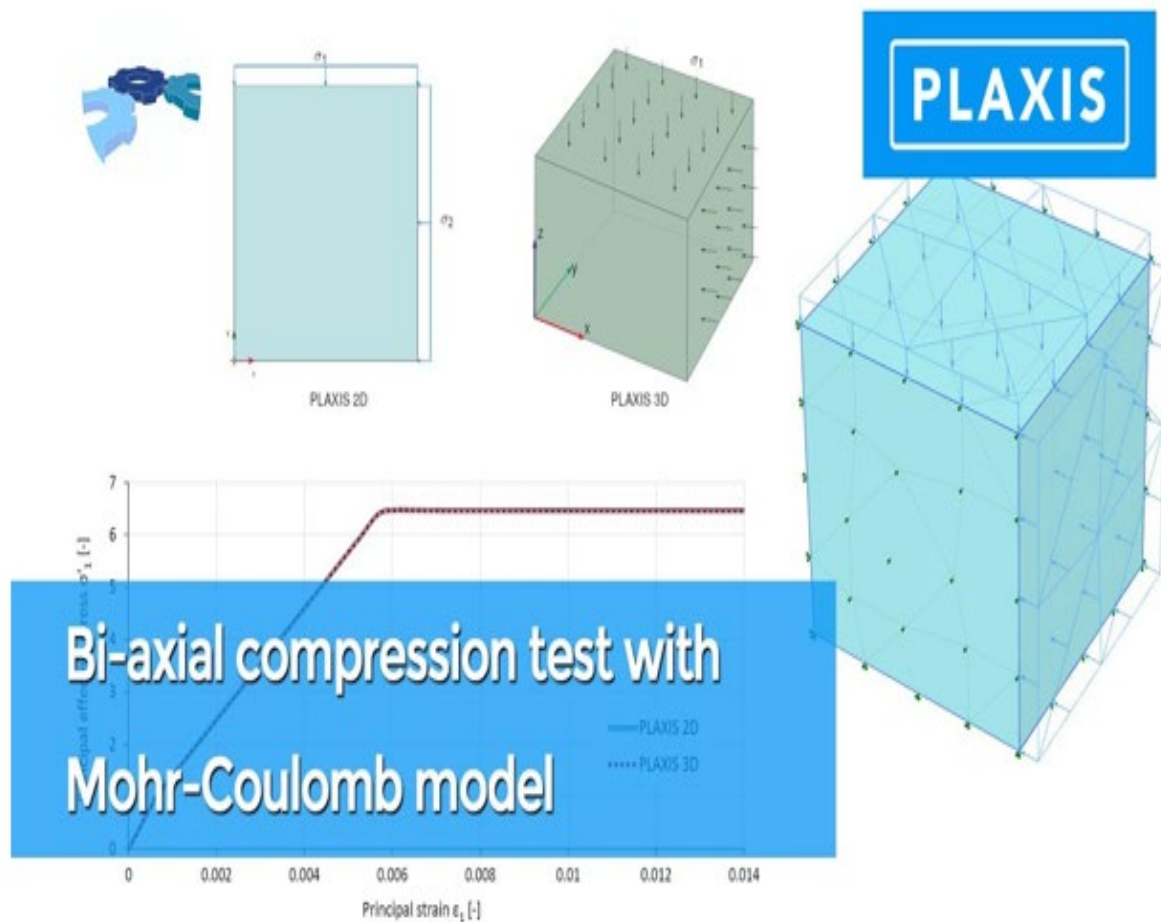


Figure 9.2: Mohr-Coulomb Model in PLAXIS 2D

(<https://i.ytimg.com/vi/m46rPeuQjX8/sddefault.jpg>)

9.5 Applications of the Mohr-Coulomb Model

- Slope stability analysis
- Excavation and retaining wall design
- Foundation design

The Mohr-Coulomb model in Plaxis 2D offers engineers a powerful tool for simulating the behavior of soils and rocks in geotechnical projects. By accurately representing the shear strength and frictional behavior, it enables engineers to make informed decisions, optimize designs, and ensure the stability and safety of various geotechnical structures.

9.6 HARDENING SOIL MODEL

The Hardening Soil model is an advanced constitutive model used to simulate the mechanical behaviour of soils under various loading conditions. The Hardening Soil model is an extension of the Mohr-Coulomb model and is particularly suitable for

performing dynamic analysis. This particular model is specifically used for performing all the analysis of the project as of the dynamic emphasis.

9.6.1 Importance of Soil Hardening Model

The soil hardening model is essential for capturing the nonlinear behavior of soils under cyclic loading conditions. It enables engineers to analyze and predict the response of soils subjected to repeated loading, such as in earthquake or cyclic loading scenarios.

9.6.2 Features of Soil Hardening Model

1. **Nonlinear Stress-Strain Relationship:** The Hardening Soil model represents a non-linear stress-strain relationship to capture the soil behaviour beyond its yield point.
2. **Stress-Dependent Parameters:** The Hardening Soil model parameters, such as cohesion, friction angle, and hardening modulus, are stress-dependent. This means that these parameters can vary with the stress state of the soil, providing a more realistic representation of the soil behaviour under different loading conditions.
3. **Plastic Hardening:** The model incorporates plastic hardening to represent the increase in shear strength with plastic deformation. This characteristic is particularly relevant for modelling clays and clay-like soils, which exhibit strain-hardening behaviour.
4. **Plastic Flow Rule:** The Hardening Soil model uses a plastic flow rule to ensure that the stress state remains on the yield surface during plastic deformation. The model accurately represents the stress redistribution during plasticity.
5. **Critical State Soil Mechanics:** The Hardening Soil model is based on critical state soil mechanics principles, which provide a sound theoretical framework for modelling the soil mechanical behaviour. This enhances the model's ability to simulate soil response under complex loading conditions.
6. **Volume Change:** The Hardening Soil model can capture volume change behaviour, such as dilation or compression, during shearing. This feature is essential for accurately modelling the behaviour of cohesive soils.
7. **Time-Dependent Behaviour:** The Hardening Soil model can be combined with time-dependent components to simulate time-dependent soil behaviour, such as creep and consolidation. This makes it suitable for long-term geotechnical analyses.

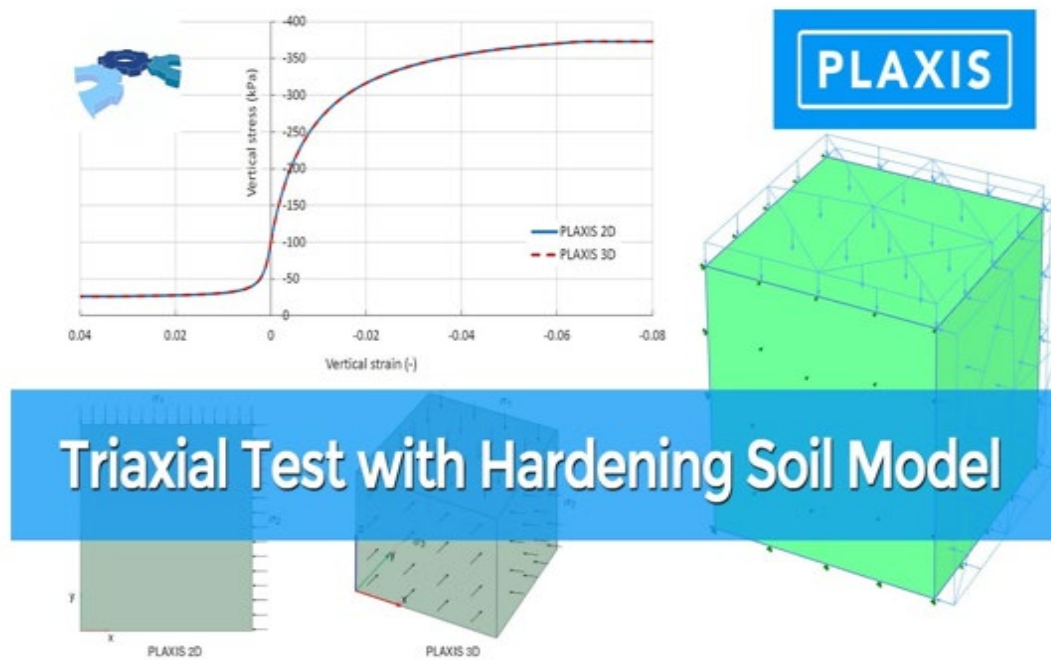


Figure 9.3: Hardening Soil Model in Plaxis 2D

(<https://i.ytimg.com/vi/mm8wCn35ggk/sddefault.jpg>)

Applications of soil hardening model

- Seismic Analysis
- Embankment Design
- Dynamic Pile analysis

The soil hardening model in Plaxis 2D provides engineers with a valuable tool for analyzing and predicting the behavior of soils under cyclic loading conditions. By accurately capturing the stiffness evolution and strain accumulation, it enables engineers to assess stability, optimize designs, and ensure the performance of geotechnical structures in seismic and cyclic loading scenarios.

CHAPTER 10

DISPLACEMENT ANALYSIS ON VARIOUS TYPES OF SOIL

10.1 Introduction

Displacement analysis is a fundamental aspect of geotechnical engineering, which allows to predict and understand the behavior of different types of soil under various loading conditions. This report aims to investigate and compare the displacement behavior of different soil types, cohesive soils (clay), cohesionless soil (sand), and a two layered soil through numerical simulations using finite element analysis (FEA) software i.e. PLAXIS 2D.

10.2 Methodology

To perform the displacement analysis, numerical simulations were carried out using PLAXIS 2D, a widely used finite element analysis software for geotechnical applications. The numerical models were developed based on field-tested soil parameters, ensuring the accuracy and reliability of the results.

10.3 Different models prepared for performing the analysis

10.3.1 Cohesionless Soil i.e., clay.

Cohesionless soils, are characterized by their high permeability and low cohesion.

- Brief description of the system:** The effect of a typical turbo generator running at a specific frequency on a double storey steel frame structure is analyzed. The structure is made of structural steel of Fe-415 and is on a M25 concrete block foundation length of 14 m with a height of 10 m. The underlying soil is a 40 m of sand layer is taken for analysis. The turbo generator lies at a distance of 5 m from the steel frame with a height of 2.5 m and width of 5 m respectively running at 50 Hz frequency.

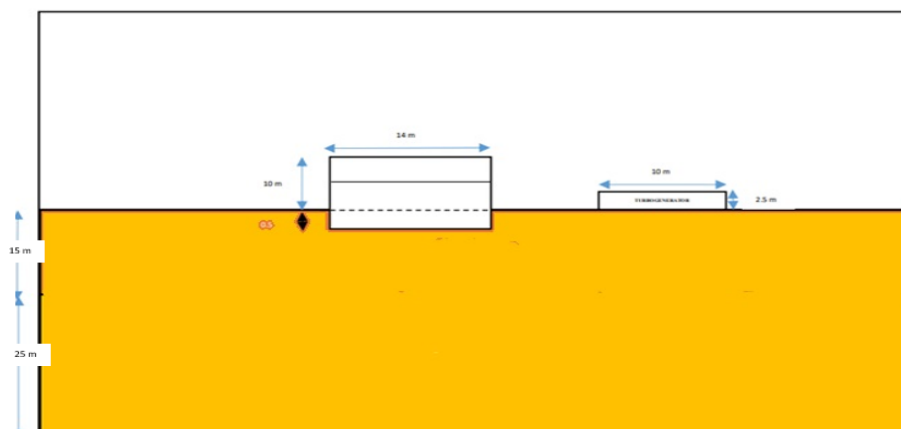


Figure 10.1: Layout of the model

The properties of underlying sand layer are shown in the table below.

Table 10.1: Properties of Sand Layer

Parameter	Name	Value	Unit
General			
Material Model	Model	HS Small	-
Type of Material nature	Type	Drained	-
Soil unit weight (Unsaturated)	γ_{unsat}	20	kN/m ³
Soil Unit Weight (Saturated)	γ_{sat}	20	kN/m ³
Parameters			
Young's Modulus (Constant)	E	3 x 10 ⁴	kN/m ²
Poisson's Ratio	σ	0.2	-
Initial Conditions			
Cohesion	c	2	-
Friction angle	φ	28	Degrees
Dilatancy angle	ϕ	0	Degrees

These properties will be further put into the software, vis-à-vis PLAXIS 2D

The properties of steel and the turbogenerator are taken from CHAPTER. So, putting our model through displacement analysis we can obtain a generated mesh.

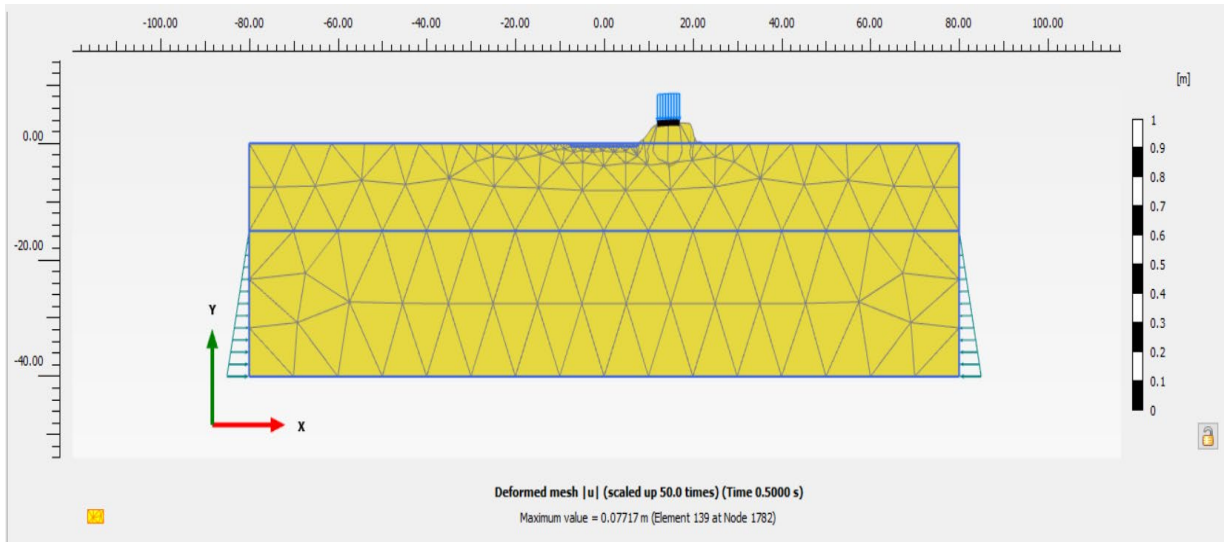


Figure 10.2: Generation of the Mesh in PLAXIS 2D

Cohesionless soils exhibit immediate settlement upon load application due to their lack of cohesion. Settlement occurs rapidly and reaches an almost immediate equilibrium state

Selection of nodes.

Three nodes are selected to extract our curves depicting the displacement analysis.



Figure 10.3: Node Selection

RESULTS

We can see the trend of the total vertical displacements in the y-direction by help of figures as shown below.

Result of Phase 1, with no loading

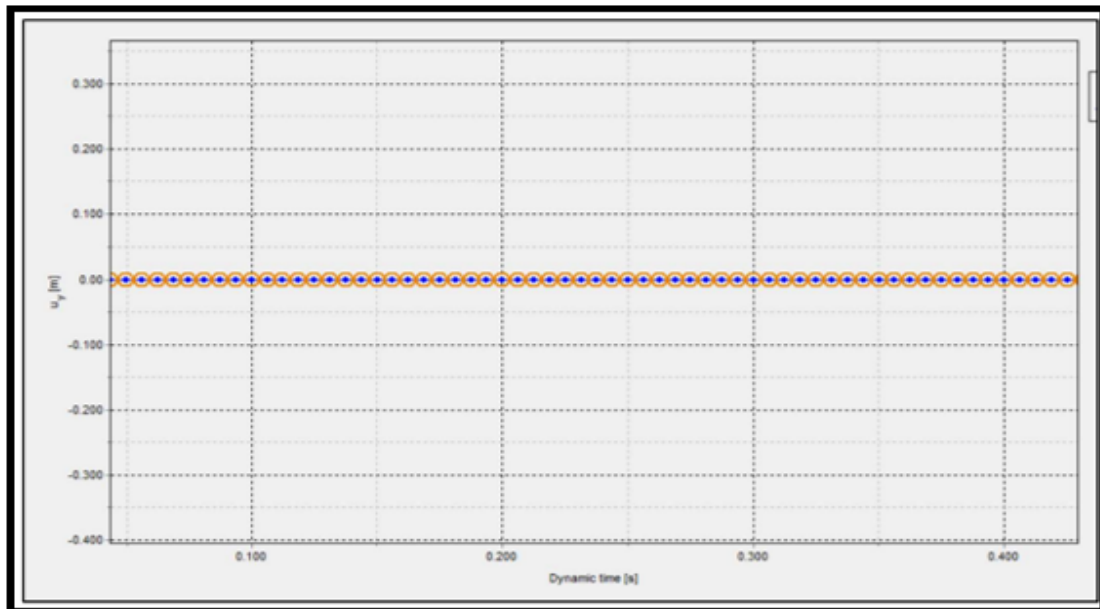


Figure 10.4: Result generated in the in-situ generator with no loading in PLAXIS 2D

Result after starting of the turbogenerator, Point on surface of soil

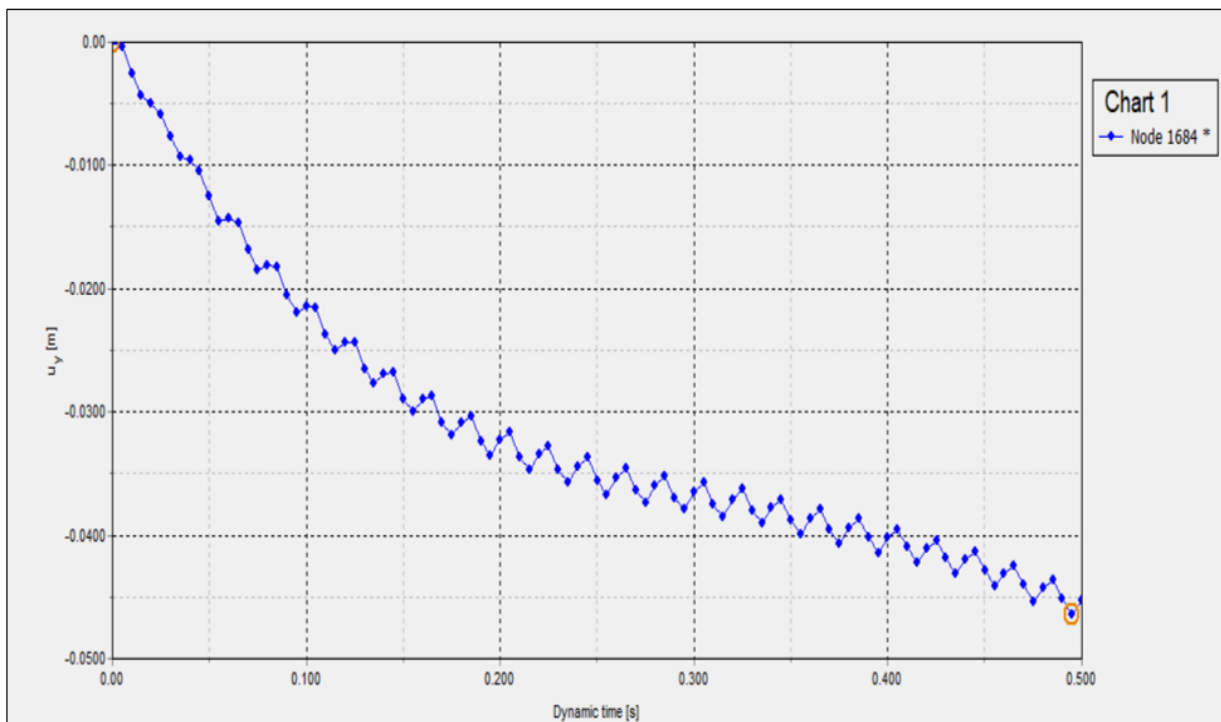


Figure 10.5: Result generated in the in-situ generator after starting of turbogenerator in PLAXIS 2D

At the bottom of steel frame foundation

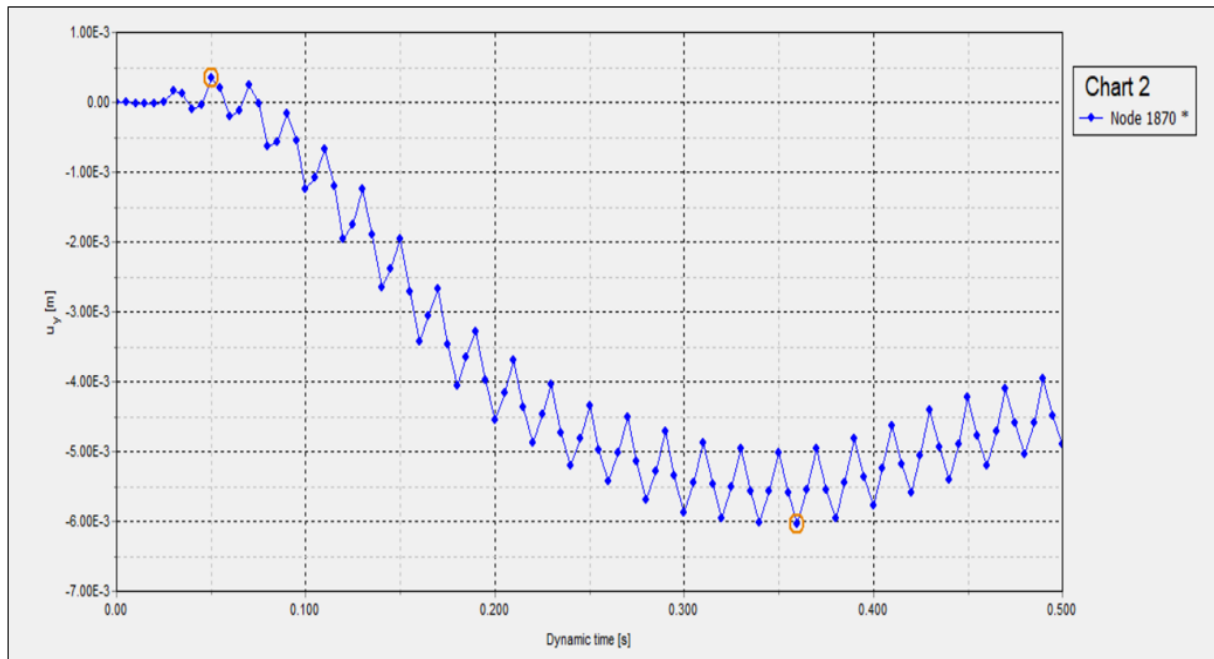


Figure 10.6: Result generated in the in-situ generator after starting of turbogenerator in PLAXIS 2D

At the middle of sand layer

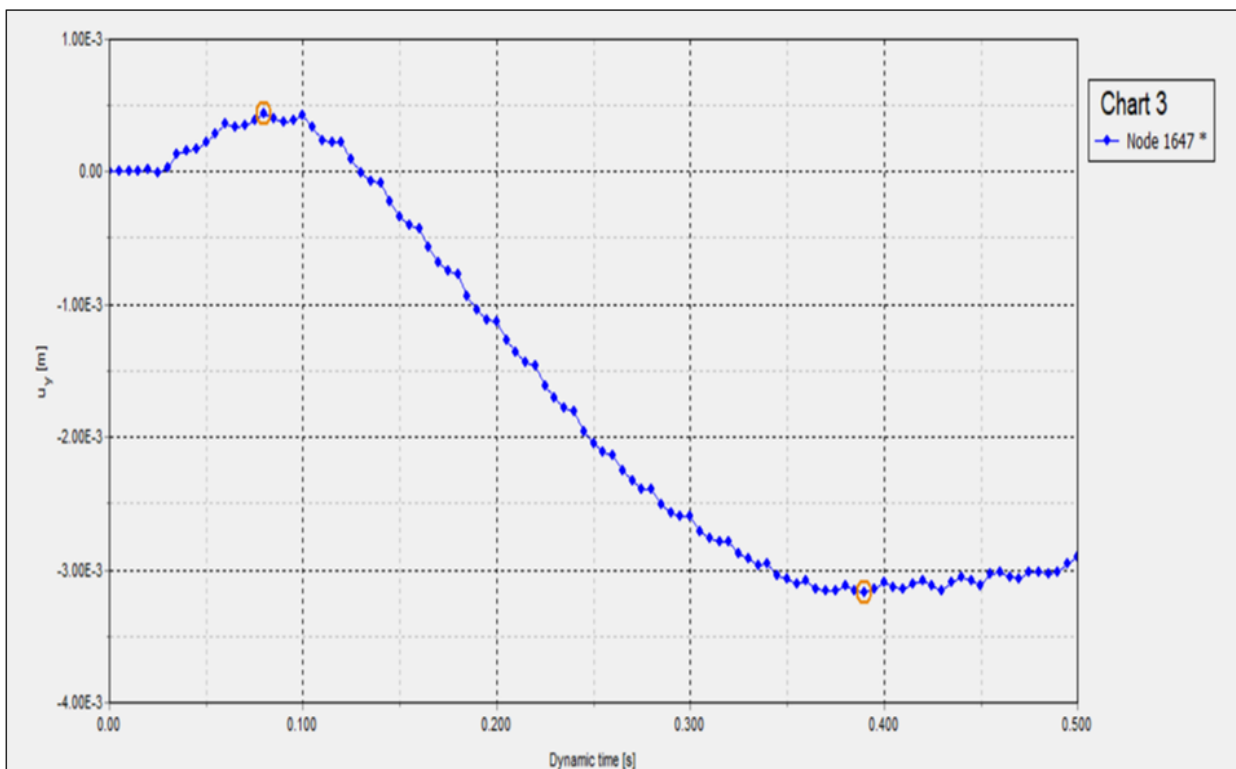


Figure 10.7: Result generated in the in-situ generator after starting of turbogenerator in PLAXIS 2D

10.4 Findings.

- After starting the Turbo generator a sharp and exponential deformation of soil is seen in each of the points considered in the mesh.
- Cohesionless soils exhibit immediate settlement upon starting of the turbo generator due to their lack of cohesion.
- Settlement occurs rapidly and reaches an almost immediate equilibrium state. The rapid settlement response is critical for our time-sensitive project.
- Under these shearing conditions, cohesionless soils tend to undergo dilation, resulting in volume expansion and additional displacements.
- Dilatancy behavior is vital for analyzing the response of cohesionless soils to dynamic loading. Dilatancy refers to the tendency of these soils to undergo volume expansion or dilation under certain loading conditions.

10.4.1 Cohesive soil i.e. clay

Cohesive soils, are characterized by their cohesive strength and low permeability.

Brief description of the system: The effect of a typical turbo generator running at a specific frequency on a double storey steel frame structure is analyzed. The structure is made of structural steel of Fe-415 and is on a M25 concrete block foundation length of 14 m with a height of 10 m. The underlying soil is a 40 m of clay layer is taken for analysis. The turbo generator lies at a distance of 5 m from the steel frame with a height of 2.5 m and width of 5 m respectively running at 50 Hz frequency.

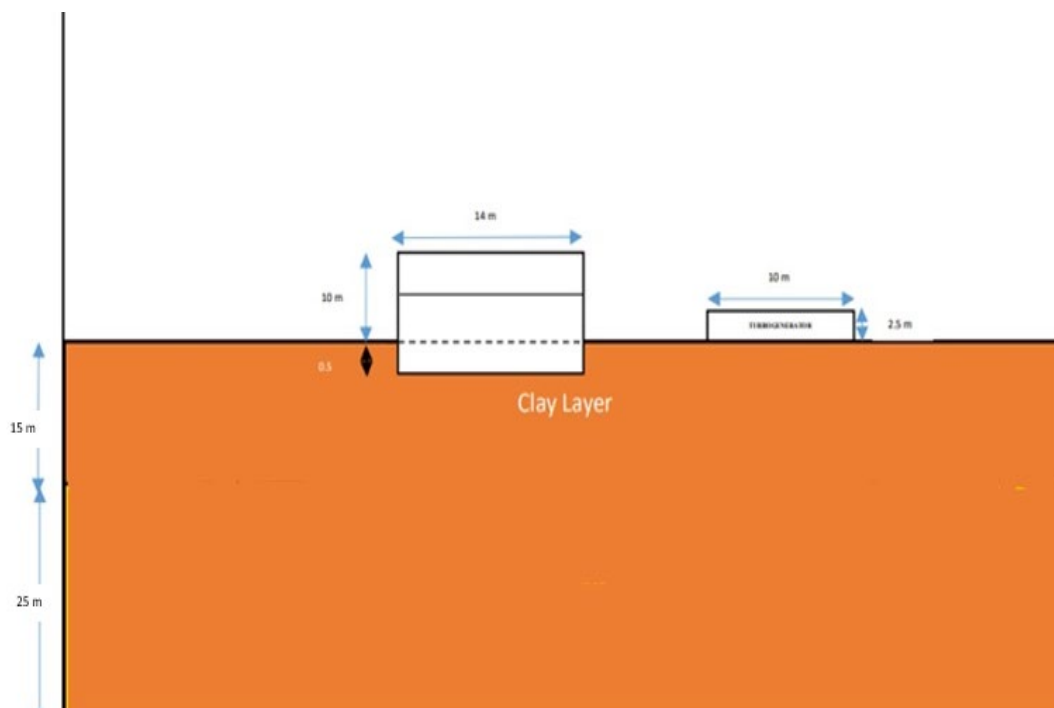


Figure 10.8: Layout of the model

Properties of clay layer.

Table 10.2: Properties of clay layer

Parameter	Name	Value	Unit
General			
Material Model	Model	HS Small	-
Type of Material nature	Type	Drained	-
Soil unit weight (Unsaturated)	γ_{unsat}	16	kN/m ³
Soil Unit Weight (Saturated)	γ_{sat}	20	kN/m ³
Parameters			
Young's Modulus (Constant)	E	2×10^4	kN/m ²
Poisson's Ratio	σ	0.2	-
Initial Conditions			
Cohesion	c	10	-
Friction angle	ϕ	--	Degrees
Dilatancy angle	φ	0	Degrees

The properties of steel and the turbogenerator are taken from CHAPTER. So putting our model through displacement analysis we can obtain a generated mesh.

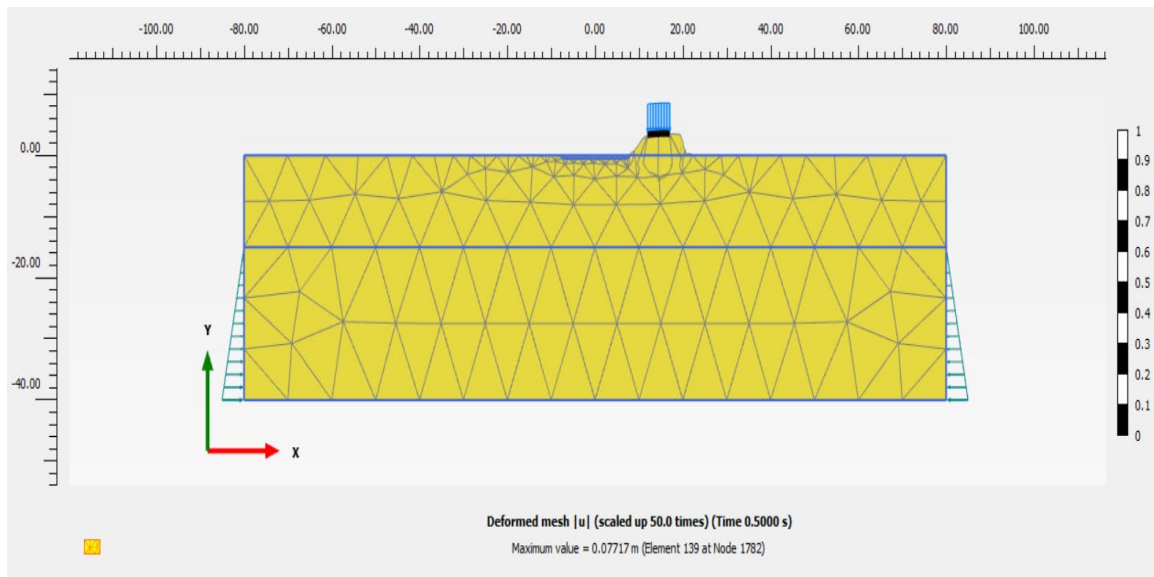


Figure 10.9: Generation of Mesh

Selection of nodes.

Three nodes are selected to extract our curves depicting the displacement analysis.



Figure 10.10: Selection of Nodes

RESULTS

We can see the trend of the total vertical displacements in the y-direction by help of figures as shown below.

Result of Phase 1, with no loading

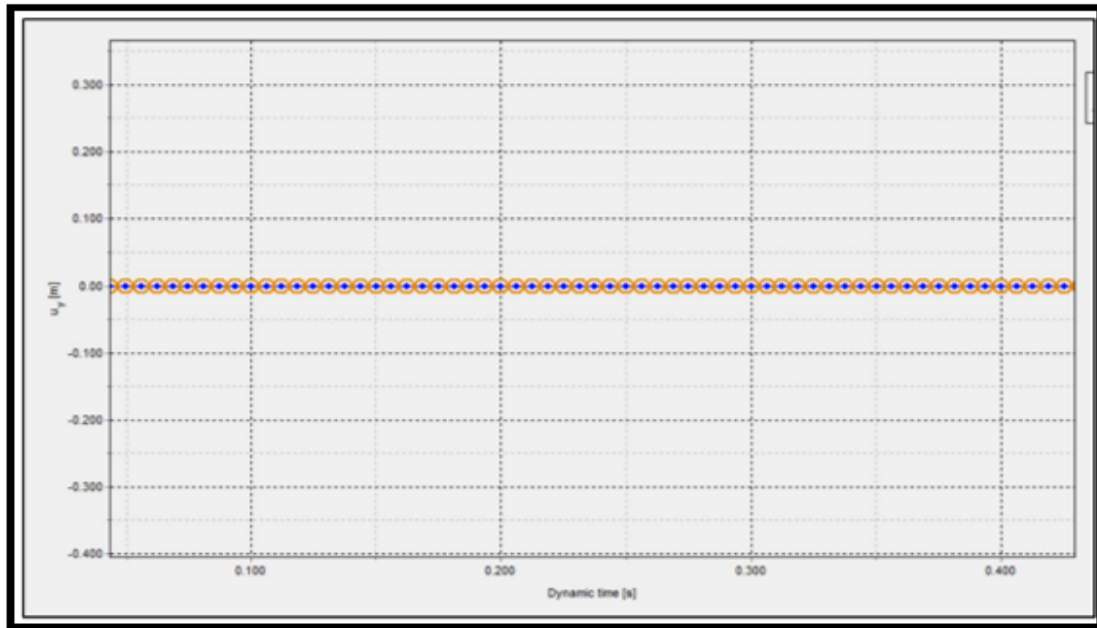


Figure 10.11: Result generated in the in-situ generator with no loading in PLAXIS 2D

Result after starting of the turbogenerator, Point on surface of soil.

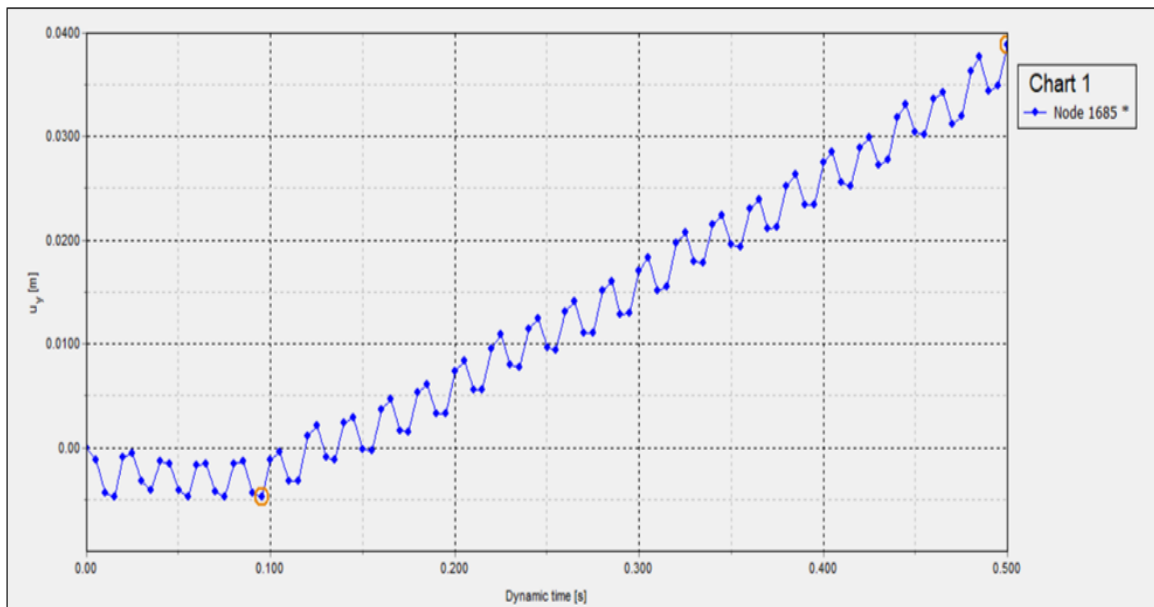


Figure 10.12: Result generated in the in-situ generator after starting of turbogenerator in PLAXIS 2D

At the bottom of steel frame foundation

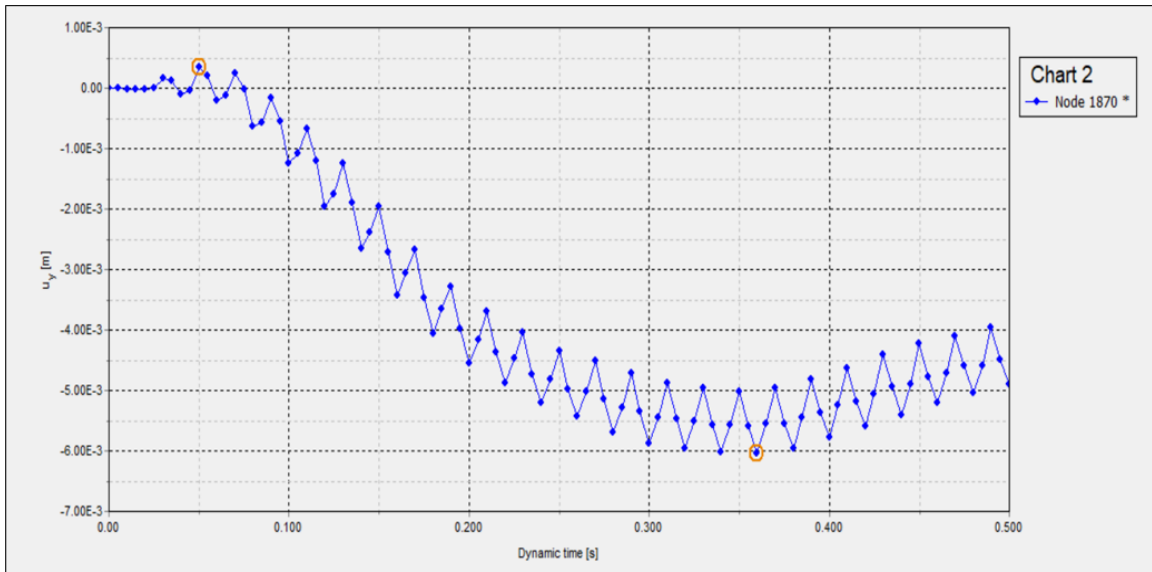


Figure 10.13: Result generated in the in-situ generator after starting of turbogenerator in PLAXIS 2D

At the middle of sand layer.

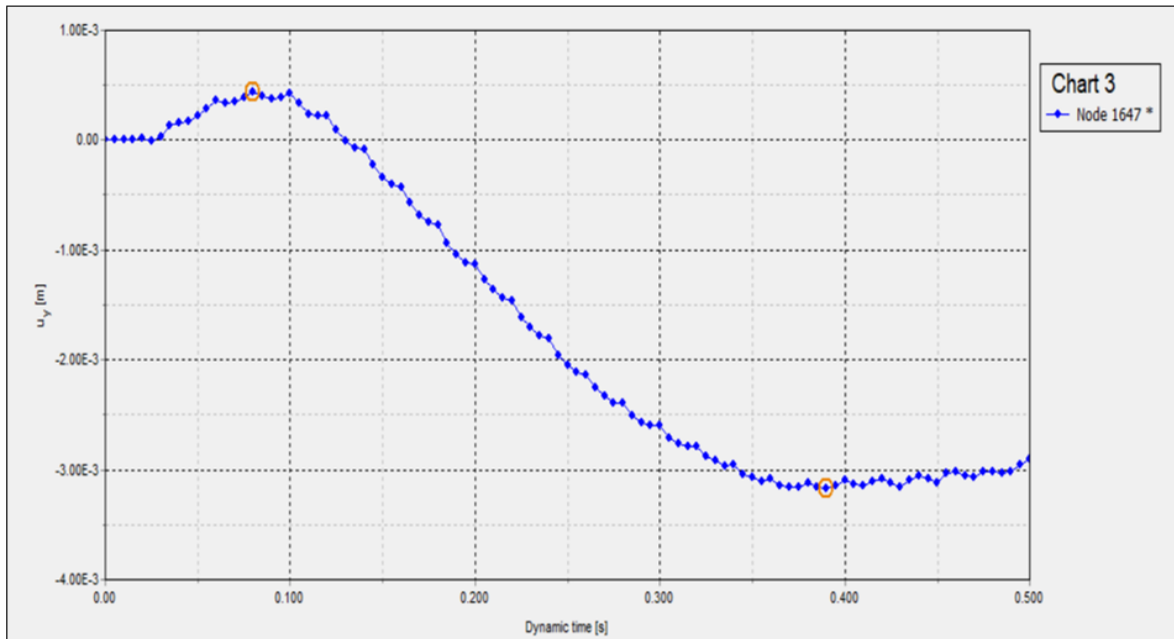


Figure 10.14: Result generated in the in-situ generator after starting of turbogenerator in PLAXIS 2D

FINDINGS.

- Compared to cohesionless soil, the deflections are fluctuating both in the x and y directions.
- Cohesive soils undergo consolidation settlement over time when subjected to loads. This graphical simulation demonstrated a gradual settlement process.
- Cohesive soil exhibits time-dependent deformation, particularly during creep analysis. The rate of creep deformation depends on the soil sensitivity and its ability to gain strength over time. Understanding the creep behavior is crucial for predicting long-term displacements and ensuring the stability of geotechnical structures.

10.4.2 FOR A TWO LAYERED SOIL SYSTEM.

Brief description of the system: The effect of a typical turbo generator running at a specific frequency on a double storey steel frame structure is analyzed. The structure is made of structural steel of Fe-415 and is on a M25 concrete block foundation length of 14 m with a height of 10 m. The underlying soil is a cohesive soil up to 15 m and below layer consists of sand. 25 m of sand layer is taken for analysis. The turbo generator lies at a distance of 5 m from the steel frame with a height of 2.5 m and width of 5 m respectively running at 50 Hz frequency.

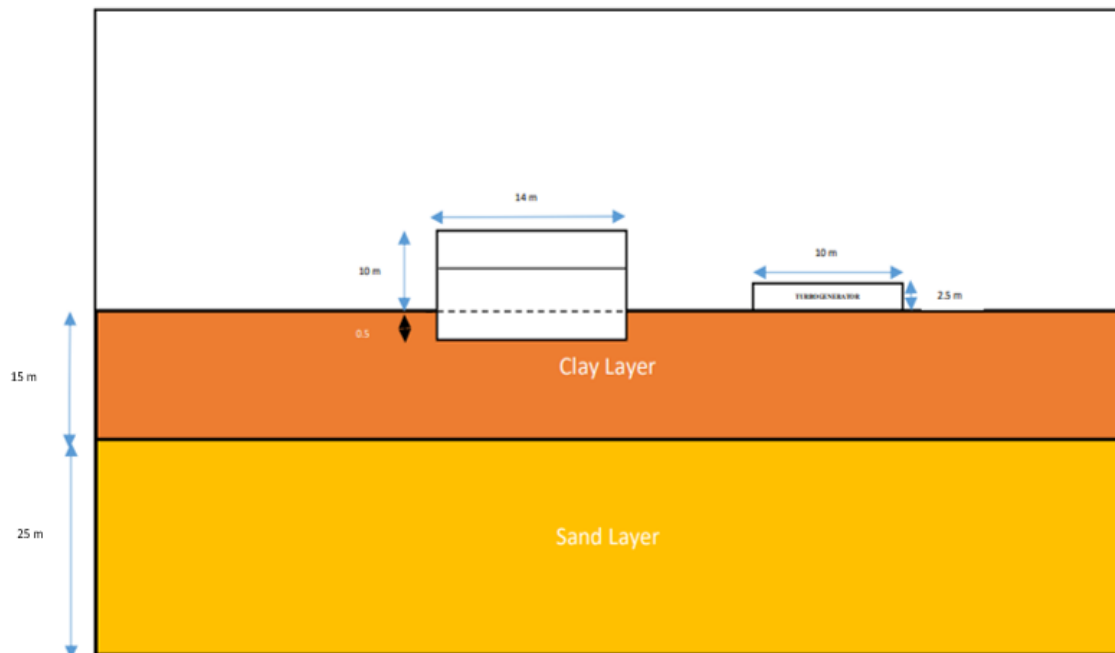


Figure 10.15: Layout of the Model

The generated mesh is shown below

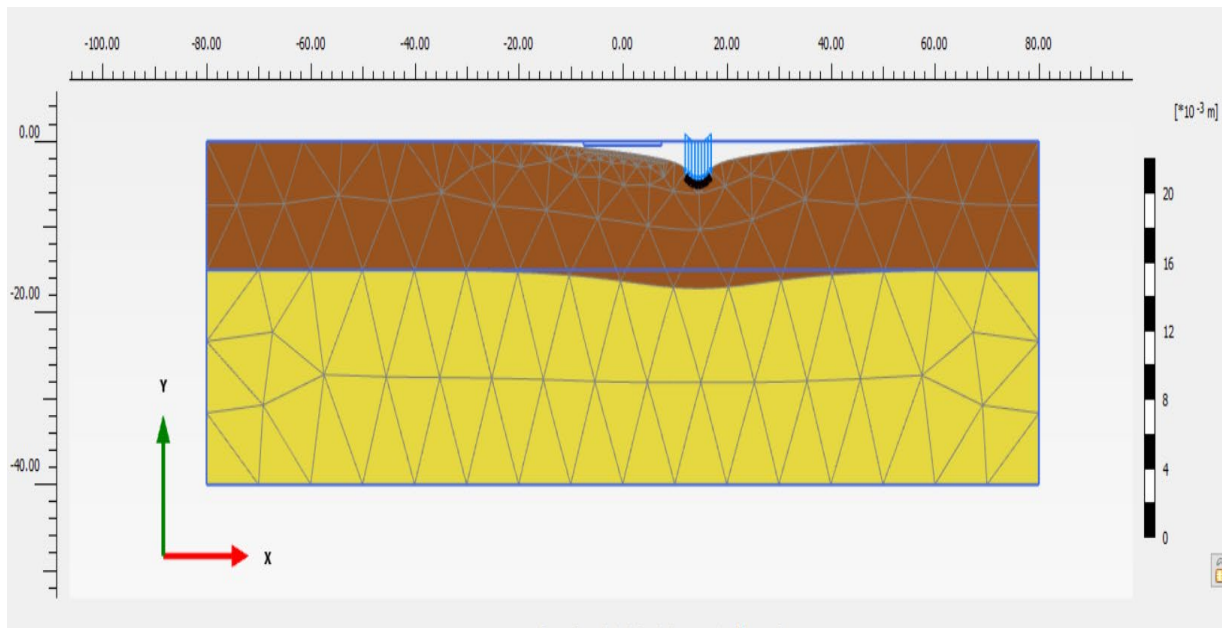


Figure 10.16: Generation of Mesh

The nodes selected for generating the displacement curves are shown below.

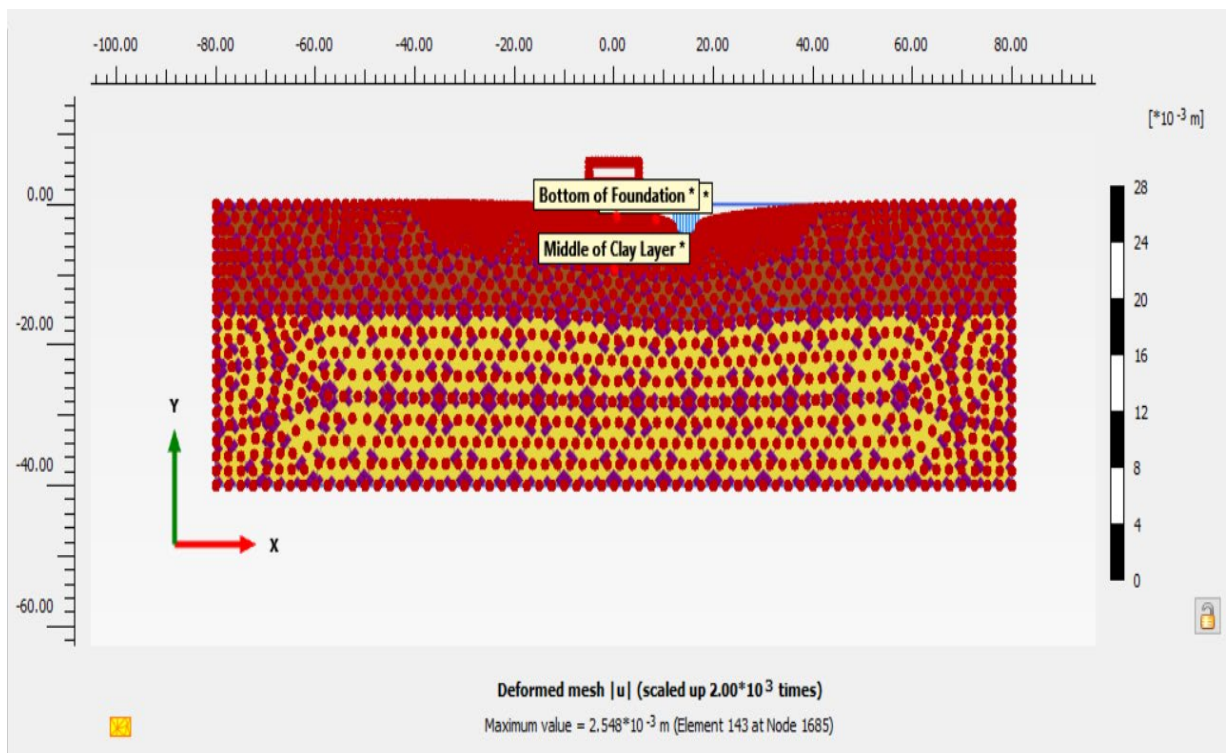


Figure 10.17: Selection of Nodes

The properties of soil, steel and the turbogenerator are kept same.

Results

Result of Phase 1, with no loading

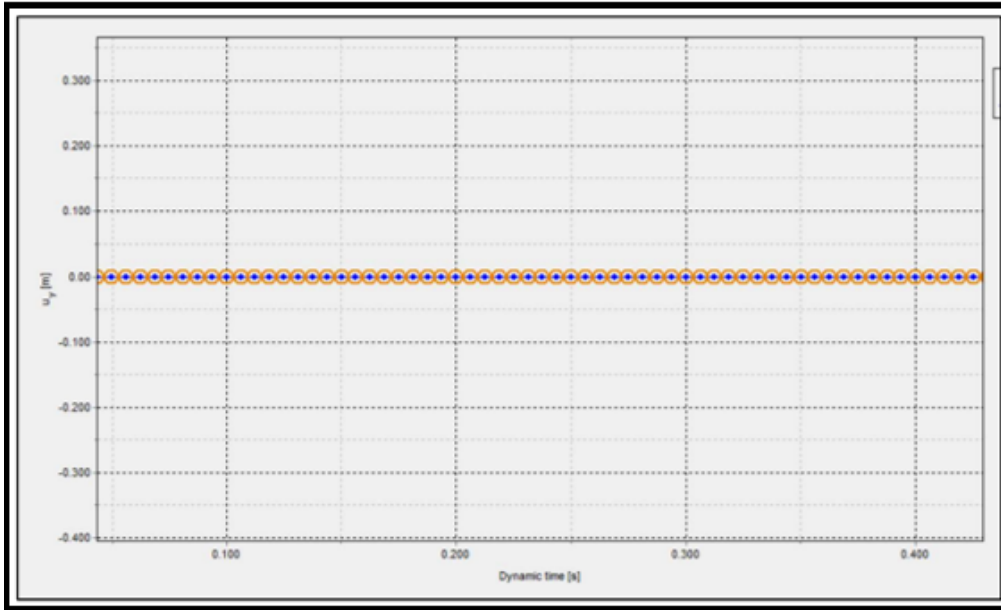


Figure 10.18: Result generated in the in-situ generator with no loading in PLAXIS 2D

Result after starting of the turbogenerator, Point on surface of soil



Figure 10.19: Result generated in the in-situ generator after starting of turbogenerator in PLAXIS 2D

At the bottom of steel frame foundation.

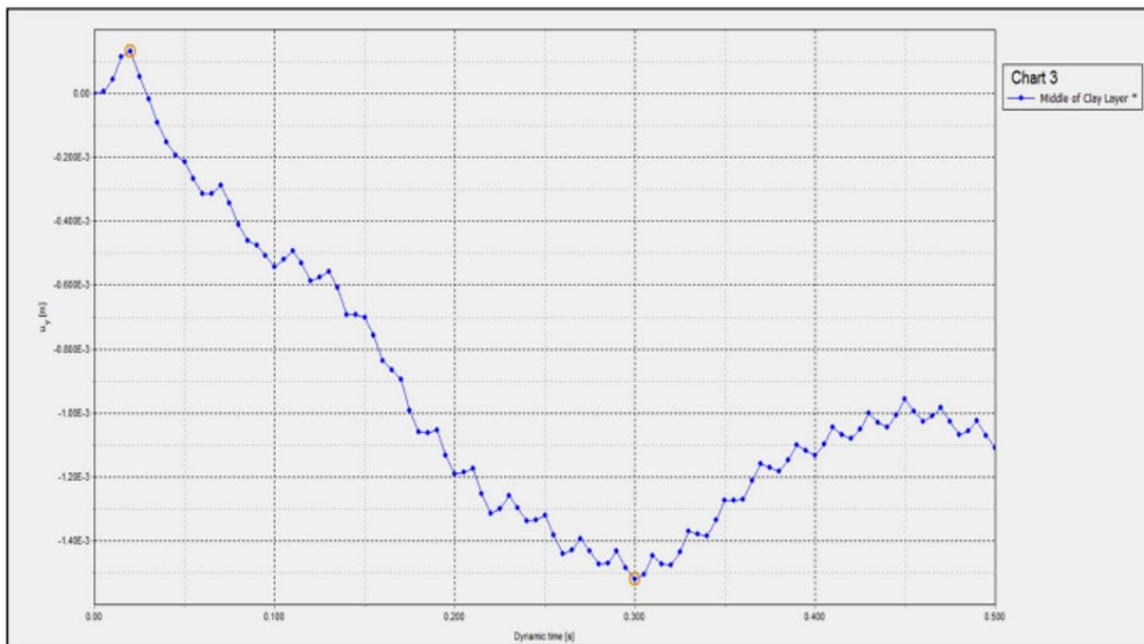


Figure 10.20: Result generated in the in-situ generator after starting of turbogenerator in PLAXIS 2D

At the middle of clay layer

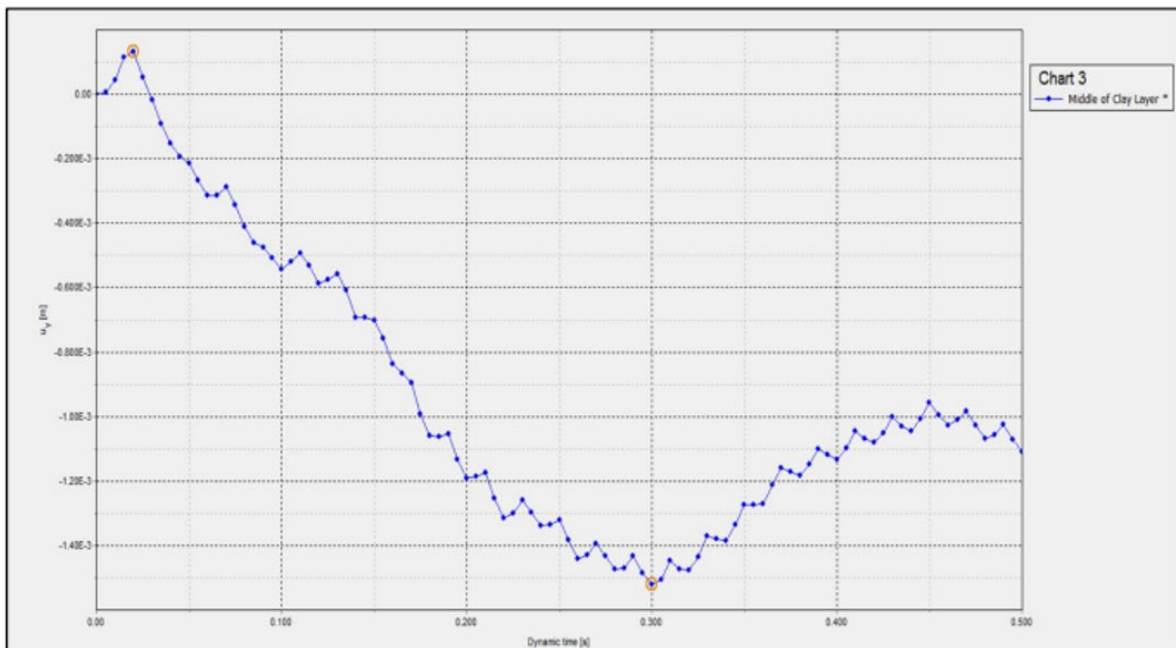


Figure 10.21: Result generated in the in-situ generator after starting of turbogenerator in PLAXIS 2D

Findings

Comparable to the sand layer values of earlier case. Effect of underlying clay layer seems to stabilize the deformations to some extent.

CHAPTER 11

EFFECT OF WATER TABLE

11.1 Introduction

The water table is a critical factor in shaping the soil environment, affecting its physical, chemical, and biological properties. Understanding the water table's dynamics is essential for sustainable land and water management practices, especially in agriculture, construction, and environmental conservation. The importance of water table for construction and foundation lies in its potential to influence the stability, integrity, and long-term performance of foundations. Understanding and managing the water table are crucial considerations during the planning and construction phases of any project. A high water table may require a foundation that is more resistant to buoyancy and water pressure, such as pile foundations or deep foundations. On the other hand, a lower water table might allow for shallow foundations to be used effectively.

11.2 Water Table effects through Plaxis 2D

- The stability and performance of foundations are crucial for the safety and longevity of structures.
- The presence of groundwater, represented by the water table, significantly influences soil behaviour and foundation response.
- This report points out PLAXIS 2D, a FEA modelling tool, to simulate different water table conditions and evaluate their effects on various soil types.
- PLAXIS 2D uses finite element methods to calculate the foundation response under different water table scenarios.
- The results are analysed to determine the effects of the water table on foundation settlements, bearing capacities, and potential risks.

11.3 Water Table effect on Cohesionless soil.

The water table has a significant effect on cohesion less soils.

- Cohesionless soils highly permeable. When the water table is below the ground surface, the soil pores are filled with air, and the permeability is relatively high. However, when the water table rises and saturates the soil, the permeability decreases significantly due to the presence of water in the pores.
- Cohesionless soils rely on the concept of effective stress to bear loads. Effective stress is the difference between total stress and pore water pressure. When the water table is low, the pore water pressure is low, and the effective stress between soil particles is higher, providing better load-bearing capacity. As the water table rises, the pore water pressure increases, reducing the effective stress and potentially causing a decrease in soil strength.

- The water table can influence the settlement and consolidation behaviour of cohesion less soils. When the water table rises, excess pore water pressures can develop, causing settlement and consolidation of the soil layers.

11.4 The effects of water table in Cohesionless soil.

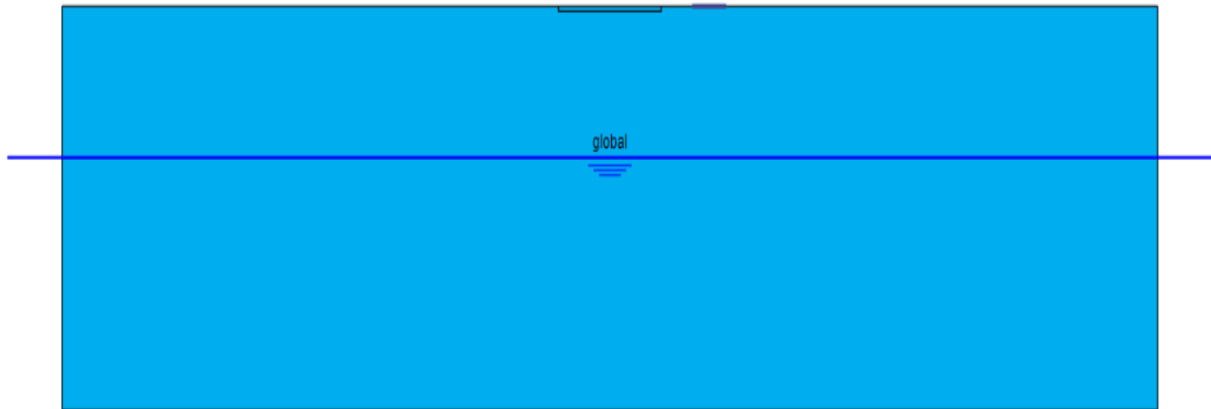


Figure 11.1: System with Global water level

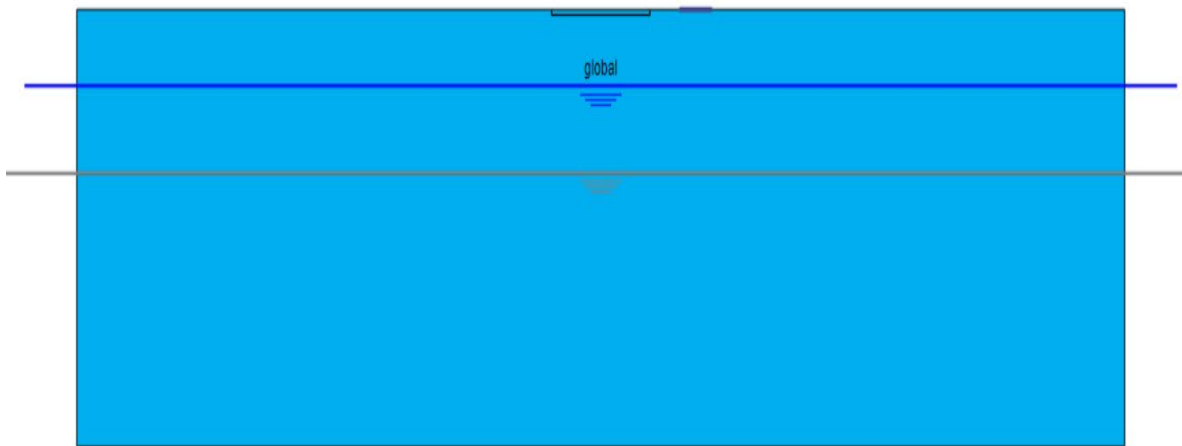


Figure 11.2: Manually raised water level to study the effects

11.5 Comparing the load vs settlement, we get.

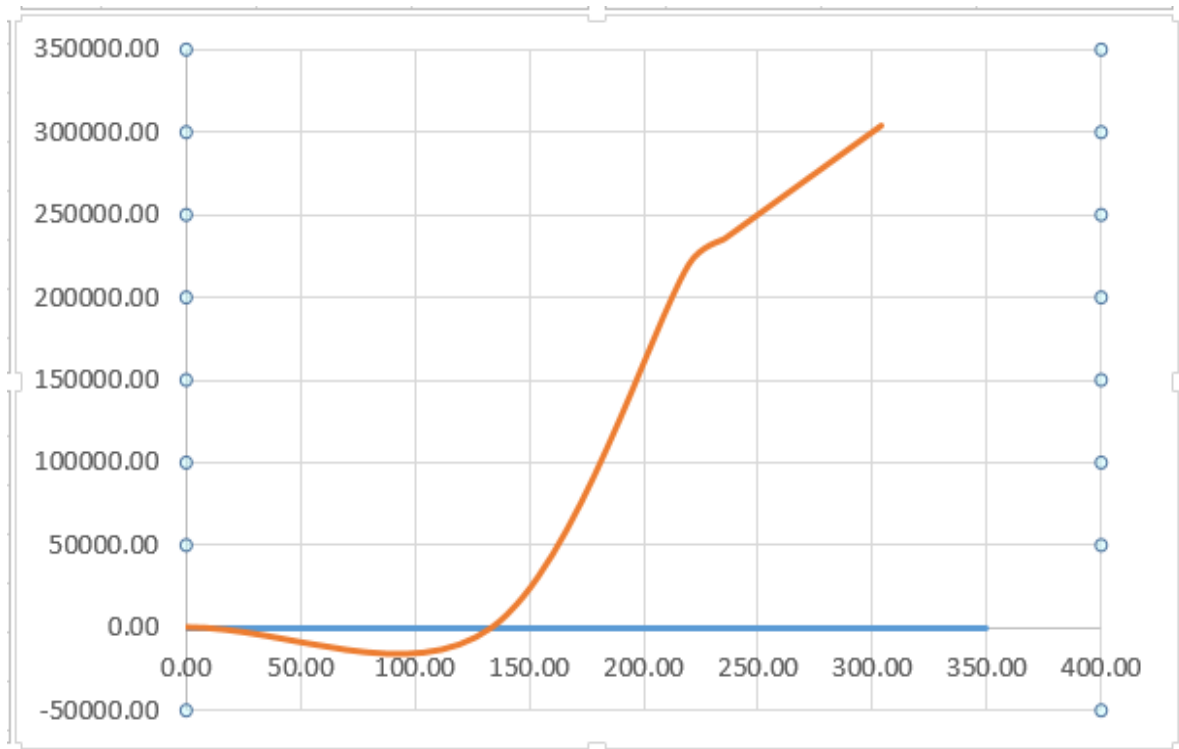


Figure 11.3: Graphical representation of comparing the load vs settlement

X-axis- LOAD

Y-axis- SETTLEMENT

----- load vs settlement with raised water levels.

----- load vs settlement with global water levels.

The graph shows that as the water table rises, the settlement of the cohesionless soil increases under the same applied load. This is due to the reduction in effective stress caused by the rise in pore water pressure, which decreases the soil shear strength and allows more settlement to occur.

As the load increases for a given water table position, the settlement of the soil is expected to increase as well. Higher loads lead to higher stress levels in the soil, resulting in more significant deformation and settlement.

11.6 Effects of water table in cohesive soil.

The water table plays an important role in the behaviour and stability of cohesive soils. The presence and position of the water table can have various effects on cohesive soils, influencing their strength, volume change, and overall engineering behaviour.

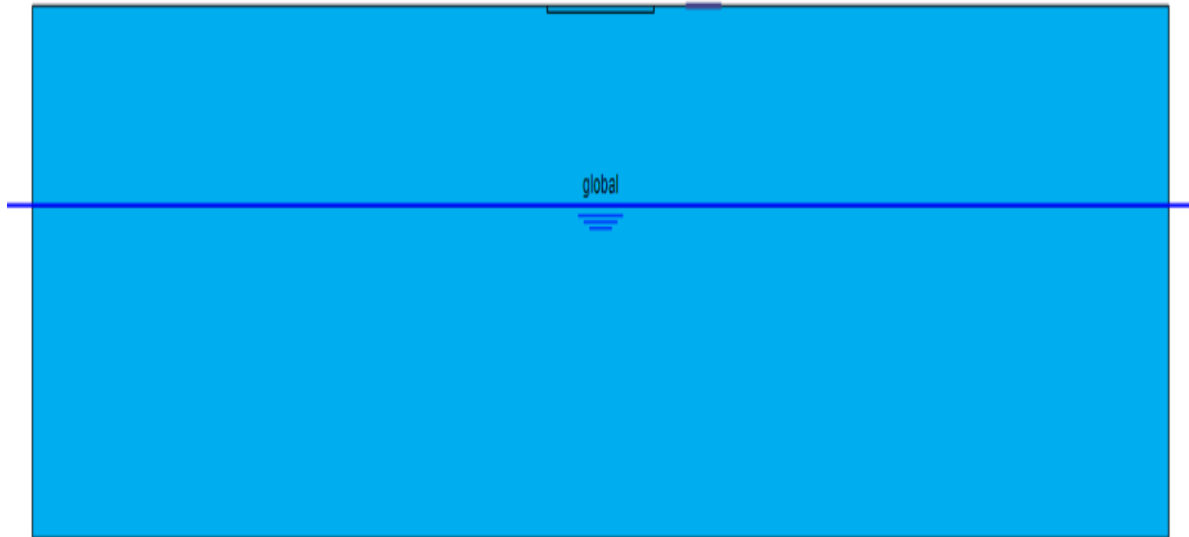


Figure 11.4: System with Global water level

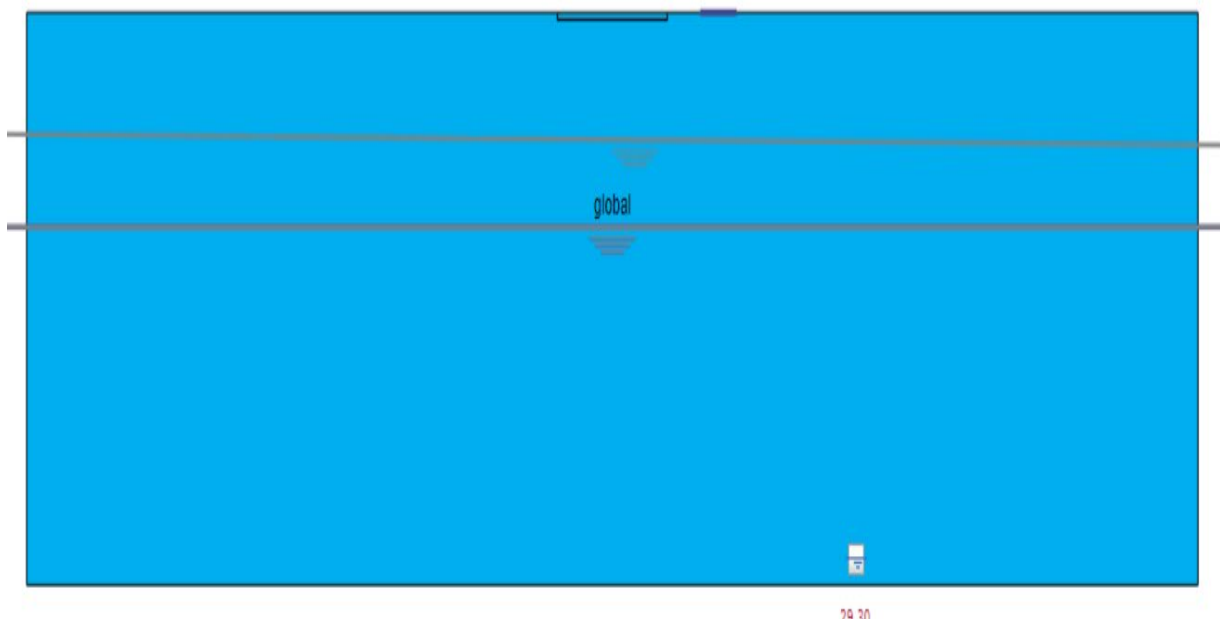


Figure 11.5: Manually raised water level to study the effects

11.7 Comparing the load vs settlement, we get.

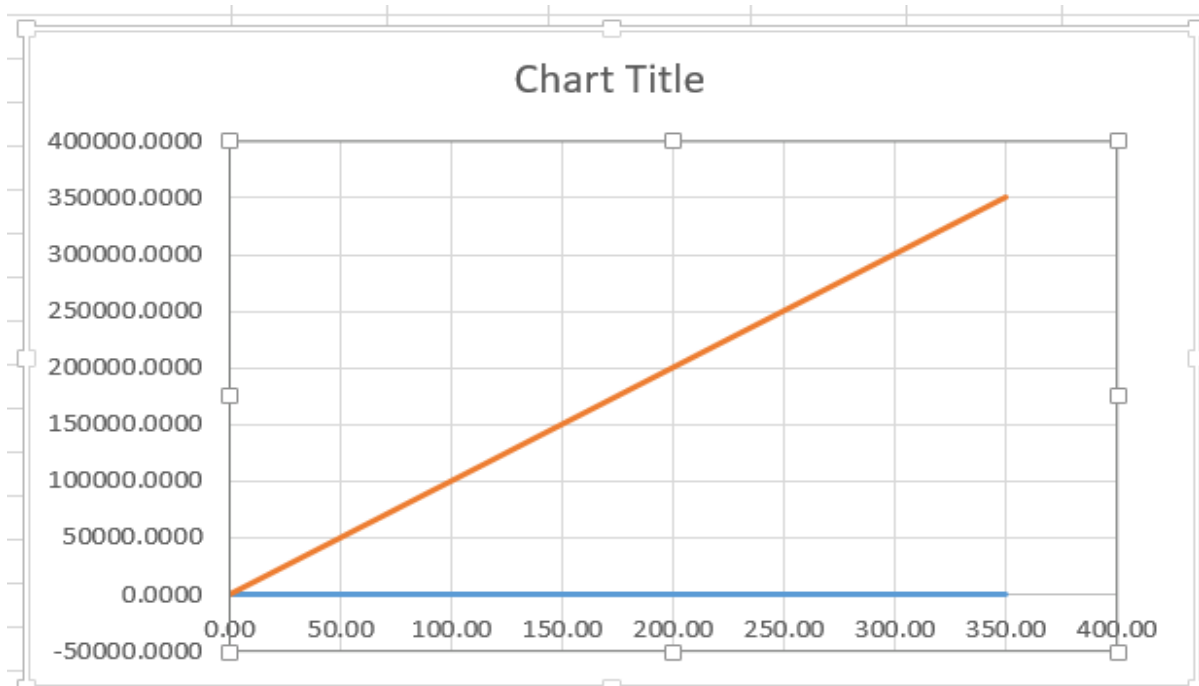


Figure 11.6: Graphical representation of comparing the load vs settlement

X-axis- LOAD

Y-axis- SETTLEMENT

----- load vs settlement with raised water levels.

----- load vs settlement with global water levels.

The graph illustrates that a raised water table can have a profound impact on the settlement behaviour of cohesive soils. As the water table rises, it reduces the effective stress and strength of the soil, leading to increased settlement rates.

11.8 Mitigation of rising water levels.

Mitigating the effects of rising water levels is essential to prevent any potential damage to structures and infrastructure. Some effective mitigation measures to consider are noted below:

1. **Site Selection and Planning:** To conduct a thorough site investigation to understand the groundwater conditions and potential risks associated with rising water levels.
2. **Elevating Structures:** Designing buildings and foundations with elevated foundations to raise potential flood levels. This can reduce the risk of damage and allow floodwater to pass underneath without causing significant harm.

3. **Proper Drainage System:** Implementing a well-designed and adequately maintained drainage system to divert excess water away from critical areas. By using surface channels, ditches, and underground drainage networks to control the flow of water.
4. **Dewatering and Pumping:** For temporary water level rises, dewatering techniques and pumps to lower the groundwater level and maintain a stable working environment are used.
5. **Subsurface Drainage:** Installing subsurface drainage systems, such as French drains or well points, to control the water table and reduce pore water pressure in the cohesive soil.
6. **Grading and Slope Modification:** Properly grading the land and modify slopes to direct water away from critical areas and prevent erosion.
7. **Vegetation and Erosion Control:** Planting vegetation, such as grass or trees, can help stabilize the soil and reduce erosion caused by water movement.
8. **Retaining Walls:** Constructing retaining walls to stabilize slopes and prevent soil erosion during periods of rising water levels.
9. **Public Awareness and Emergency Planning:** Educate the public about flood risks, evacuation procedures, and emergency response plans to minimize potential hazards during rising water events.

CHAPTER 12

ANALYSIS OF DAMPING EFFECT

12.1 Introduction

Damping plays a crucial role in the dynamic behaviour of soils under various loading conditions. When subjected to external forces, soils tend to exhibit vibrational responses, and damping is responsible for energy dissipation during these vibrations. Understanding the impact of damping on different soil types is essential in designing resilient and safe structures. This report presents an analysis of the effect of damping on different types of soil using PLAXIS 2D, a powerful finite element software for geotechnical engineering applications. The study aims to understand how the presence of damping influences the behaviour of soils under different loading conditions. The analysis involves the use of PLAXIS 2D to model soil response with varying damping properties and presents the findings through a series of simulations and results.

12.2 Rayleigh damping

- Rayleigh damping is a type of damping used in dynamic analysis to model the energy dissipation in structures subjected to dynamic loads.
- It is named after Lord Rayleigh, who proposed a damping model that combines both mass-proportional and stiffness-proportional damping.
- To define Rayleigh damping parameters in PLAXIS 2D, two pieces of information are provided: the mass-proportional damping coefficient (α) and the stiffness-proportional damping coefficient (β).

The Rayleigh damping coefficients (α and β) are defined based on the following equations:

$$C = \alpha \cdot M + \beta \cdot K$$

Where:

- C is the Rayleigh damping matrix
- M is the mass matrix
- K is the stiffness matrix
- α is the mass-proportional damping coefficient (a positive value)
- β is the stiffness-proportional damping coefficient (a positive value)

12.3 Damping analysis in cohesionless soil

Rayleigh damping is entered in the material data set. The following steps are followed

1. The material data set of the soil is opened.

2. In the General tab sheet the box next to the Rayleigh α parameter is clicked.
3. In order to introduce 5% of material damping, the value of the ξ parameter is set to 5% for both targets.
4. The frequency values to 1 and 10 for the Target 1 and Target 2 respectively.

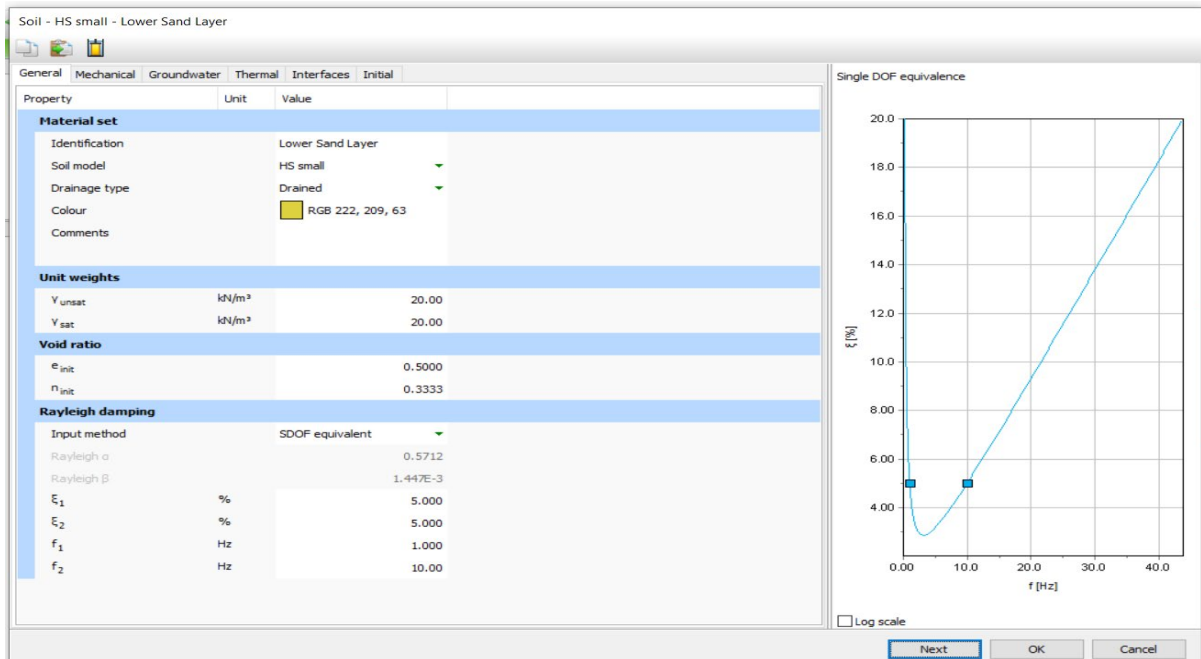


Figure 12.1: Damping is introduced

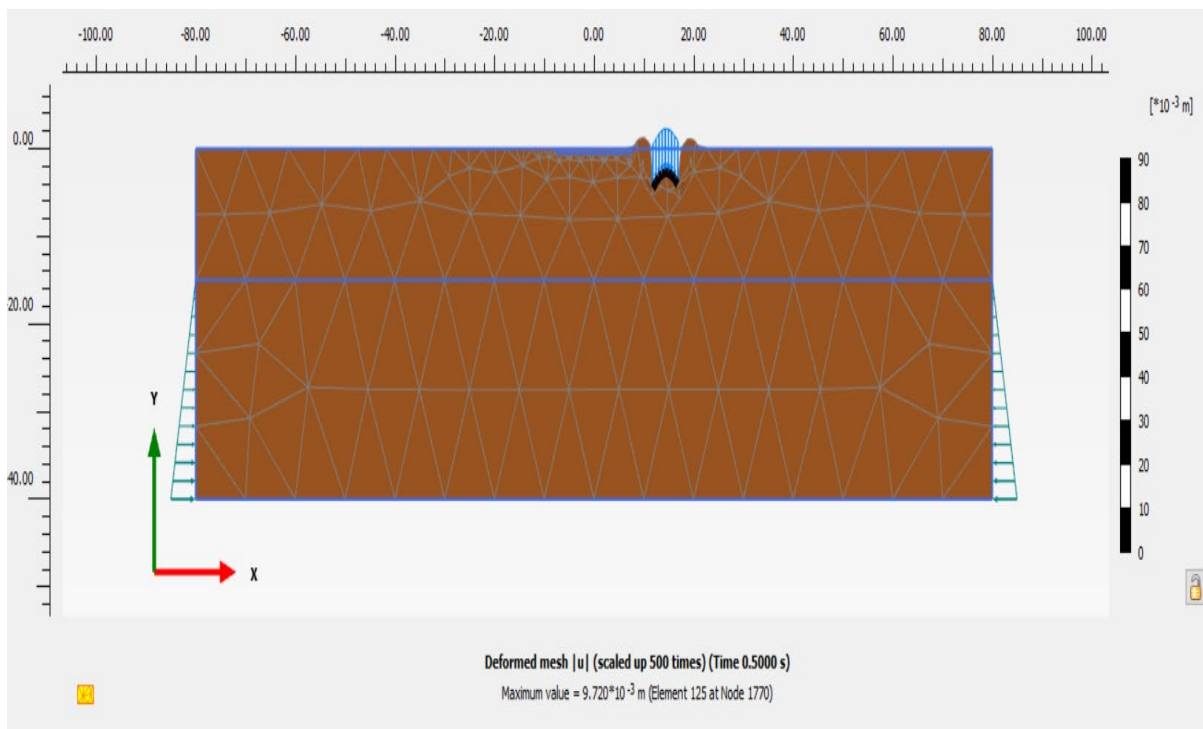


Figure 12.2: Generation of mesh

12.4 Results of analysis performed

12.4.1 Without damping.

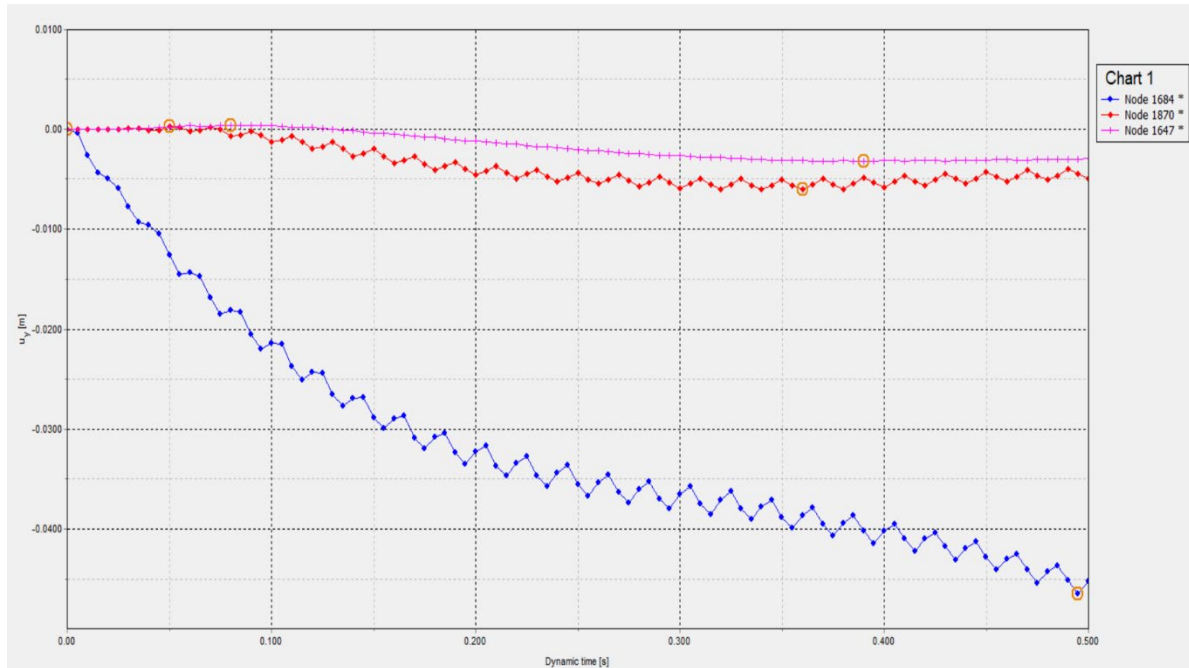


Figure 12.3: Result generated in in-situ generator analysis performed without damping

12.4.2 With damping

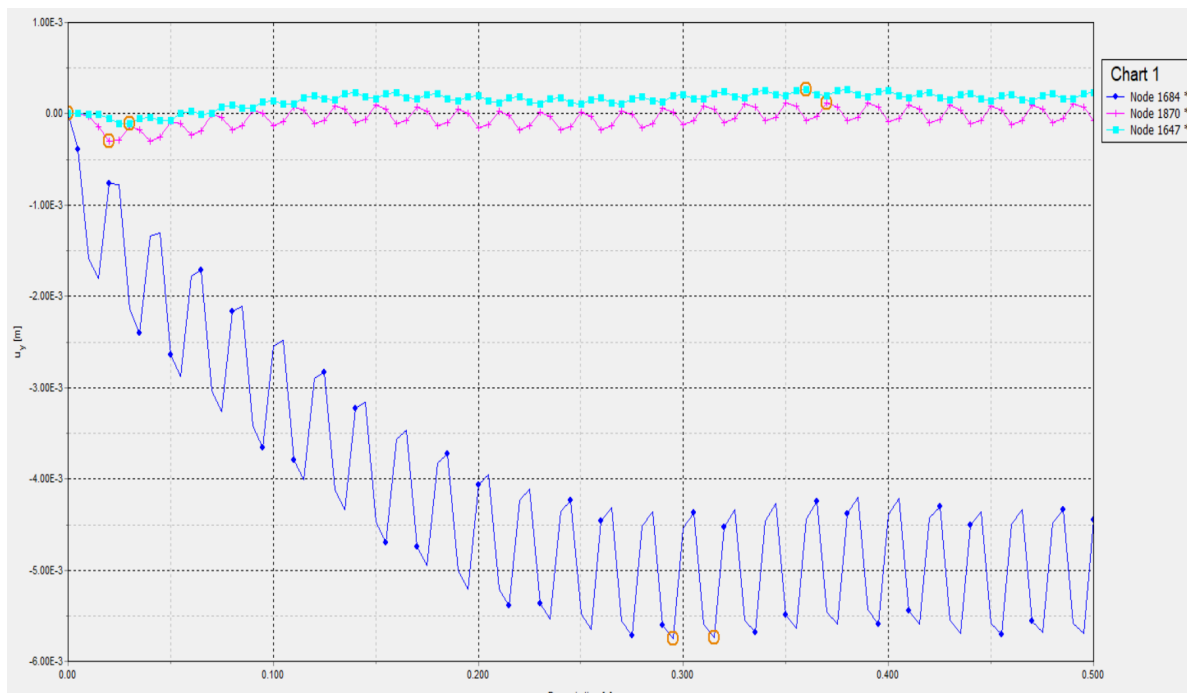


Figure 12.4: Result generated in in-situ generator analysis performed with damping

12.5 Damping analysis in cohesive soil

Rayleigh damping is entered in the material data set. The following steps are followed

1. The material data set of the soil is opened.
2. In the General tab sheet the box next to the Rayleigh α parameter is clicked.
3. In order to introduce 5% of material damping, the value of the ξ parameter is set to 5% for both targets.
4. The frequency values to 1 and 10 for the Target 1 and Target 2 respectively.

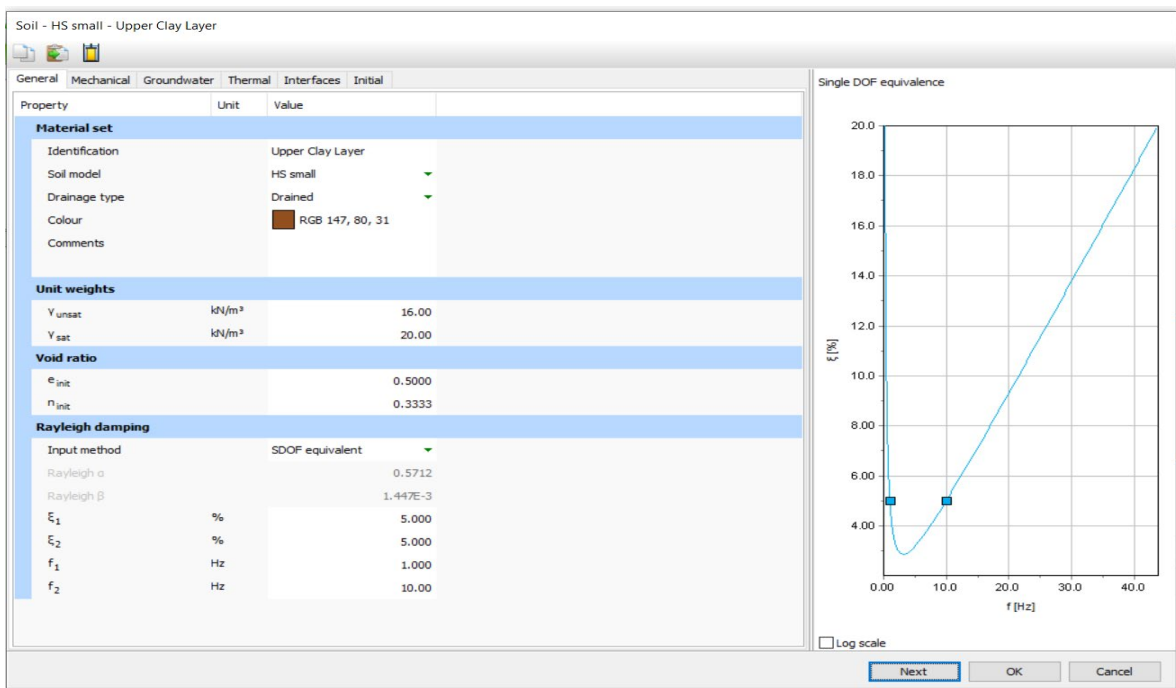


Figure 12.5: Damping is introduced into the soil layer

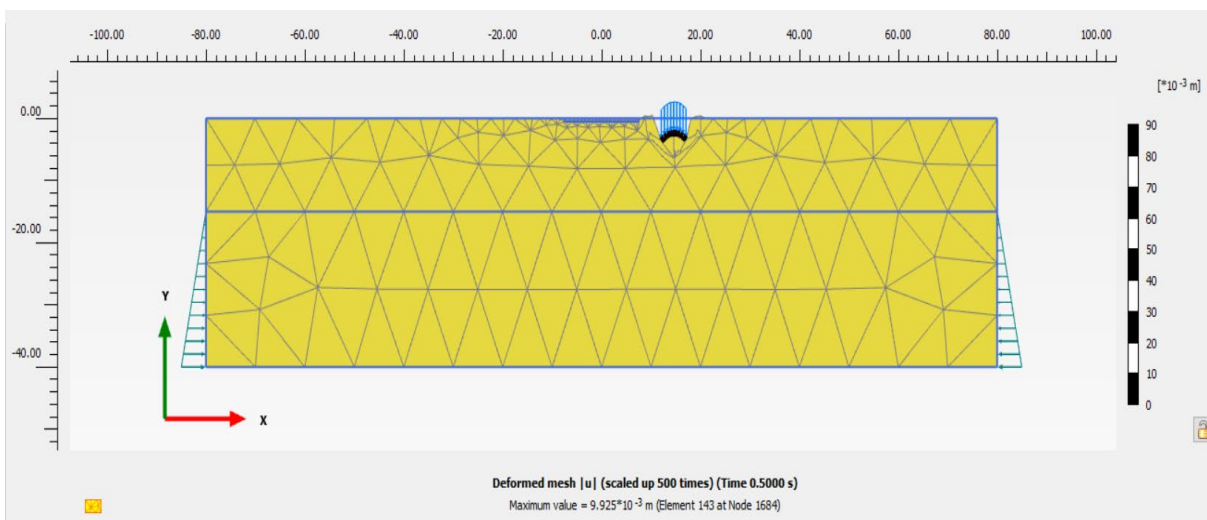


Figure 12.6: Mesh is generated

12.6 Results of analysis performed

12.6.1 Without damping.

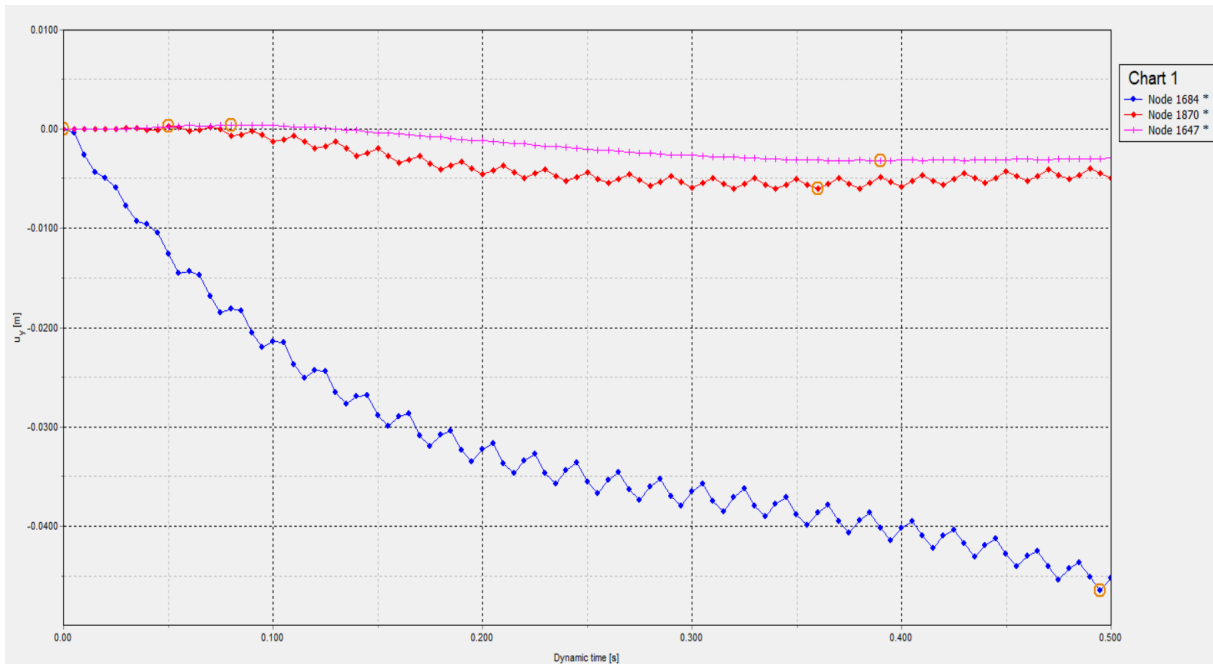


Figure 12.7: Result generated in in-situ generator analysis performed without damping

12.6.2 With damping

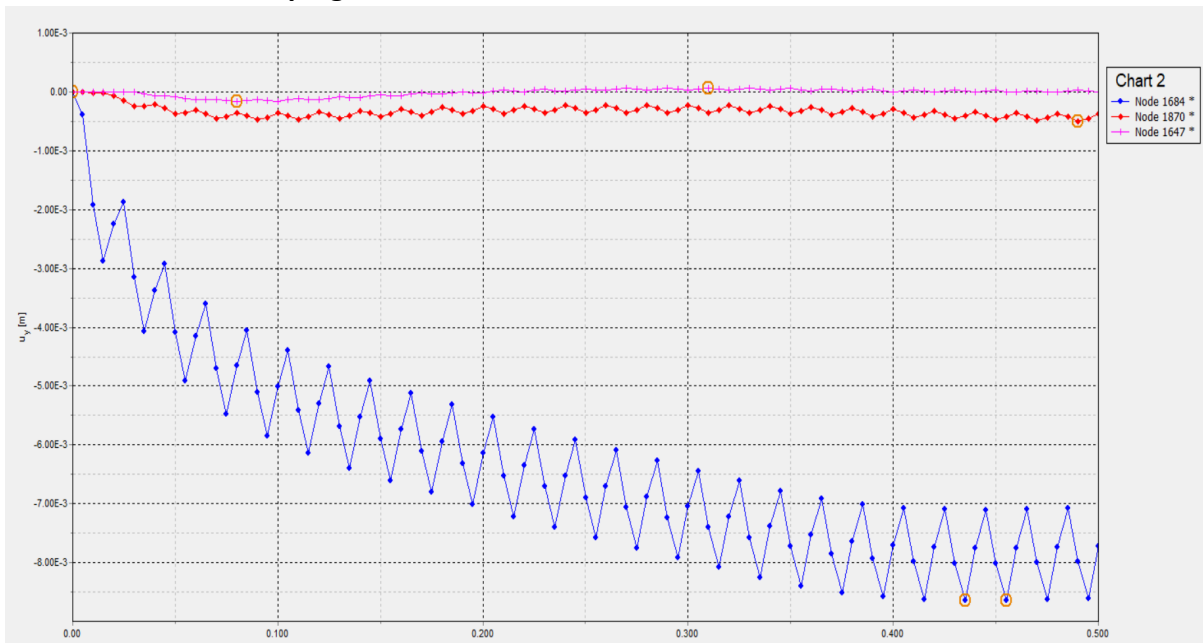


Figure 12.8: Result generated in in-situ generator analysis performed with damping

12.7 Damping analysis in Two Layered soil

Rayleigh damping is entered in the material data set. The following steps are followed

1. The material data set of the soil is opened.

2. In the General tab sheet the box next to the Rayleigh α parameter is clicked.
3. In order to introduce 5% of material damping, the value of the ξ parameter is set to 5% for both targets.
4. The frequency values to 1 and 10 for the Target 1 and Target 2 respectively.

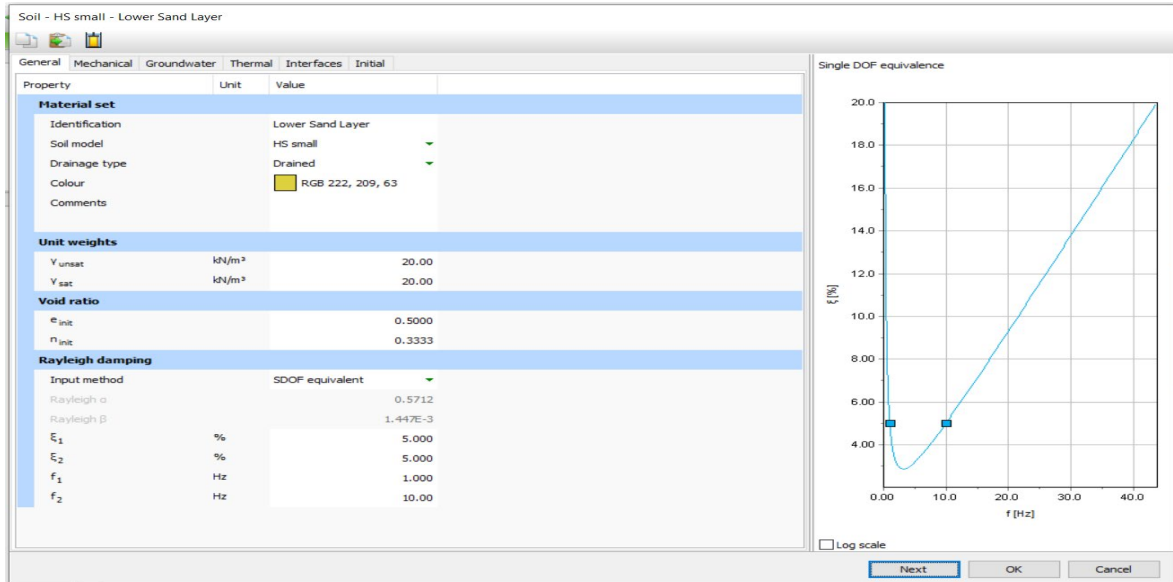


Figure 12.9: Damping is introduced for Sand layer

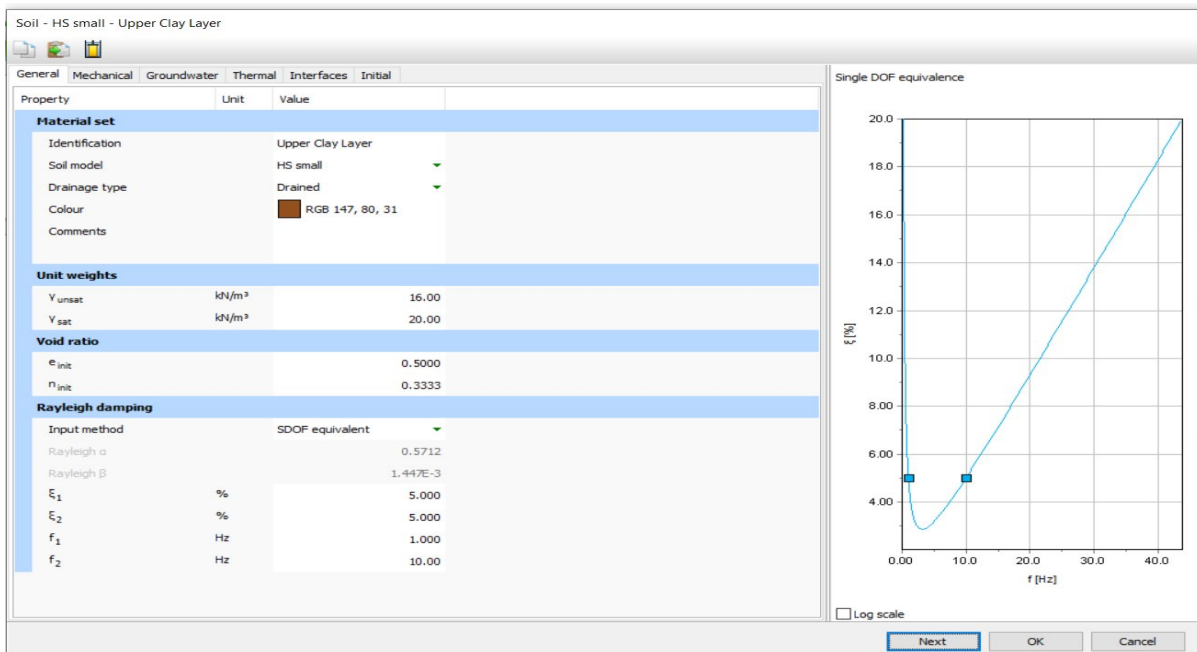


Figure 12.10: Damping is introduced for clay layer

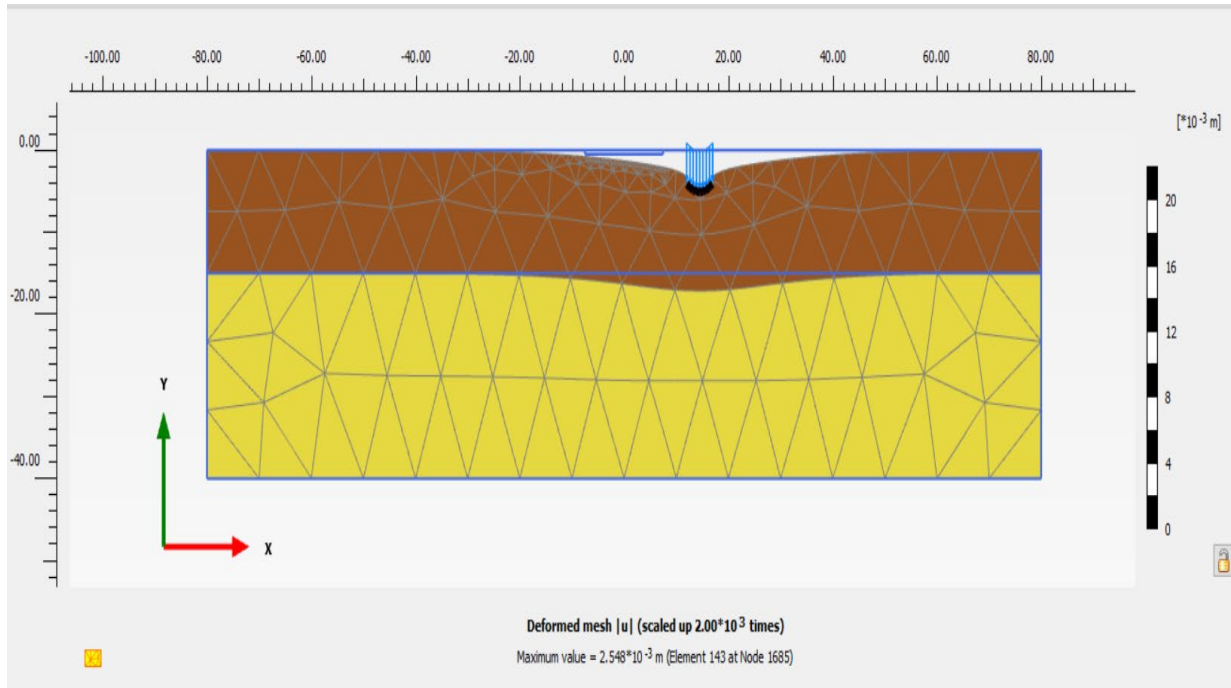


Figure 12.11: Generation of mesh

12.8 Results of analysis performed

12.8.1 Without damping.

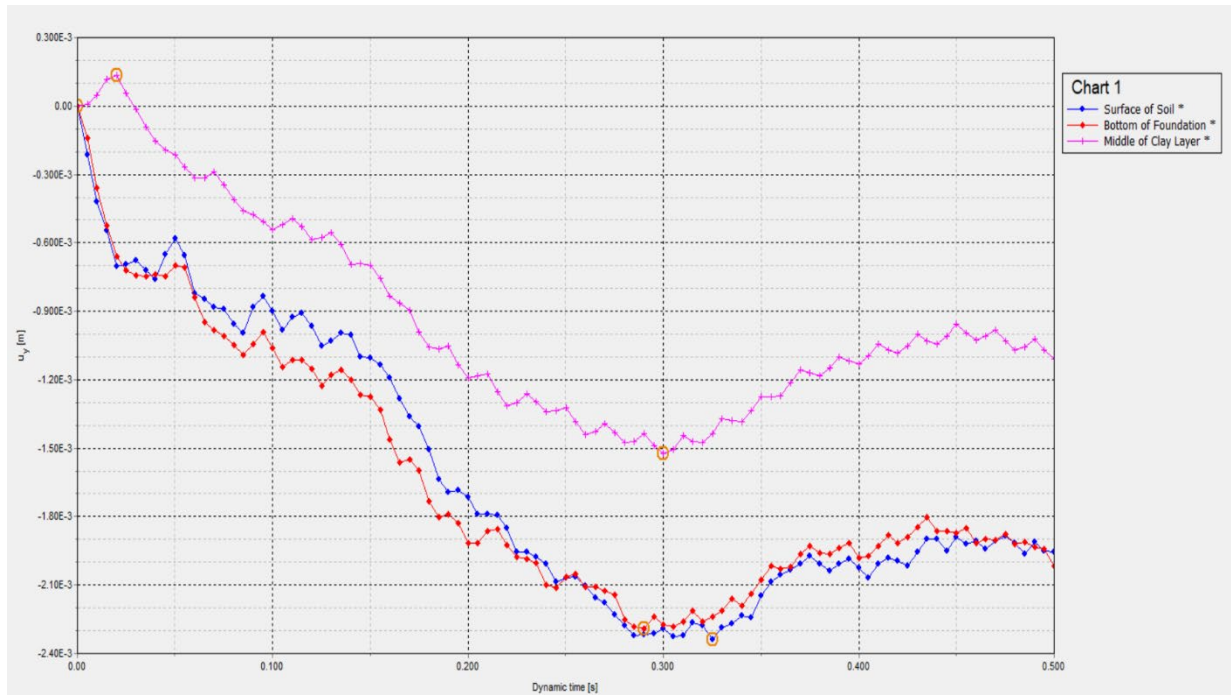


Figure 12.12: Result generated in in-situ generator analysis performed without damping

12.8.2 With Damping

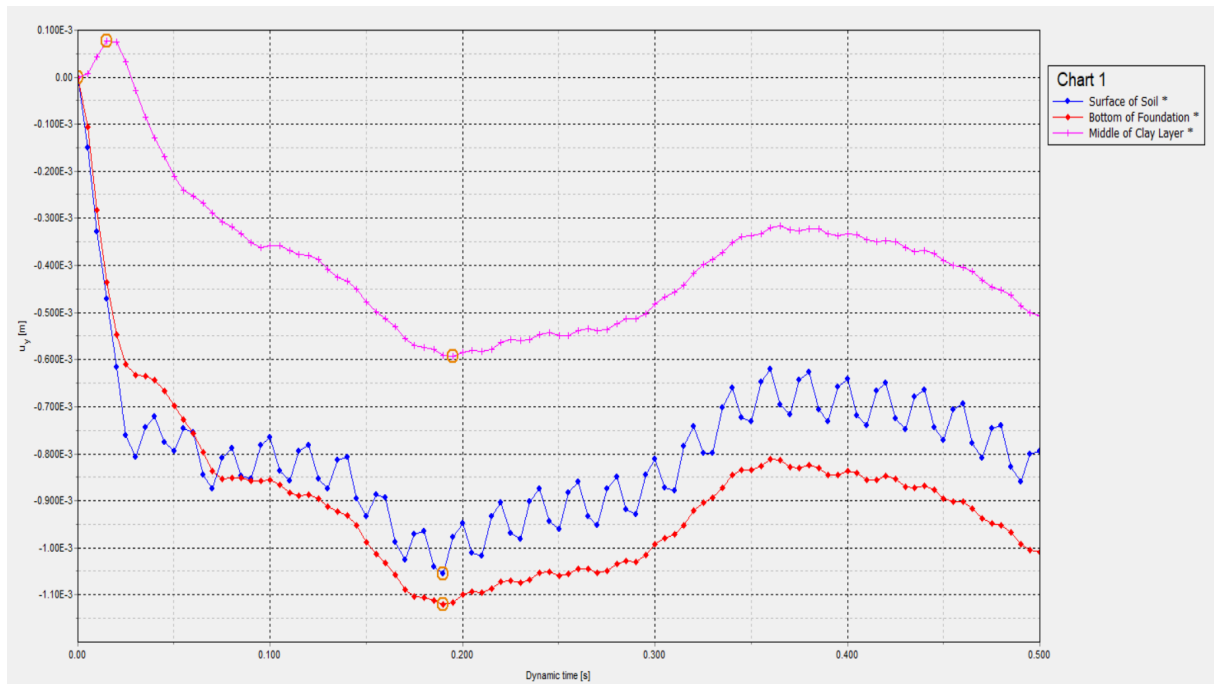


Figure 12.13: Result generated in in-situ generator analysis performed with damping

After conducting the analysis of the damping effect on various types of soil using PLAXIS 2D, the following conclusions can be drawn from the graphs obtained.

- The graphs demonstrate that the presence of damping significantly reduces the vibrational response of soils under dynamic loading conditions.
- As the damping coefficient increases, the amplitude of displacements and accelerations decreases, indicating that damping effectively dissipates energy and dampens vibrations.
- Cohesive soil show a more noticeable reduction in vibrational response with increasing damping coefficients compared to Cohesionless soil. This is because soft soils are more susceptible to dynamic deformations, and damping helps in mitigating these deformations effectively.
- Damping plays a crucial role in mitigating resonance effects in soils. Resonance can occur when the excitation frequency matches the natural frequency of the soil, leading to amplified displacements and stresses. By adjusting the damping coefficient appropriately, it is possible to avoid resonance and prevent potential failures.
- In the two-layered soil profile, each layer exhibit different damping characteristics. The interaction between the two layers significantly influences the overall damping behaviour of the system

- Here the upper layer has higher damping than the lower layer, energy dissipation in the upper layer may reduce the energy transmitted to the lower layer, affecting the response of the entire system.

CHAPTER 13

CALCULATION OF SAFE DISTANCE

13.1 Introduction

The safe distance between the foundations and turbo generator is important to prevent adverse interactions such as settlements, tilting, and vibrations. PLAXIS 2D uses finite element analysis for the following analysis. This chapter outlines the methodology and results of calculating the safe distance between the foundation and the turbo generator.

13.2 Methodology

This calculation involves evaluating the potential impact of the foundation loading on the turbo generator and vice versa. This is achieved through finite element analysis in PLAXIS 2D, which simulates the soil-structure interaction and provides insights into the soil behaviour and potential deformations.

13.3 Analytical calculation of safe distance in cohesive soil

13.3.1 Generation of geometry and mesh.

Brief description of the system: The effect of a typical turbo generator running at a specific frequency on a double storey steel frame structure is analyzed. The structure is made of structural steel of Fe-415 and is on a M25 concrete block foundation length of 14 m with a height of 10 m. The underlying soil is a 40 m of clay layer is taken for analysis. The turbo generator lies at a distance of 9.5m from the steel frame with a height of 2.5 m and width of 5 m respectively running at 50 Hz frequency.

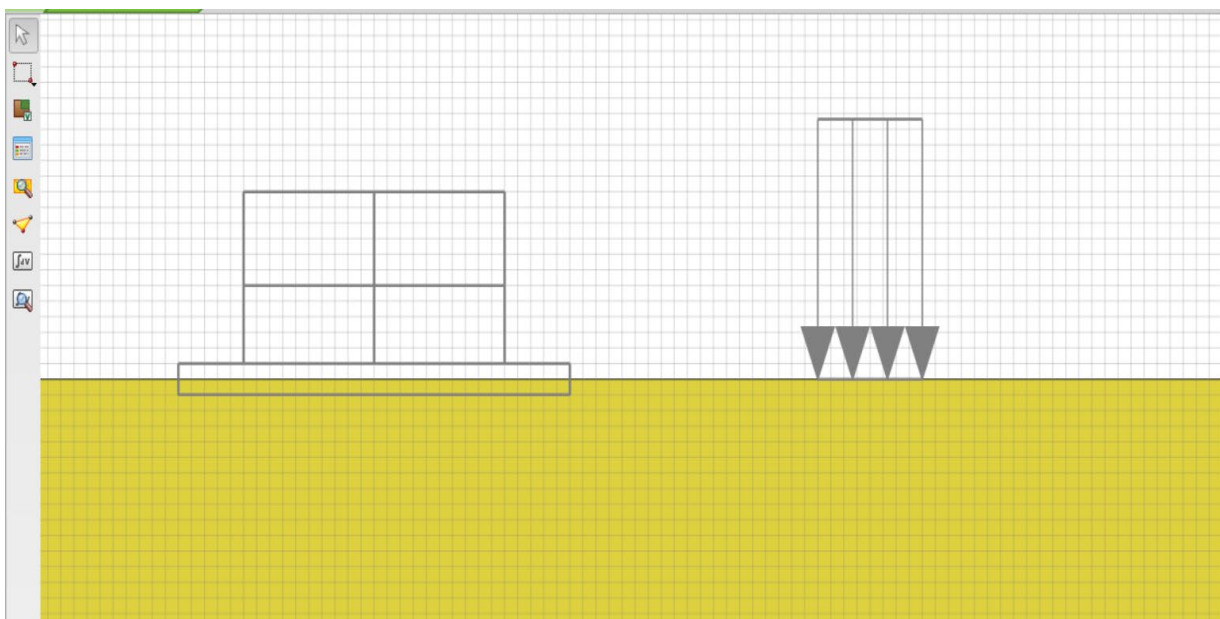


Figure 13.1: The foundation and machine are modelled as separate entities

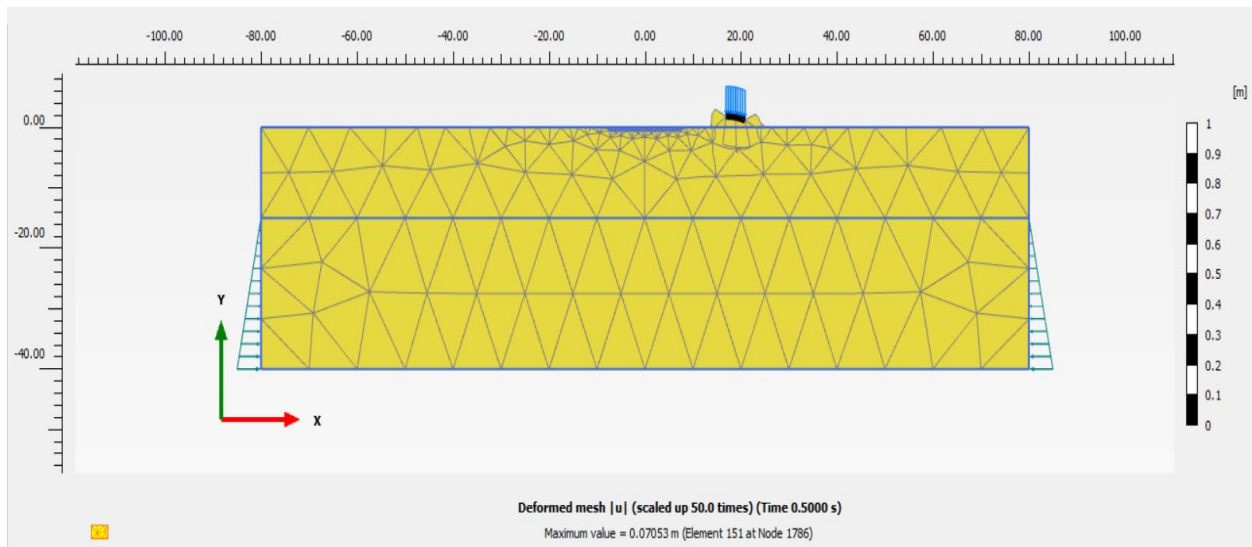


Figure 13.2: Generation of mesh

Material Properties: Material properties such as soil stiffness, cohesion, and friction angle were assigned based on references from Chapter 8. Structural properties of the foundation and machine components, including elastic modulus and Poisson's ratio, were also defined. Appropriate boundary conditions are applied to the model to simulate real-world constraints. These conditions included fixed boundaries, and constraints on the machine's components.

After generation of the mesh, three nodes were selected for the displacement analysis.

Results.

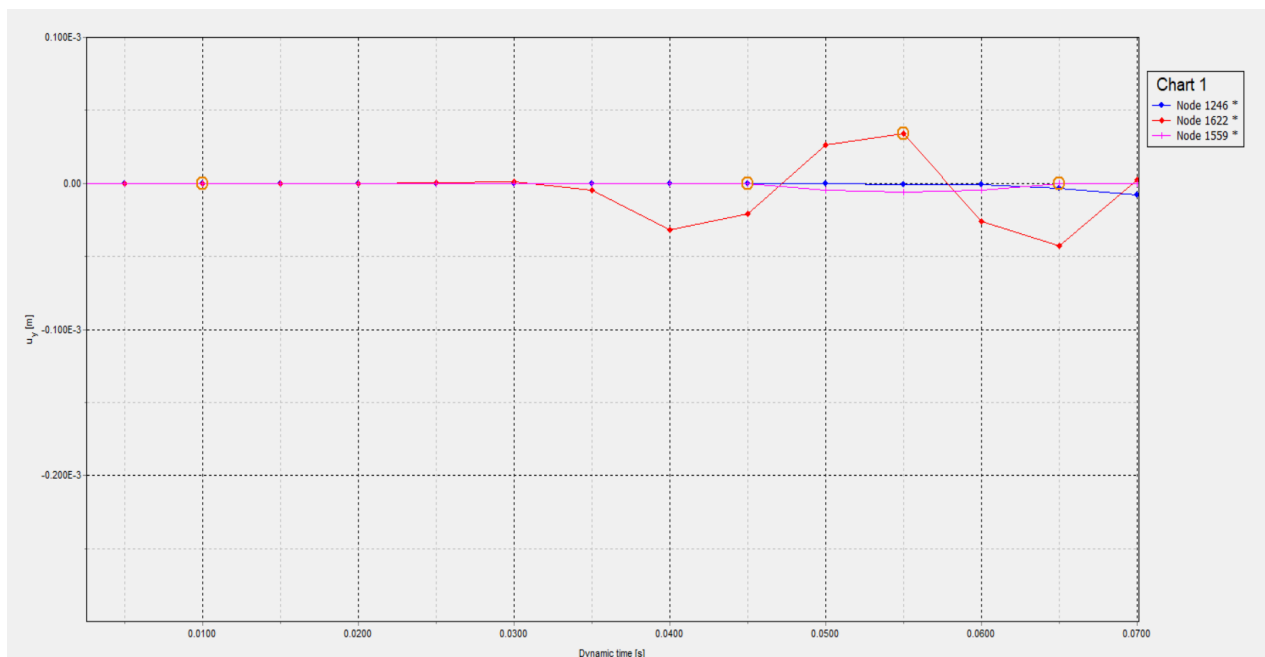


Figure 13.3: The dynamic time vs. displacement graph is shown below

Point	Step	Dynamic time [s]	u_y [m]
11	10	0.000	0.000
12	10	0.005	0.000
13	11	0.010	0.000
14	12	0.015	0.000
15	13	0.020	0.000
16	14	0.025	0.000
17	15	0.030	0.000
18	16	0.035	0.000
19	17	0.040	0.000
20	18	0.045	0.000
21	19	0.050	0.000

Figure 13.4: Tabulated data showing minimal to no deformation for the safe distance in PLAXIS 2D

Point	Step	Dynamic time [s]	u_y [m]
11	10	0.000	0.000
12	10	0.005	0.000
13	11	0.010	0.000
14	12	0.015	0.000
15	13	0.020	0.000
16	14	0.025	0.000
17	15	0.030	0.000
18	16	0.035	0.000
19	17	0.040	0.000
20	18	0.045	0.000
21	19	0.050	0.000

Figure 13.5: Tabulated data showing minimal to no deformation for the safe distance in PLAXIS 2D

Point	Step	Dynamic time [s]	u_y [m]
11	10	0.000	0.000
12	10	0.005	0.000
13	11	0.010	0.000
14	12	0.015	0.000
15	13	0.020	0.000
16	14	0.025	0.000
17	15	0.030	0.000
18	16	0.035	0.000
19	17	0.040	0.000
20	18	0.045	0.000
21	19	0.050	0.000

Figure 13.6: Tabulated data showing minimal to no deformation for the safe distance in PLAXIS 2D

The analysis yields valuable insights into the behaviour of the system. The tabulated data shows no deformation in the y direction which have significant implications for the safety, reliability, and longevity of the steel structure. The stable graphs resulting from the stability analysis provide strong evidence of the structural system's ability to withstand various loading conditions without experiencing deformation.

13.4 Analytical calculation of safe distance in cohesionless soil.

13.4.1 Generation of geometry and mesh.

Brief description of the system: The effect of a typical turbo generator running at a specific frequency on a double storey steel frame structure is analyzed. The structure is made of structural steel of Fe-415 and is on a M25 concrete block foundation length of 14 m with a height of 10 m. The underlying soil is a 40 m of sand layer is taken for analysis. The turbo generator lies at a distance of 8m from the steel frame with a height of 2.5 m and width of 5 m respectively running at 50 Hz frequency.

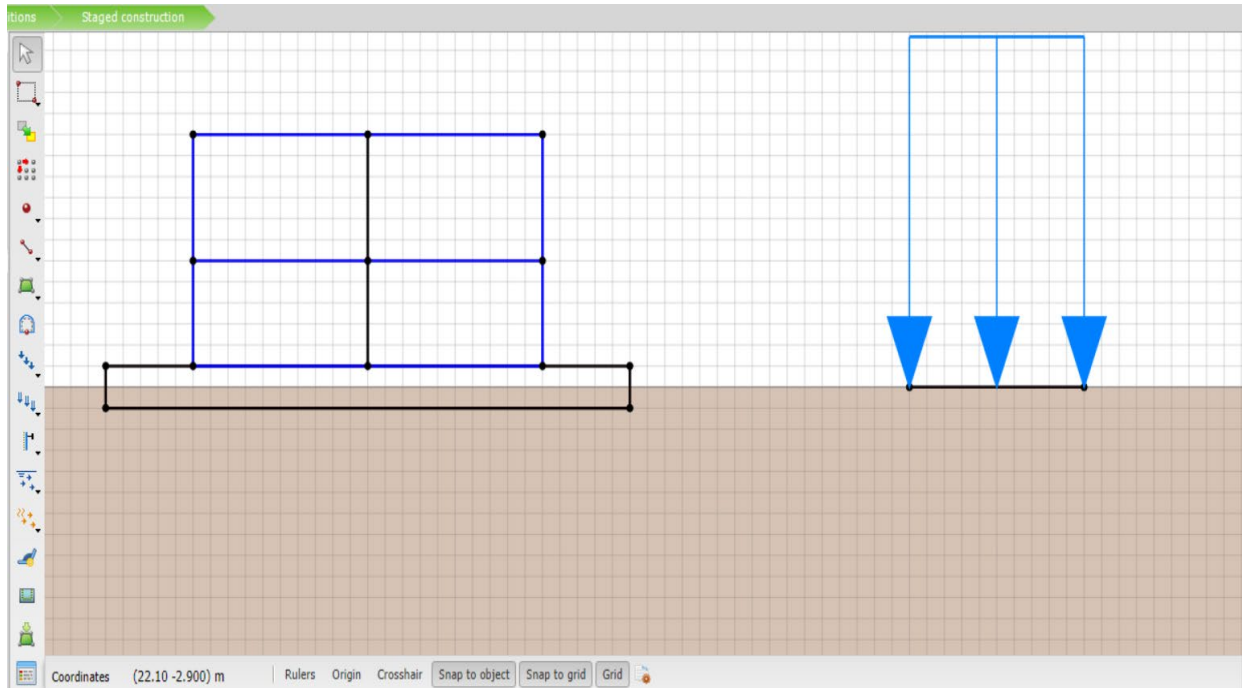


Figure 13.7: The foundation and machine are modelled as separate entities

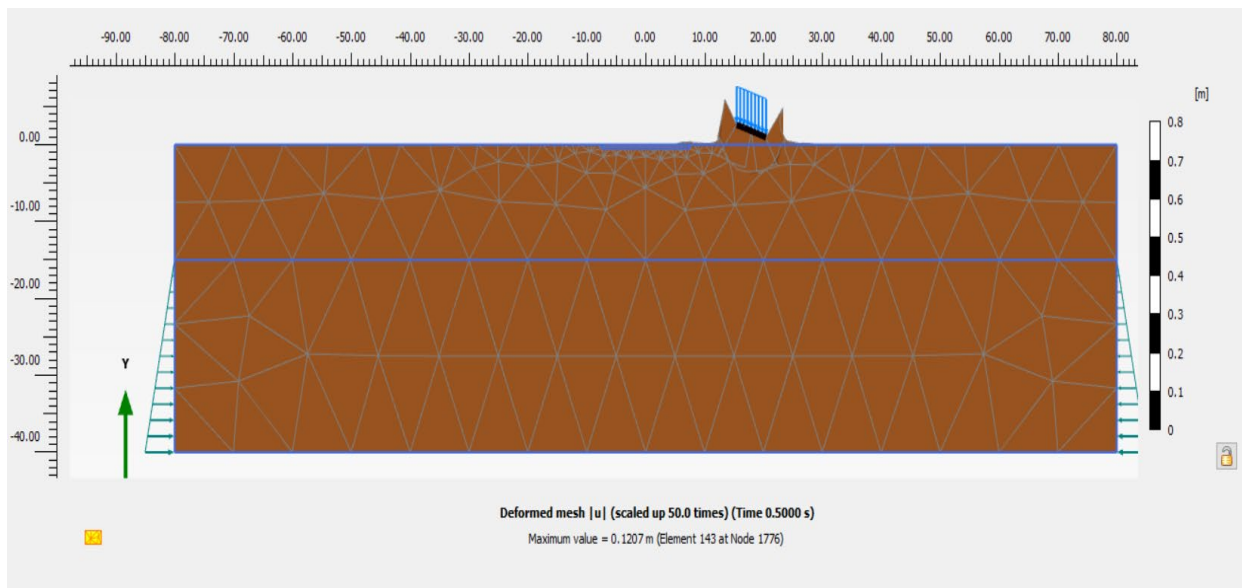


Figure 13.8: Generation of mesh

Material Properties: Material properties such as soil stiffness, cohesion, and friction angle were assigned based on references from Chapter 8. Structural properties of the foundation and machine components, including elastic modulus and Poisson's ratio, were also defined. Appropriate boundary conditions are applied to the model to simulate real-world constraints. These conditions included fixed boundaries, and constraints on the machine's components.

After generation of the mesh, three nodes were selected for the displacement analysis.

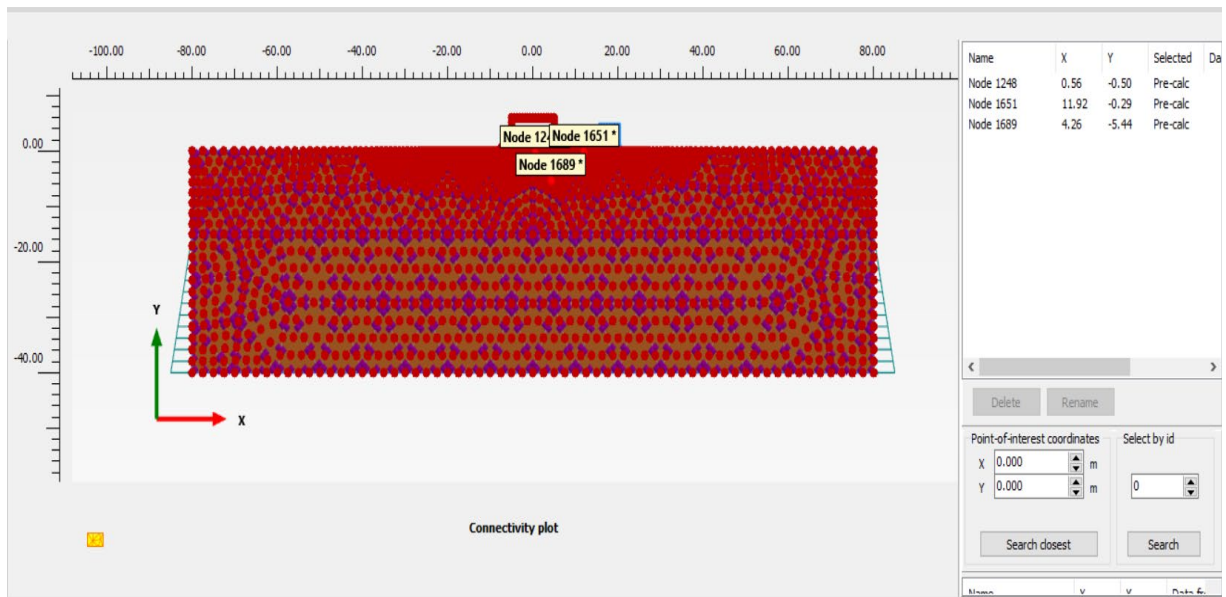


Figure 13.9: Selection of nodes

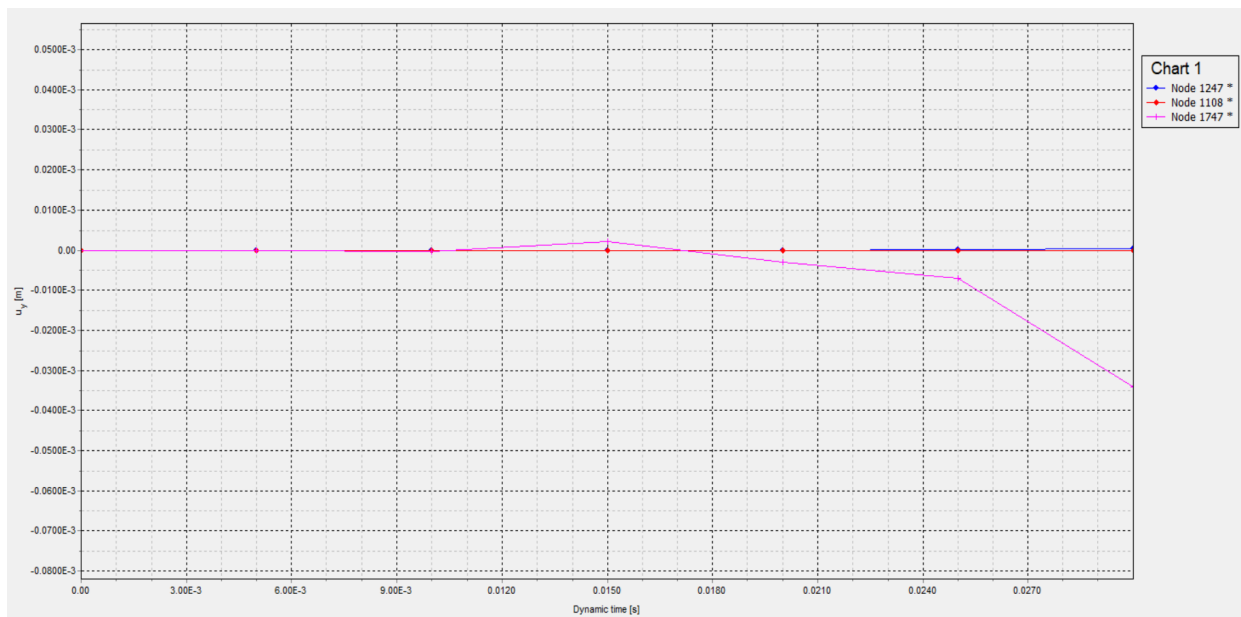


Figure 13.10: The dynamic time vs. displacement graph is shown below

The analysis yields valuable insights into the behaviour of the system. The graphical data shows no deformation in the y direction which have significant implications for the safety, reliability, and longevity of the steel structure. The stable graphs resulting from the stability analysis provide strong evidence of the structural system's ability to withstand various loading conditions without experiencing deformation.

13.5 Analytical calculation of safe distance in two layered soil.

13.5.1 Generation of geometry and mesh.

Brief description of the system: The effect of a typical turbo generator running at a specific frequency on a double storey steel frame structure is analyzed. The structure is made of structural steel of Fe-415 and is on a M25 concrete block foundation length of 14 m with a height of 10 m. The underlying soil is a cohesive soil up to 15 m and below layer consists of sand. 25 m of sand layer is taken for analysis. The turbo generator lies at a distance of 7 m from the steel frame with a height of 2.5 m and width of 5 m respectively running at 50 Hz frequency.

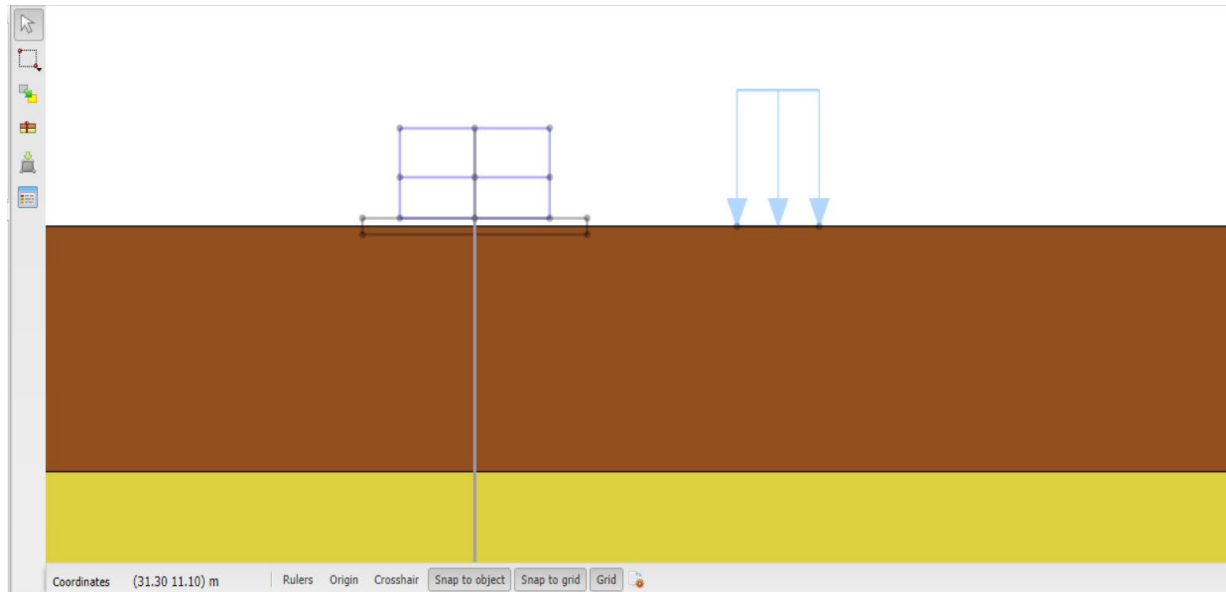


Figure 13.11: The foundation and machine are modelled as separate entities

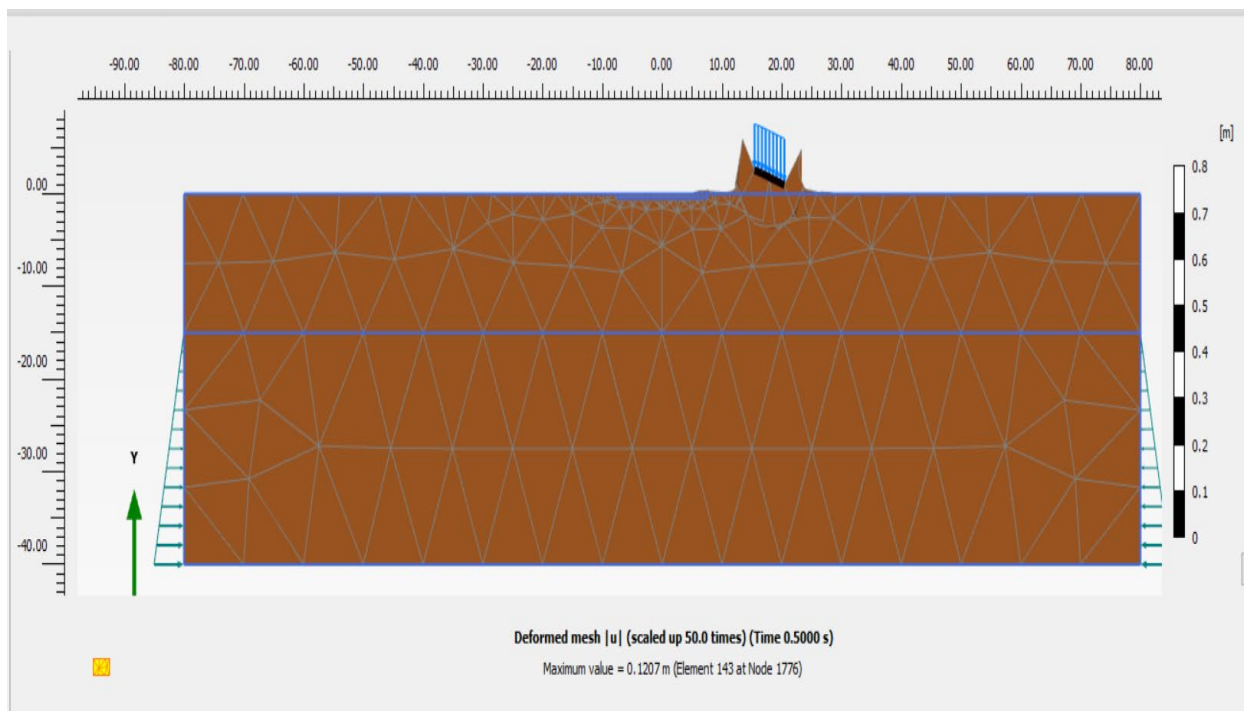


Figure 13.12: Generation of mesh

Material Properties: Material properties such as soil stiffness, cohesion, and friction angle were assigned based on references from Chapter. Structural properties of the foundation and machine components, including elastic modulus and Poisson's ratio, were also defined. Appropriate boundary conditions are applied to the model to simulate real-world constraints. These conditions included fixed boundaries, and constraints on the machine's components.

After generation of the mesh, three nodes were selected for the displacement analysis.

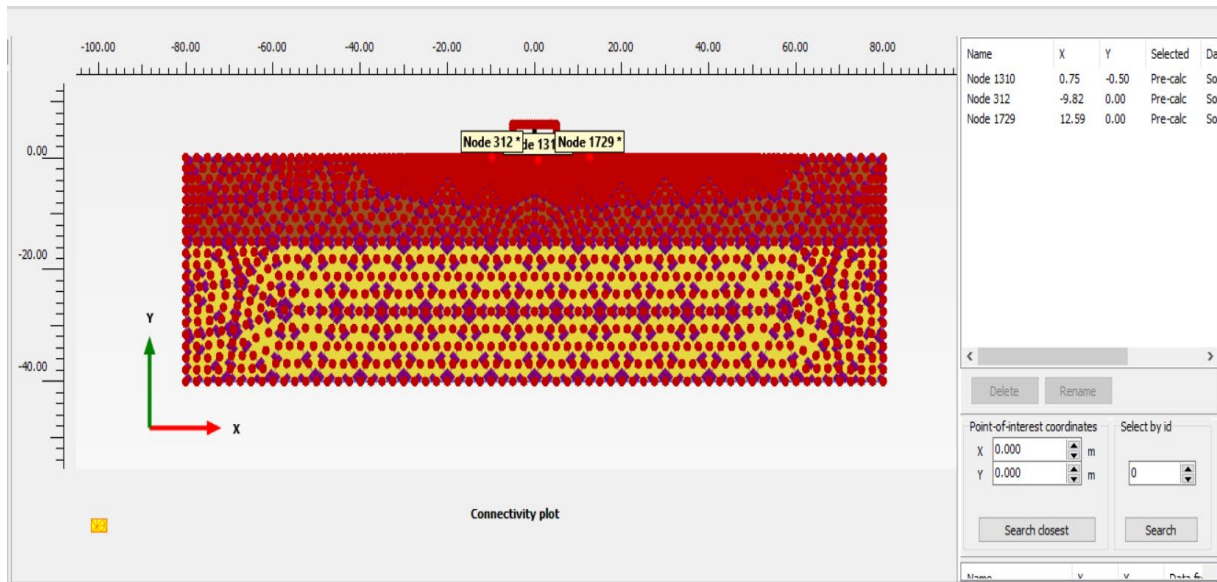


Figure 13.13: Selection of nodes

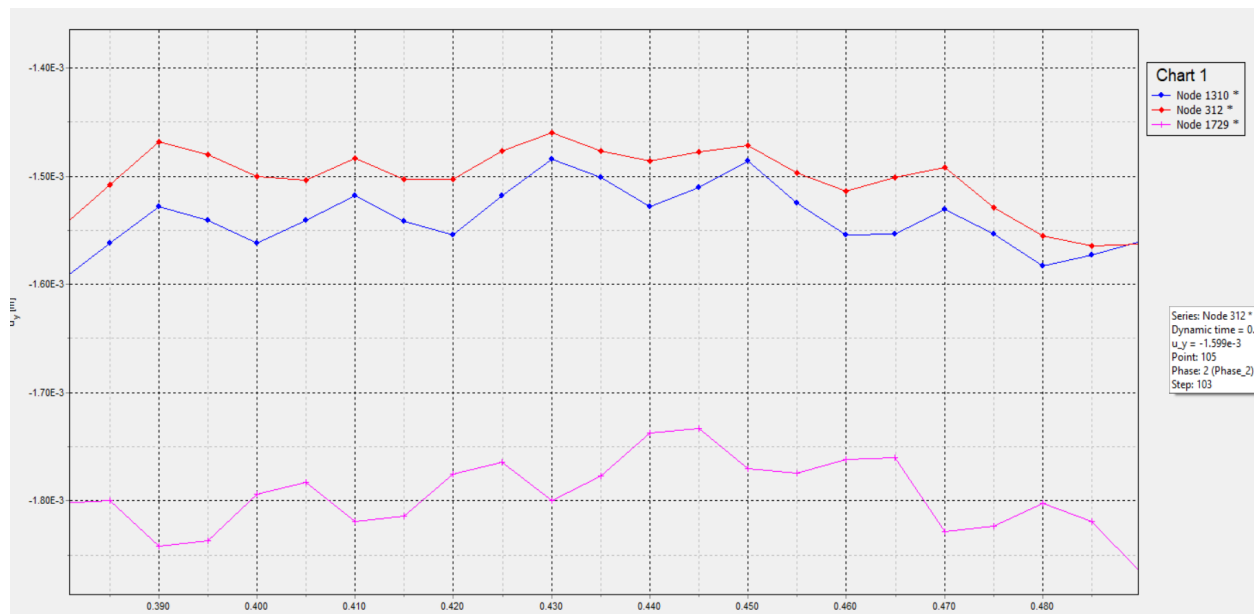


Figure 13.14: The dynamic time vs. displacement graph is shown below

FINDINGS

In a two-layered soil consisting of both sand and clay layers, determining the safe distance as 7 m between the turbo generator and the building becomes more complex due to the different properties of each layer. The interaction between the layers significantly impact how vibrations and forces are transmitted through the soil. This analysis considers the transmission of dynamic loads from the turbo generator to the building, as well as the potential for ground movement and settlement. This interaction is known as soil-structure interaction (SSI).

The analysis yields valuable insights into the behaviour of the system. The graphical data shows lesser deformation in the y direction which have significant implications for the safety, reliability, and longevity of the steel structure. The stable graphs resulting from the stability analysis provide strong evidence of the structural system's ability to withstand various loading conditions without experiencing deformation.

CHAPTER 14

CONCLUSIONS

14.1 GENERAL

This simulation study conducted using PLAXIS 2D for the design of a turbo generator foundation has provided valuable insights into the structural behaviour and stability of the foundation system with respect to the designed steel structure. This study aimed to ensure the safe and effective installation of the turbo generator while accounting for the complex interactions between the foundation, soil, and dynamic loads

Through the analysis performed by PLAXIS 2D, various critical aspects were examined:

14.2 Soil-Structure Interaction:

The simulation specified the dynamic interaction between the foundation structure and the underlying soil layers. This interaction is crucial in determining how loads from the turbo generator are distributed, absorbed, and transmitted to the surrounding ground.

14.3 Vibration and Settlement Analysis:

By modelling the dynamic loads generated by the turbo generator, we assessed potential vibrations and the resulting settlements. This enabled us to predict any adverse effects on the structural integrity of both the foundation and the adjacent steel structure. The conclusion from the analysis is given in Table 14.1

Table 14.1: Vibration and Settlement Analysis of types of Soil.

SL NO.	SOIL TYPE	POSITION OF NODES	RESULT
1.	Cohesionless Soil	At Surface of soil	A Sharp deformation with peak values 0.046×10^3 , 0.039×10^3 , 0.056×10^3 meter respectively are observed followed by uniform deformation
		At Bottom of steel foundation	
		At Middle of Soil Layer	
2	Cohesive Soil	At Surface of soil	A Sharp deformation with peak values 0.036×10^3 , 0.047×10^3 , 0.039×10^3 meter respectively are observed followed by uniform deformation
		At Bottom of steel foundation	
		At Middle of Soil Layer	
3	Two Layered Soil	At Surface of soil	A Sharp deformation with peak values 0.031×10^3 , 0.03×10^3 , 0.03×10^3 meter respectively are observed followed by more stable deformation
		At Bottom of steel foundation	
		At Middle of Soil Layer	

14.4 Damping Analysis:

The simulation provided a detailed view of stress distribution within the foundation and soil layers. This insight was essential in identifying potential stress concentrations and

ensuring that the foundation's design is robust enough to handle the loads without exceeding safe stress limits. The conclusion from the analysis is given in Table 14.2

Table 14.2: Damping Analysis in various steps of soil.

SL NO.	SOIL TYPE	RESULT AFTER DAMPING ANALYSIS
1	Cohesionless Soil	Reduces the vibrational response of the soil under dynamic loading condition with lesser peak value.
2	Cohesive Soil	More susceptible to dynamic deformation, more noticeable reduction in vibrational response
3	Two Layered Soil	Interaction between the two layers mitigates resonance and is more effective in preventing failure

14.5 Water Table Analysis:

The influence of the water table on the soil properties and behaviour was considered, as it can significantly affect the foundation's stability and damping characteristics. The simulation allowed for a thorough exploration of the impact of varying water table levels. The following table 14.3 allows us to conclude the following simulations.

Table 14.3: Water Table Analysis of soil.

SL NO.	SOIL TYPE	GRAPHICAL CONCLUSION
1	Cohesionless Soil	A rise in load vs settlement graph is seen with raising the water table with load 133.82 KN with settlement of 0.86 m
2	Cohesive Soil	A rise in the load vs settlement graph is seen with raising the water table at the initial loading conditions

14.6 Calculation of safe distance:

Establishing the optimal safe distance between the turbo generator and the building is a complex endeavour that encompasses a wide array of interrelated factors. These factors encompass not only the physical characteristics of the generator and the building but also broader aspects that significantly influence the dynamics of the system. Through integration of these diverse factors, the safe distance between a turbo generator and a building can be defined to strike a balance between operational functionality and structural security. This ensures that the coexistence of the turbo generator and the building is characterized by minimized structural stress, controlled noise levels, and a safeguarded environment for all stakeholders involved. The safe distance calculated for various types of soil is given in Table 14.4

Table 14.4: Calculated safe distance of various types of soil.

SL NO.	SOIL TYPE	SAFE DISTANCE
1	Cohesionless Soil	Safe distance is calculated to be 9.5 m and more
2	Cohesive Soil	Safe distance is calculated to be 8 m and more
3	Two Layered Soil	Safe distance is calculated to be 7 m and more

14.7 Validation and Optimization:

The simulation results were validated with inbuilt properties taken from the various journals, enhancing the accuracy and reliability of the analysis. Iterative simulations and parameter adjustments enabled optimization of the foundation design to meet desired performance criteria.

The outcomes of this simulation study will play a pivotal role in the finalization of the turbo generator foundation design. By accounting for the intricate interactions between the structure, soil, and loads, we have ensured that the foundation will provide stable support for the turbo generator's operation while maintaining the structural integrity of the surrounding environment.

14.8 Future Scope:

Our present study was limited to 2D modelling of the foundation, but a 3D model will give a more precise result. Some specific future scopes are noted

- Investigation of more advanced material models that can capture the nonlinear behaviour of soils and concrete under dynamic loading.
- The analysis can be extended to consider the effects of seismic loading on turbo generator foundations. This could involve studying how different seismic intensities and ground motion characteristics impact the foundation's response.
- Thermal analysis can be considered to analyze the effects of thermal intensities on the foundation.
- The effect of Multiple vibrations can be considered.

In embracing these future directions, the dynamic analysis of turbo generator foundations in PLAXIS 2D can pave the way for safer, more efficient, and environmentally conscious energy infrastructure. As technology evolves and knowledge deepens, engineers and researchers have the opportunity to shape the future of foundation design, contributing to the reliability and resilience of power generation systems worldwide.

REFERENCE

1. "The turbogenerator – A continuous engineering challenge", C. Ginet, R. Joho, Member, IEEE, M. Verrier. Archived from the original on 2010-08-21.
2. Fleischer, P. S., & Trombik, P. G. (2008, October). Turbo generator machine foundations subjected to earthquake loadings. In The 14th World Conference on Earthquake Engineering, Beijing, China.
3. Hokmabadi, A. S., & Fatahi, B. (2016). Influence of foundation type on seismic performance of buildings considering soil–structure interaction. *International Journal of structural stability and dynamics*, 16(08), 1550043.
4. Jagtap, H. P., Bewoor, A. K., Kumar, R., Ahmadi, M. H., & Chen, L. (2020). Performance analysis and availability optimization to improve maintenance schedule for the turbo-generator subsystem of a thermal power plant using particle swarm optimization. *Reliability Engineering & System Safety*, 204, 107130.
5. Jayarajan, P., & Kouzer, K. M. (2014). Dynamic analysis of turbo-generator machine foundations. *Journal of Civil Engineering and Environmental Technology*, 1(4), 30- 35.
6. Madhu Priya, M., Chandru, P., Vijaya Sarathy, R., & Jose Ravindra Raj, B. (2016). Dynamic Analysis and Structural Design of Turbo Generator Frame Foundation–A Review. *International Journal of Advances in Engineering Research*, e-ISSN, 2231- 5152.
7. Meiden-Alternator JG2000 series, <https://www.meidensha.com/catalog/CB73-3137.pdf>
8. Rajkumar, K., Ayothiraman, R., & Matsagar, V. A. (2021). Effects of Soil-Structure Interaction on Torsionally Coupled Base Isolated Machine Foundation under Earthquake Load. *Shock and Vibration*, 2021, 1-18.
9. Smart, M. G., Friswell, M. I., & Lees, A. W. (2000). Estimating turbogenerator foundation parameters: model selection and regularization. *Proceedings of the Royal Society of London. Series A: Mathematical, Physical and Engineering Sciences*, 456(1999), 1583-1607.
10. Star, L. M., Givens, M. J., Nigbor, R. L., & Stewart, J. P. (2015). Field-testing of structure on shallow foundation to evaluate soil-structure interaction effects. *Earthquake Spectra*, 31(4), 2511-2534.
11. Sun, Y. H., & Zhang, Q. (2013). Study on optimization of dynamic characteristics of turbo generator foundation. In *Advanced Materials Research* (Vol. 625, pp. 45-52). Trans Tech Publications Ltd.
12. Tripathy, S., & Desai, A. K. (2015). Dynamic analysis of turbo generator frame foundation using SAP: 2000 v 17.1 software. In *Fiftieth Indian geotechnical conference*.
13. Turbo Generator - https://en.wikipedia.org/wiki/Turbo_generator
14. https://communities.bentley.com/cfs-file/__key/communityserver-wikis-components-files/00-00-00-01-05/Use_5F00_of_5F00_ShotCrete_5F00_UDSM_5F00_notchedbeammixedfracturemode_5F00_abc.png
15. <https://i.ytimg.com/vi/m46rPeuQjX8/sddefault.jpg>
16. <https://i.ytimg.com/vi/mm8wCn35ggk/sddefault.jpg>